

1  
2  
3 **1 Late Triassic tectonic inversion in the upper Yangtze Block: insights from**  
4 **2 detrital zircon U–Pb geochronology**  
5  
6  
7  
8  
9  
10

11  
12  
13  
14  
15  
16  
17  
18  
19  
20  
21  
22  
23  
24  
25  
26  
27  
28  
29  
30  
31  
32  
33  
34  
35  
36  
37  
38  
39  
40  
41  
42  
43  
44  
45  
46  
47  
48  
49  
50  
51  
52  
53  
54  
55  
56  
57  
58  
59  
60

1  
2  
3  
4  
5  
6  
7  
8  
9  
10  
11  
12  
13  
14  
15  
16  
17  
18  
19  
20  
21  
22  
23  
24  
25  
26  
27  
28  
29  
30  
31  
32  
33  
34  
35  
36  
37  
38  
39  
40  
41  
42  
43  
44  
45  
46  
47  
48  
49  
50  
51  
52  
53  
54  
55  
56  
57  
58  
59  
60

Zhaokun Yan<sup>1,3</sup>, Yuntao Tian<sup>2,3</sup>, Rui Li<sup>2</sup>, Pieter Vermeesch<sup>3</sup>, Xilin Sun<sup>4</sup>, Yong Li<sup>1</sup>, Martin Rittner<sup>3</sup>,  
Andrew Carter<sup>5</sup>, Chongjian Shao<sup>1</sup>, Hu Huang<sup>1</sup>, Xiangtian Ji<sup>1</sup>

<sup>1</sup> State Key Laboratory of Oil and Gas Reservoir Geology and Exploitation (Chengdu University of  
Technology), Sichuan Chengdu, 610059, China

<sup>2</sup> School of Earth Sciences and Engineering, Sun Yat-sen University, Guangzhou, 510275, China

<sup>3</sup> Department of Earth Sciences, University College London, London, WC1E 6BT, UK

<sup>4</sup> Cluster Geology and Geochemistry, VU University Amsterdam, De Boelelaan 1085, 1081 HV  
Amsterdam, The Netherlands

<sup>5</sup> Department of Earth and Planetary Science, Birkbeck University of London, Malet Street,  
Bloomsbury, London WC1E 7HX, UK

Corresponding author:

Yuntao Tian

School of Earth Sciences and Engineering

Sun Yat-sen University

Guangzhou, China

Email: tianyuntao@mail.sysu.edu.cn

**ABSTRACT**

Closure of the Paleo-Tethys Ocean during the Middle – Late Triassic saw the Sichuan Basin region, located at the western margin of the Yangtze Block, transition from a passive continental margin into a foreland basin. To understand if and how the regional sediment routing system adjusted to these changes we applied detrital zircon U-Pb analyses to representative stratigraphic samples from the southwestern edge of the Sichuan Basin to monitor sediment provenance. Integration of the results with paleocurrent and published detrital zircon data from other parts of the basin identified a marked change in provenance between Early - Middle Triassic samples, dominated by Neoproterozoic (~700-900Ma) zircons sourced mainly from the Kangdian Oldland to the south, and Late Triassic sandstones that contain a more diverse range of zircon ages similar to the Songpan-Ganzi terrane located further away to the northwest. This change reflects a major drainage adjustment in response to the Late Triassic closure of the Paleo-Tethys Ocean and significant shortening in the Longmen Shan thrust belt and the eastern Songpan-Ganzi terrane. This study highlights the importance of tectonic events in reorganizing drainage and sediment supply system in foreland basins.

## INTRODUCTION

The Sichuan Basin, located in the southwest China, shares common borders with three major tectonic terrains – the Qinling-Dabie orogen to the north, the eastern Tibetan Plateau to the west and south, and the eastern Sichuan fold-and-thrust belt to the east (Fig. 1). Numerous structural, geochronological, and sedimentary studies suggested that these areas had experienced a significant phase of crustal shortening and rock exhumation during the Triassic (Zhang *et al.*, 1995; Burchfiel *et al.*, 1995; Yin, 1996; Meng & Zhang, 2000; Li *et al.*, 2003a; Wang *et al.*, 2005; Jia *et al.*, 2006), and the Sichuan Basin changed from a passive continental margin to a foreland basin.

In the context of these changes, the provenance of sediments deposited in the Sichuan Basin have seen extensive study, much based on detrital zircon U-Pb geochronology work (Deng *et al.*, 2008; Chen, 2011; Luo *et al.*, 2014; Zhang *et al.*, 2015; Shao *et al.*, 2016; Li *et al.*, 2016). Results from previous work suggest that the sediments in the basin were mainly sourced from the Qinling-Dabie orogen, to the north, and the Longmen Shan thrust belt and the Songpan-Ganzi terrane to the west. However, most of those previous studies focused on the post Late Triassic foreland basin sediments in the western and northern part of the Sichuan Basin. The provenance of pre-Late Triassic passive continental margin clasts remains elusive. Constraining the provenance of the sediments deposited before and after the Late Triassic tectonic inversion could provide significant insights into whether the sediment routing system into the basin had significantly changed by the inversion event.

Previous sedimentary and stratigraphic studies suggested that during the Early – Middle Triassic, the southwestern basin margin was bounded by a highland, as indicated by a lateral sedimentary facies transition from clastic to carbonate away from the basin edge to interior (Liu & Tong, 2001; Long *et al.*, 2011; Zhao *et al.*, 2012; Wei *et al.*, 2014; Tan *et al.*, 2014). The highland consists of Neoproterozoic basement and is referred to as the Kangdian Oldland or Kangdian Axis by Chinese researchers (Li, 1963; Luo, 1983; Wang *et al.*, 1983; Dai *et al.*, 2012; Tan *et al.*, 2013) (Fig. 2). The lithology of Late Triassic sediments in the southern Sichuan Basin is similar to those in other parts of the basin, sourced mainly from the Longmen Shan thrust belt and the Qinling-Dabie orogen. This implies that a significant change in sediment provenance might have occurred during the Late Triassic basin inversion. To test this, we applied detrital zircon geochronology to nine Early - Late Triassic sandstone and one volcanic tuff outcrop samples collected from the southwestern part of the Sichuan Basin. The results are interpreted together with previously mapped stratigraphic correlations and paleocurrent data, so as to constrain the paleogeographic evolution of the southwestern margin of the Sichuan Basin during Early - Late Triassic time, and to test if the afore-mentioned tectonic events had influenced the sedimentary delivery network in the basin margin.

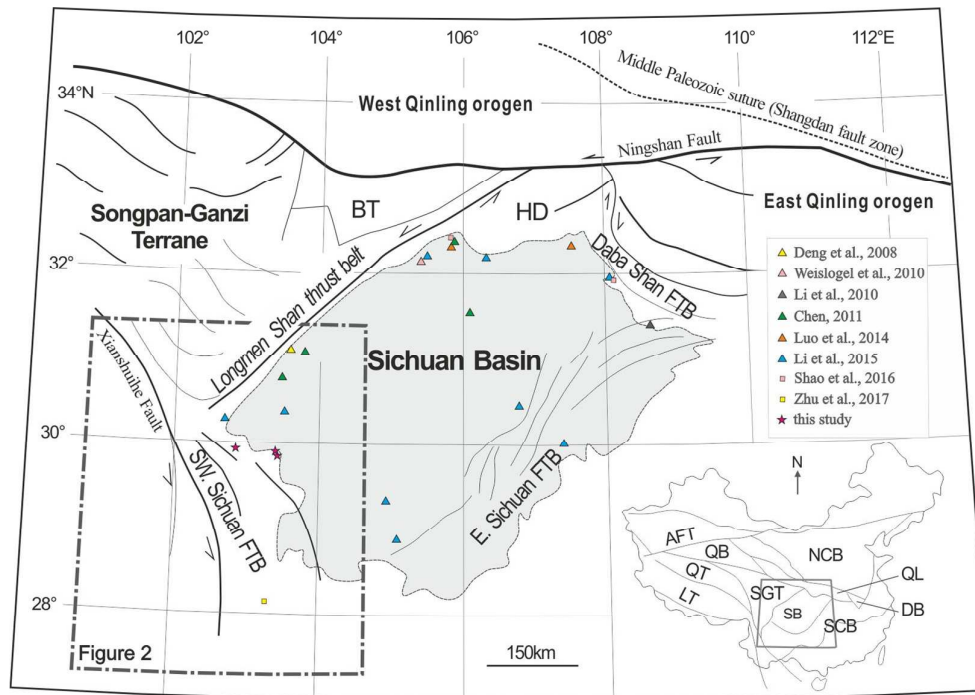


**Fig. 1.** Simplified tectonic map of the Sichuan Basin and adjacent regions. Sites of previous detrital zircon geochronology studies of the Sichuan Basin are shown in the figure. Inset shows main tectonic elements of China. ATF—Altyn Tagh fault; BT—Bikou terrane; DB—Dabie orogen; FTB—fold-thrust belt; HD—Hannan dome; LT—Lhasa terrane; NCB—North China Block; QB—Qaidam basin; QL—Qinling orogen; QT—Qiangtang terrane; SB—Sichuan Basin; SCB—South China Block; SGT—Songpan-Ganzi terrane. Modified from Tian *et al.* (2012a).

## 85 GEOLOGICAL SETTING

86 The southwestern part of Sichuan Basin is bounded by the Kangdian basement to the south and  
 87 southeastern Songpan-Ganzi terrane and Longmen Shan to the west (Figs. 1, 2). The geological  
 88 evolution of these major terranes is summarized below.

### 89 Sichuan Basin

90 The geological evolution of the Sichuan Basin can be divided into three major stages: a passive  
 91 margin stage characterized by platform carbonates during Paleozoic to Middle Triassic time (Xu *et al.*,  
 92 1997), a Late Triassic foreland basin characterized predominantly by continental siliciclastic  
 93 sedimentation and a terrestrial foreland basin or intracratonic stage from the Jurassic to Quaternary (Li  
 94 *et al.*, 2003a). The eastern and central Sichuan Basin experienced a prolonged phase of denudation  
 95 since late Cretaceous time, as shown by thermochronological studies (Tian *et al.*, 2012a, b). In this  
 96 study, we focus on the Triassic strata in the southwest that consists of Feixianguan, Jialingjiang,  
 97 Leikoupo, Maantang, Xiaotangzi and Xujiuhe Formations, from bottom to top.

98 (1) The marine Feixianguan Formation is widely distributed in the Sichuan Basin, but shows  
 99 marked lateral lithofacies variations. The formation consists of purple shale and sandy shale,  
 100 interbedded with grey limestone, oolitic limestone, marl and sandstone in the western Sichuan Basin,

1  
2  
3 101 but change into limestone toward the eastern basin (BGMRS, 1997). The biostratigraphic age of the  
4 102 formation is Early-Early Triassic (based on bivalves and ammonites such as *Claraia*, *Eumorphotis*,  
5 103 *Oxytoma*, *Ophiceratidae*) (BGMRS, 1997). Several volcanic ash beds at the bottom of the formation  
6 104 compare well with the ash sequence of the Global Stratotype Section (Meishan section) (Huang *et al.*,  
7 105 2017) that has ash beds (~252Ma) (Burgess *et al.*, 2014) providing a quantitative constraint for the age  
8 106 of the Feixianguan Formation.

9  
10  
11 107 (2) The marine Jialingjiang Formation conformably overlies the Feixianguan Formation, and is  
12 108 mainly composed of limestone and dolomite (BGMRS, 1997). In the formation, Late-Early Triassic  
13 109 bivalves (including *Eumorphotis*, *Claraia*, *Myophoria*, *Leptochondria*), ammonites (including  
14 110 *Meekoceras*, *Paranannites*, *Tirolites*, *Dinarites*), foraminiferas (*Glomospira*) and conodonts (including  
15 111 *Hindeodalla*, *Neospathodus*, *Neogondolella*) have been discovered (BGMRS, 1997). The top of the  
16 112 formation is marked by a widespread thin layer (the thickness is 10s cm – 1 m) of altered tuff (named  
17 113 as “green-bean rocks” in early Chinese literature) (Zhu & Wang, 1986), that has been dated to ~247 Ma  
18 114 (Ovtcharova *et al.*, 2006; Xie *et al.*, 2013; Lehrmann *et al.*, 2015).

19  
20  
21 115 (3) The marine Leikoupo Formation mainly consists of dolomite and argillaceous dolomite,  
22 116 interbedded with limestone and gypsum layers (BGMRS, 1997). It contains Middle Triassic bivalves  
23 117 such as *Eumorphotis* (*Asoella*), *Myophoria* (*Costatoria*) and ammonites such as *Progonoceratites*,  
24 118 *Beyrichites* (BGMRS, 1997). The boundary between the Leikoupo and Jialingjiang formations is the  
25 119 altered tuff.

26  
27 120 (4) The marine Maantang Formation, distributed in the western Sichuan Basin, mainly consists of  
28 121 marine black mudstone and shale interbedded with siltstone, marl, oolitic and bioclastic limestones and  
29 122 sponge reefs (BGMRS, 1997; Li *et al.*, 2003a). It is regarded as Carnian in age on the basis of its  
30 123 fossil content, which includes ammonoid, bivalve and conodont taxa (Shi *et al.*, 2016). The  
31 124 Kuahongdong Formation represents equivalent coeval strata in the southwestern margin of the Sichuan  
32 125 Basin, and is composed of conglomerate, mudstone, argillaceous limestone and argillaceous dolomite.  
33 126 Marine fossils identified in the Kuahongdong Formation include bivalves (*Plagiostoma*, *Cassianella*,  
34 127 *Halobia*, *Burmesia*), brachiopods (*Aulacothyropsis*) and ammonoids (*Paratibetites*, *Clionites*,  
35 128 *Trachyceras*) (BGMRS, 1997).

36  
37  
38 129 (5) The Xiaotangzi Formation (equivalent to the first member of the Xujiache Formation), is  
39 130 composed of black marine shale, mudstone, quartz arenite, lithic arenite and siltstone, and can be  
40 131 divided into three parts: a lower part, composed of black shale interbedded with quartz arenite, a  
41 132 middle part, composed of lithic arenite and black shale, and an upper part, composed of arkose. The  
42 133 formation coarsens upwards and is thought to represent a transition from marine shelf to delta  
43 134 environments. It has an early Norian age based on its fossil content, including plants such as  
44 135 *Thaumatopteris* *sp.*, *Lepidopteris* *sp.*, *Clathropteris meniscioides*, bivalves (*Burmesia lirata* Healey,  
45 136 *Halobia cf. fallax* Mojs, *Myophoria* (*Costatoria*) *seperata*, *Pteria krumbecki*, *Myophoria seperata*) and  
46 137 spores (*Protoanemitee*, *Taeniaesporites*, *Discisporites*) (Li *et al.*, 2003a).

47  
48  
49 138 (6) The Xujiache Formation conformably overlies the Xiaotangzi Formation in the western  
50 139 Sichuan Basin, and unconformably overlies Middle Triassic limestone of the Leikoupo Formation in  
51 140 the central and eastern Sichuan Basin. Widely distributed in the Sichuan Basin, the lithology and facies  
52 141 of the formation changes from coarse-grained sediments, including alluvial conglomerate bodies in  
53 142 front of the Longmen Shan thrust belt, to fine-grained lacustrine deposits in the basin interior. The  
54 143 depocenter is located in front of the middle section of the Longmen Shan thrust belt where the Xujiache  
55 144 Formation is up to 4 km thick (Meng *et al.*, 2005). Depositional age of the formation is late Norian to  
56  
57  
58  
59  
60

1  
2  
3 145 Rhaetian based on the fossil content that include plants, spores and bivalves (WGCMSPISB, 1984; Li  
4 146 *et al.*, 2003a).

5 147 Previous sedimentary studies suggested that the clastic deposits of Feixianguan, Jialingjiang and  
6 148 Leikoupo formations in the southwestern margin of the Sichuan Basin sourced from the south, as  
7 149 shown by a facies transition from clastic to carbonate deposits from the margin to the interior of the  
8 150 basin (Feng *et al.*, 1997; Tan *et al.*, 2014; Sun *et al.*, 2015). The Kangdian Oldland might be the source  
9 151 of Upper Triassic sediments, as suggested by studies on the detrital mineral assemblage, sedimentary  
10 152 system and conglomerate composition (Xie *et al.*, 2006; Jiang *et al.*, 2007; Shi *et al.*, 2010). However,  
11 153 nonmarine Upper Triassic sediments unconformably overlie rocks of the Kangdian Oldland (BGMRSF,  
12 154 1991) indicating that the region was likely an area of deposition rather than erosion (Liu & Tong, 2001;  
13 155 Yi *et al.*, 2014).

### 18 156 **Kangdian Oldland**

19  
20 157 The Kangdian Oldland is the western margin of the Yangtze Block and extends for over 700 km  
21 158 from the Kangding in the north to Yuanmou in the south (Zhou *et al.*, 2002a; Zhu *et al.*, 2011), is  
22 159 located in the western margin of the Yangtze Block (Fig. 2). It mainly consists of Precambrian  
23 160 basement, overlain by marine Paleozoic cover and locally by Upper Triassic to Cenozoic terrestrial  
24 161 sediments (Fig. 2, BGMRSF, 1991). Extensive Neoproterozoic magmatism (mainly ~740–870 Ma) is  
25 162 probably associated with the breakup of the supercontinent Rodinia due to a mantle plume (Li *et al.*,  
26 163 2003b), or the subduction of the Mozambique oceanic slab beneath the western margin of the Yangtze  
27 164 Block (Zhao & Zhou, 2007; Sun *et al.*, 2009).

28  
29 165 There is a debate on the geological evolution of Kangdian Oldland throughout the Paleozoic and  
30 166 Mesozoic. One school of thought is that the oldland was a region of erosion between the Ordovician  
31 167 and Carboniferous (Li, 1963), followed by a rift stage from Late Permian to Jurassic (Luo, 1983). A  
32 168 different point of view is that the Paleozoic - Mesozoic geological evolution of the region can be  
33 169 divided into three stages: a stable marine platform from the Cambrian to Early Permian, an uplift stage  
34 170 affected by Emeishan mantle plume from Late Permian to Middle Triassic, and foreland basin from the  
35 171 Late Triassic to Jurassic (Feng *et al.*, 1994; Wang *et al.*, 1994; He *et al.*, 2003).

### 40 172 **Longmen Shan**

41  
42 173 The Longmen Shan approximately 500km long and 30-50km wide, defines a major part of the  
43 174 highly dissected eastern margin of Tibetan Plateau. Neoproterozoic basement rocks, surrounded by  
44 175 Paleozoic sedimentary strata, outcrop in the Longmen Shan. Zircon U-Pb analyses of the basement  
45 176 rocks yielded ages of 770-890 Ma (Fu *et al.*, 2013).

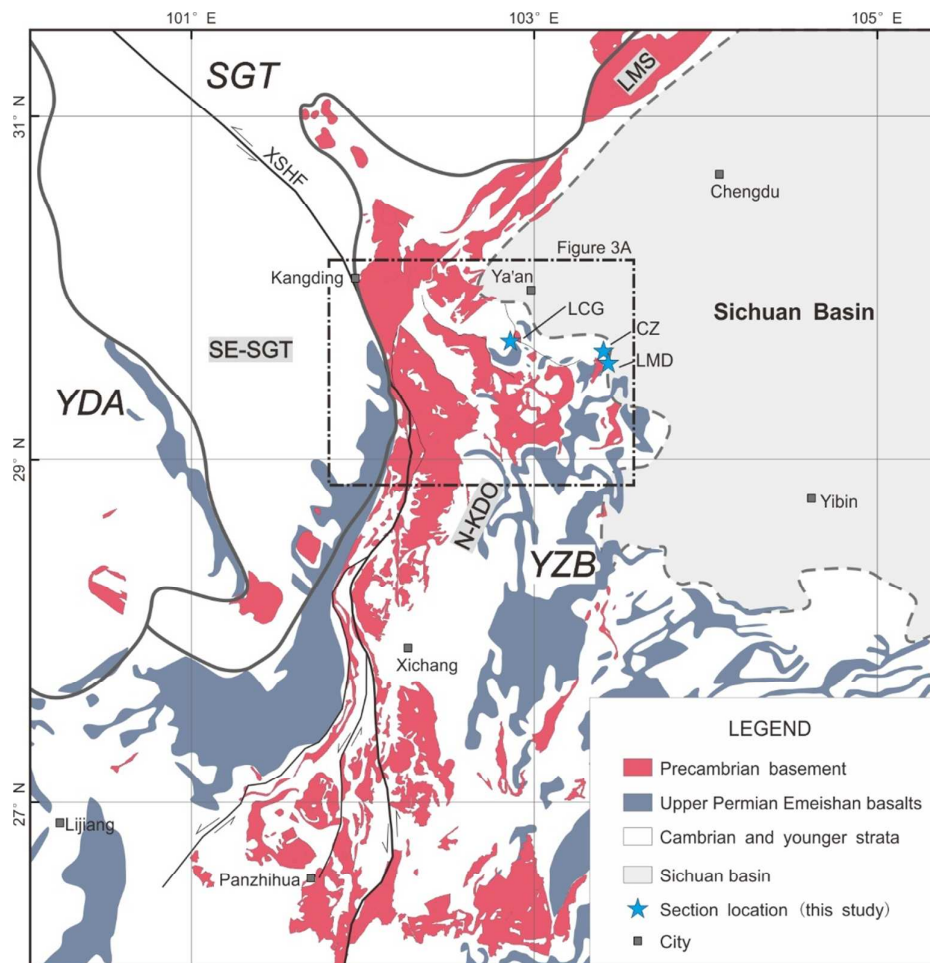
46 177 The Longmen Shan thrust belt experienced three phases of intra-continental orogenic shortening  
47 178 in the early Mesozoic and late Cenozoic (e.g., Burchfiel *et al.*, 1995; Yan *et al.*, 2011).  
48 179 Geochronological data suggests that the first phase of deformation had initiated before or at 237-190  
49 180 Ma (Huang *et al.*, 2003; Weller *et al.*, 2013): (i) the oldest U–Th–Pb monazite and Sm–Nd garnet ages  
50 181 (204-190 Ma), derived from metamorphosed rocks in the Danba Antiform, immediately south of the  
51 182 Longmen Shan, were interpreted as dating the timing of Barrovian metamorphism associated with the  
52 183 deformation (Huang *et al.*, 2003; Weller *et al.*, 2013). (ii) muscovite  $^{40}\text{Ar}/^{39}\text{Ar}$  dating of early Paleozoic  
53 184 schistose rocks from the northern Longmen Shan yielded ages between 237-208 Ma, which were  
54 185 interpreted as minimum age constraints for Mesozoic shortening (Yan *et al.*, 2011).

186 A recent structural and synkinematic mica  $^{40}\text{Ar}/^{39}\text{Ar}$  geochronological study by Tian *et al.* (2016)  
 187 suggest a late Cretaceous – early Paleogene phase of deformation, characterized by contemporaneous  
 188 hinterland-ward shearing and foreland-ward thrusting in the back and front sides of the Longmen Shan  
 189 thrust belt, respectively. In the late Cenozoic, pre-existing structures were reactivated by the eastward  
 190 growth of the Tibetan Plateau (e.g. Wang *et al.*, 2012; Tian *et al.*, 2013).

### 191 Songpan-Ganzi terrane

192 More than 80% of the Songpan-Ganzi terrane is covered by thick Triassic turbidites, which was  
 193 mainly sourced from the Qinling-Dabie orogen to the northeast and terranes to the north  
 194 (Enkelmann *et al.*, 2007; Ding *et al.*, 2013). By latest Triassic, the Songpan - Ganzi basin had  
 195 shallowed, as documented by coeval coal-bearing clastic deposits (BGMRS, 1991; Chang, 2000).  
 196 In response to the closure of the paleo-Tethys Ocean the flysch basin evolved into a fold belt (Xu  
 197 *et al.*, 1992; Roger *et al.*, 2011). Except for Pliocene - Quaternary glacial and fluvial sediments,  
 198 Jurassic – Cenozoic deposits, are regionally absent from the terrane (Figs. 1, 3).

199 The Songpan-Ganzi terrane was intruded by Upper Triassic–Jurassic granitoids (Roger *et al.*,  
 200 2011). Metamorphic grade varies across the Songpan-Ganzi terrane. In general, the metamorphic  
 201 overprint is relatively strong along the terrane margins where mudstones were metamorphosed to  
 202 phyllite, but weak within the interior (Chang, 2000).



203

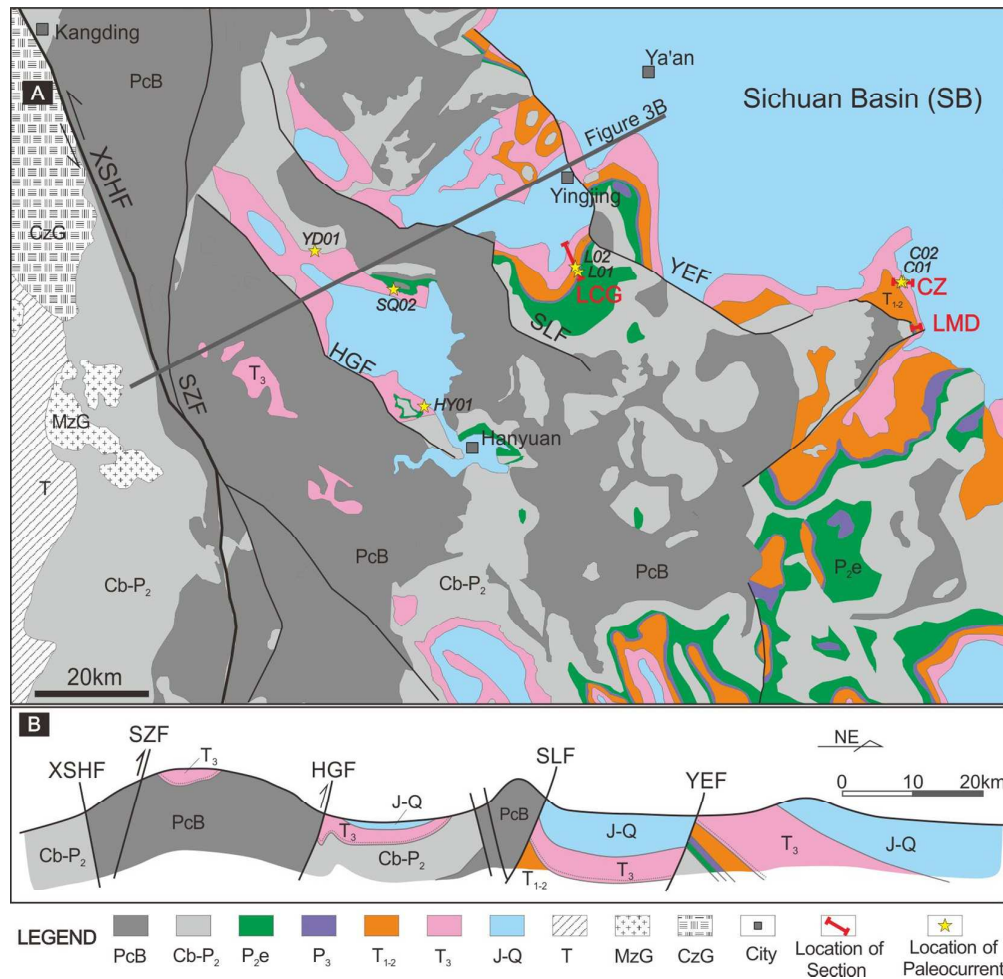
204 Fig. 2. Geological map of the western Yangtze Block. Modified from Wang & Pan, 2013.

59

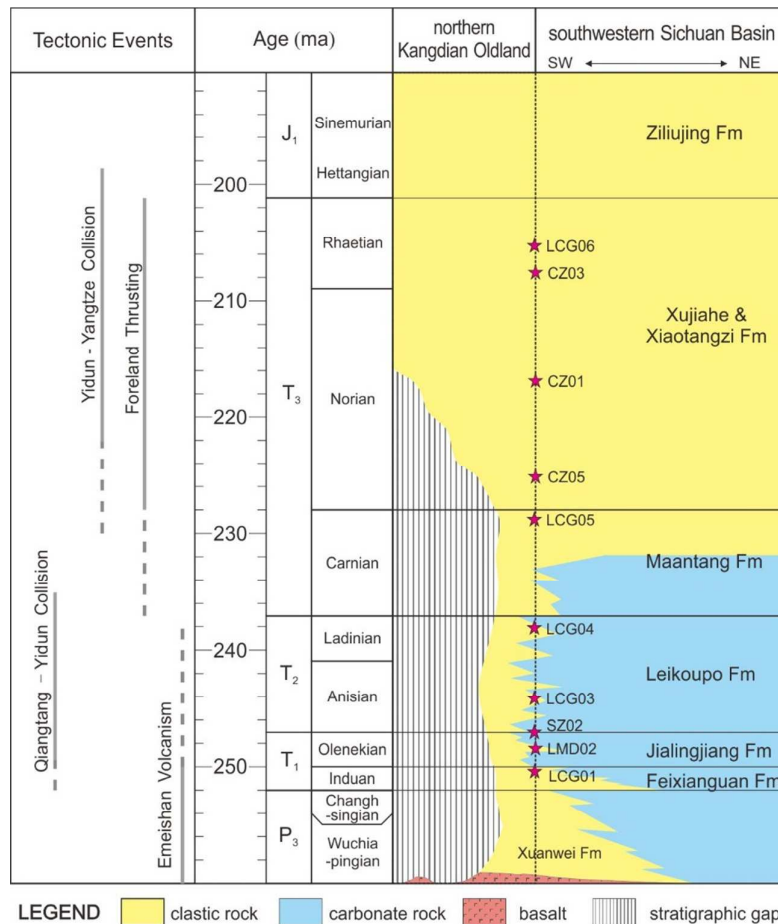
60



205 LMS—Longmen Shan thrust belt; N-DKO—Northern Kangdian Oldland; SE-SGT— southeastern  
 206 Songpan-Ganzi terrane; SGT—Songpan-Ganzi terrane; YZB—Yangtze Block; YDA—Yidun Arc. The  
 207 distribution of the Upper Permian Emeishan basalts is modified from [Xu et al., 2004](#).  
 208  
 209



210  
 211 **Fig. 3.** Geological sketch map of the study area (A) and structural profile of northern Kangdian  
 212 Oldland (B). The location of Fig.3A is shown in Fig. 2. PcB—Precambrian Basement;  
 213 Cb-P<sub>2</sub>—Cambrian- Middle Permian; P<sub>2e</sub>—Upper Permian Emeishan basalts; P<sub>2</sub> —Upper Permian  
 214 Xuanwei Formation; T<sub>1,2</sub>—Lower and Middle Triassic; T<sub>3</sub>—Upper Triassic; J-Q—Jurassic to  
 215 Quaternary; T—Triassic in southeastern Songpan-Ganzi terrane; CzG—Cenozoic Granite;  
 216 HGF—Hanyuan-Ganluo fault; MzG—Mesozoic Granite; SLF—Sanhe-Leibo fault;  
 217 SZF—Shimian-Zhaojue fault; XSHF—Xianshuihe fault; YEF—Yingjing-Emei fault. Red solid lines  
 218 and text makes the localities of the Longcanggou (LCG), Chuanzhu (CZ) and Longmendong (LMD)  
 219 sections, from which samples were collected. Fig. 3A is modified from BGSP (1974). Fig. 3B is  
 220 modified from [Chen et al., 2011](#).



221

222 **Fig. 4.** Stratigraphic nomenclature, age of the southern Sichuan Basin and northern Kangdian Oldland.  
 223 Tectonic events are after Hou *et al.* (2004), Reid *et al.* (2005), and Xu *et al.* (2008), Weislogel *et al.*  
 224 (2010), Wang *et al.* (2011). Time scale is from Gradstein *et al.* (2012). P<sub>3</sub>—the Late Permian; T<sub>1</sub>—the  
 225 Early Triassic; T<sub>2</sub>—the Middle Triassic; T<sub>3</sub>—the Late Triassic; J<sub>1</sub>—the Early Jurassic.

226

## 227 PREVIOUS DETRITAL ZIRCON STUDIES

228 Over the past decade, the provenance of the Upper Triassic clastic sediments in the Sichuan Basin  
 229 has been intensively studied, especially by detrital zircon geochronology (Fig. 1), but this has led to  
 230 conflicting conclusions. Deng *et al.* (2008) reported age spectra of four Upper Triassic sandstone  
 231 samples from the western Sichuan Basin and the eastern Songpan-Ganzi terrane, and suggested that the  
 232 Upper Triassic Xujiage Formation was sourced from the Songpan-Ganzi terrane and Longmen Shan  
 233 thrust belt. By contrast the study of Chen (2011) based in the northern and western parts of the Sichuan  
 234 Basin indicated that the Qinling orogen to the north was the main source of sediments. Recently work  
 235 by Luo *et al.* (2014), Zhang *et al.*, (2015) and Shao *et al.*, (2016), suggest that the Longmen Shan thrust  
 236 belt and the Songpan-Ganzi terrane in the west and the Qinling-Dabie orogen in the north sourced the  
 237 Upper Triassic sediments in the western and northern Sichuan Basin, respectively. Zhang *et al.* (2015)  
 238 and Shao *et al.* (2016) also indicated the minor role of the north Yangtze Block in supplying sediments  
 239 to the northern Sichuan Basin. Shao *et al.* (2016) suggested that sediments of the western, southern and



1  
2  
3 240 eastern parts of basin shared the same sources that include the southern North China Block and Qinling  
4 241 orogen, and the eastern Songpan-Ganzi terrane via the Longmen Shan thrust belt. Zhu *et al.* (2017)  
5 242 reported age spectra of four Middle-Upper Triassic sandstone samples from the southwestern Sichuan  
6 243 Basin, and suggested that Middle Triassic sediments mainly sourced from the Kangdian Oldland and  
7 244 Emeishan Large Igneous Province to the south, whereas Upper Triassic sediments mainly from the  
8 245 Songpan-Ganzi terrane and Yidun Arc to the west with a minor component from the Qinling orogen to  
9 246 the north and Jiangnan Xuefeng thrust belt (southeastern Yangtze Block) to the east. Importantly, all  
10 247 these previous studies focused on the Upper Triassic; little is known about the source of the Lower  
11 248 Triassic clastic rocks. One of the core aims of this study therefore, is to try and resolve the ongoing  
12 249 debate about the sources of the Triassic sediments.

## 17 250 **SAMPLING AND ANALYTICAL METHODS**

19 251 Ten samples were collected, including two samples from the Early Triassic Feixianguan ( $T_{1f}$ ) and  
20 252 Jialingjiang Formation ( $T_{1j}$ ), one volcanic tuff sample from the boundary between the Jialingjiang  
21 253 Formation ( $T_{1j}$ ) and Leikoupo ( $T_{2l}$ ), two samples from the Middle Triassic Leikoupo Formation ( $T_{2l}$ )  
22 254 and five samples from the Upper Triassic Xiaotangzi ( $T_{3xt}$ ) and Xujiuhe formations ( $T_{3x}$ ). These  
23 255 samples were collected from three sections, namely the Longmendong and Chuanzhu sections in the  
24 256 Emeishan area, and Longcanggou section in Yingjing area (Figs. 3, 5 and 6).

25 257 Where possible, more than 100 U/Pb ages were derived by LA-ICP-MS using the facilities at the  
26 258 London Geochronology Centre, University College London, which include a New Wave NWR193  
27 259 excimer laser ablation system and an Agilent 7700x quadrupole mass spectrometer. The laser was set to  
28 260 produce  $\sim 2.5$  J/cm<sup>2</sup> energy density at 8 Hz repetition rate for 25 seconds. The spot diameter was set to  
29 261 25  $\mu$ m for all analyses. Repeated measurements of internal U/Pb age standard Plešovice [TIMS  
30 262 reference age of  $337.13 \pm 0.37$  Ma (Sláma *et al.*, 2008)] and NIST-610 silicate glass (Jochum *et al.*,  
31 263 2011) were used to correct for instrumental mass bias and laser-pit-depth-dependent isotopic  
32 264 fractionation. GJ-1 (Jackson *et al.*, 2004) and 91500 zircon (Wiedenbeck *et al.*, 2004) were used as  
33 265 external standards. Data reduction was processed using the GLITTER software package (Griffin *et al.*,  
34 266 2008).

35 267 The paleocurrent data were determined in the field based on cross-bedding and ripples in  
36 268 sandstone beds. The orientations of trough cross laminations were measured using the method  
37 269 described by DeCelles *et al.* (1983).

## 44 270 **RESULTS**

### 47 271 **Stratigraphy and sedimentology**

49 272 Provided below is a brief description of the sedimentary features of each studied formation, which  
50 273 have been dated mostly by paleontology and locally by isotopic geochronology. Worth noting is that  
51 274 the Longmendong and Chuanzhu sections in the Emeishan have been intensively-studied by previous  
52 275 work (Wang & Ceng, 1982; Lin *et al.*, 1982; Zhao *et al.*, 1996).

1  
2  
3 276 *Lower Triassic (Feixianguan and Jialingjiang Formation)*

4  
5 277 The Lower Triassic strata studied here are from the Longcanggou and Longmendong sections  
6 278 (Figs. 5 and 6). The Feixianguan Formation (~130 m and ~180 m thick) conformably overlies the  
7 279 Upper Permian Xuanwei Formation. The Feixianguan Formation consists of purple sandstone, fine  
8 280 sandstone interbedded with conglomerate and sandy conglomerate. Sedimentary features include  
9 281 large-scale trough cross-bedding, tabular cross-bedding, parallel bedding and scour structures that  
10 282 collectively indicate fluvial facies (Fig. 6). The paleocurrent in the Feixianguan formation is eastward,  
11 283 as determined from cross-bedding in sandstone beds (Fig. 5).

12  
13 284 The Jialingjiang Formation (~110 m and ~240 m thick), consists of dolomites, limestones and  
14 285 mudstones interbedded with sandstones and conglomerates in the southwestern Sichuan Basin. This  
15 286 lithology is very different from the coeval carbonate deposits (dolomites and limestones) in the main  
16 287 part of Sichuan Basin. The formation can be divided into two parts: the lower part, composed of purple  
17 288 grey, greenish grey lithic sandstones and interbedded with limestones, the upper part, composed of  
18 289 dolomites and limestones (Fig. 6). Sedimentary features indicate upward retrogradation from fluvial to  
19 290 tidal flat facies (Lin *et al.*, 1982).

20  
21  
22  
23  
24 291 *Middle Triassic (Leikoupo Formation)*

25  
26 292 The Middle Triassic Leikoupo Formation is also from the Longcanggou and Longmendong  
27 293 sections. The formation (~50 m and ~460 m thick) conformably overlies altered tuff (Zhu & Wang,  
28 294 1986).

29  
30 295 The formation is composed of dolomites and limestones in the Longmendong section, but of  
31 296 dolomites interbedded with sandstones and mudstones in the Longcanggou section (Figs. 5, 6).  
32 297 Previous studies suggested that the Leikoupo Formation in the study area represents a tidal flat facies,  
33 298 influenced by input of terrigenous clastics (Zhao *et al.*, 1996; Tan *et al.*, 2014).

34  
35  
36  
37 299 *Upper Triassic (Maantang, Xiaotangzi and Xujiahe Formations)*

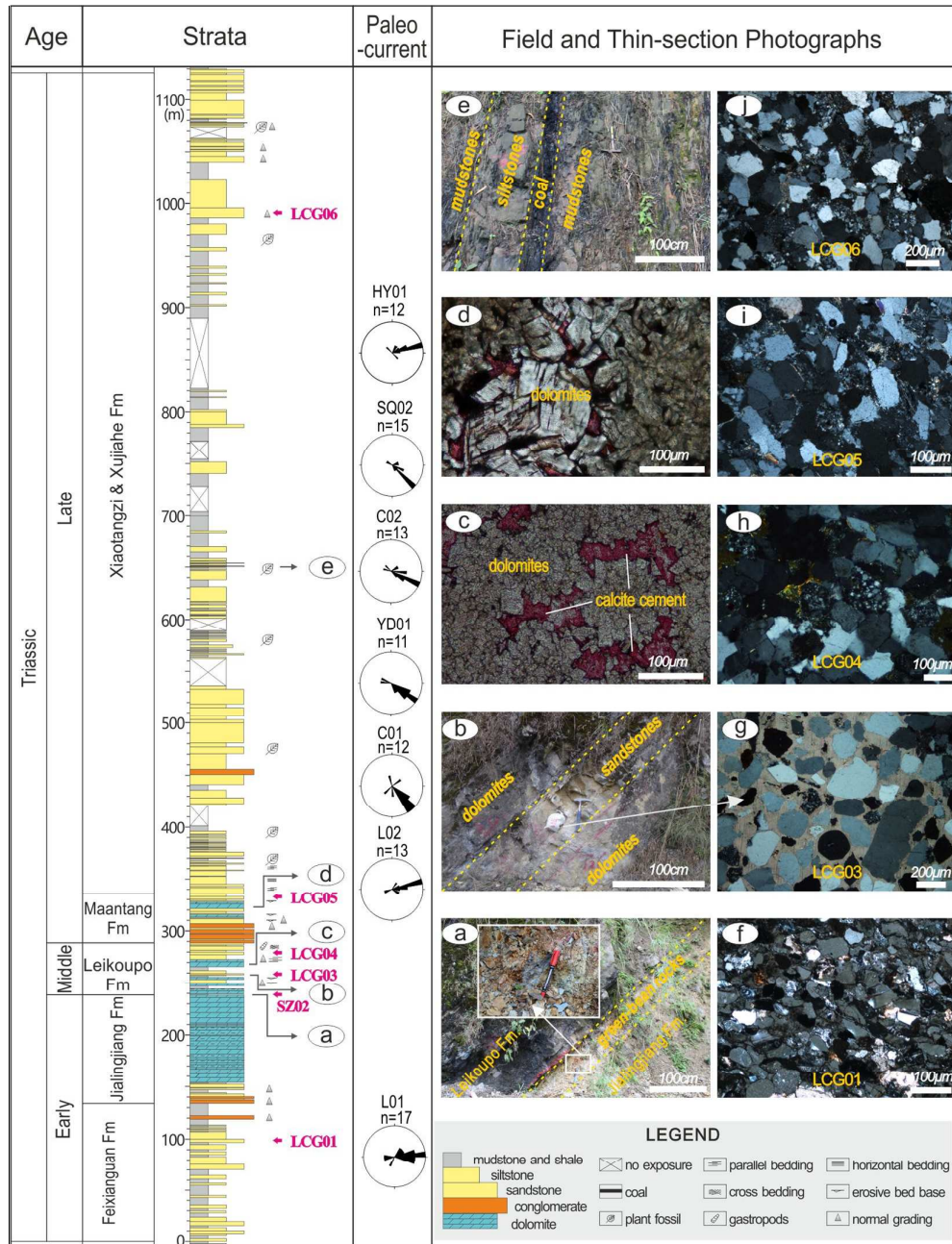
38  
39 300 The Upper Triassic strata includes the Maantang, Xiaotangzi and Xujiahe Formations, are studied  
40 301 here in the Longcanggou and Chuanzhu sections. In the Longcanggou section, the Mantang Formation  
41 302 is ~40 m thick and consists of conglomerates, sandstones, mudstones interbedded with dolomites (Fig.  
42 303 5, BGSP, 1974); while it is only ~26m thick in the Chuanzhu section and composed of grey black  
43 304 mudstone interbedded with argillaceous limestone (Fig. 6). The Maantang Formation has a parallel  
44 305 unconformable contact with the overlying strata and the underlying Leikoupo Formation (Li *et al.*,  
45 306 2014). There is much debate as to whether the sedimentary environment of the Maantang Formation in  
46 307 the Sichuan Basin represents a shallow shelf (Deng *et al.*, 1982), littoral (Zhao *et al.*, 1996), carbonate  
47 308 ramp (Xu *et al.*, 1996; Li *et al.*, 2014), reef, lagoon, tidal flat, or delta (Shi *et al.*, 2015).

48  
49 309 The Xiaotangzi and Xujiahe Formations are ~800 m and ~730 thick in the Longcanggou and  
50 310 Chuanzhu sections (Fig. 5) (WGCMSPISB, 1984). They mainly consist of grey sandstones, gray black  
51 311 siltstones, black mudstones and interbedded with coal. Previous studies suggested that the two  
52 312 formations were deposited in a shallow lacustrine and delta environment (Lin *et al.*, 2006a; Jiang *et al.*,  
53 313 2007; Li *et al.*, 2014).

54  
55  
56 314 The paleocurrent data, measured in the Longcanggou section (L02), Chuanzhu section (C01, C02)  
57 315 and Hanyuan area (YD01, SQ02, HY01) from cross-bedding and current ripples in sandstone strata,

316 indicates eastward and southeastward paleocurrent directions for the Xiaotangzi and Xujiache  
 317 Formations (Fig.3, Fig. 5).

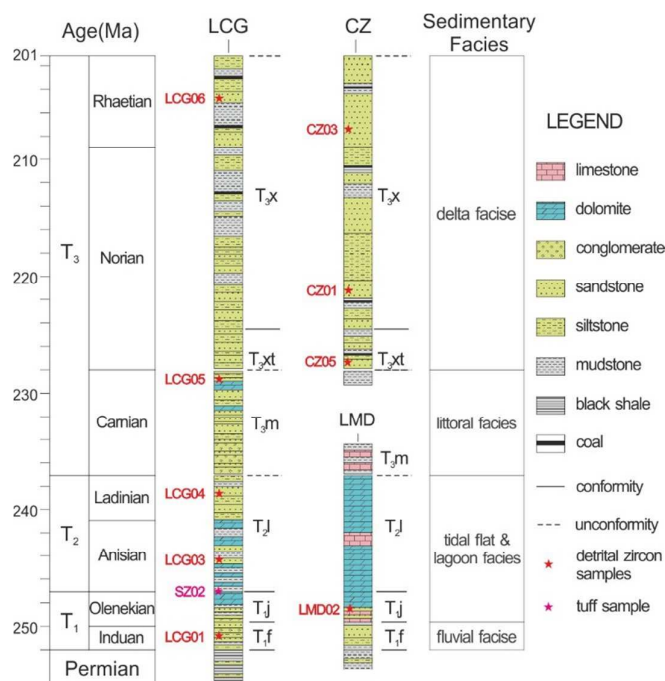
318  
 319



320

321 **Fig. 5.** Stratigraphy, rose diagrams of paleocurrent and thin-sections for the Triassic Longcanggou  
 322 section. The locations of paleocurrent measurements are shown in Fig. 3. (a) Boundary (the “ altered  
 323 tuff”) between the Lower Triassic Jialingjiang Formation and Middle Triassic Leikoupo Formation; (b)  
 324 Dolomites interbedded between sandstones (sample LCG03); (c) Thin-section photograph of dolomites  
 325 from the Leikoupo Formation; (d) Dolomites from the upper Mantang Formation; (e) Siltstones and  
 326 mudstones interbedded with coal from upper part of Xujiache Formation; (f, g, h, i, and j) Thin-sections

of sandstone from the LCG01, LCG03, LCG04, LCG05 and LCG06, collected from the Feixianguan (LCG01), Leikoupo (LCG03, LCG04), Mantang (LCG05) and Xujiuhe (LCG06) Formations.



330

331 **Fig. 6.** Triassic stratigraphy of the western Sichuan Basin. CZ (Chuanzhu) section is compiled from  
 332 (WGCMSPIB, 1984), LMD (Longmendong) section is compiled from (Lin *et al.*, 1982; Xu *et al.*,  
 333 1997; BGMRS, 1997), the sedimentary facies of Lower and Middle Triassic are after Zhao *et al.*,  
 334 1996; T<sub>1f</sub>— Feixianguan Formation; T<sub>1j</sub>—Jialingjiang Formation; T<sub>2l</sub>—Leikoupo Formation;  
 335 T<sub>3m</sub>—Mantang Formation; T<sub>3xt</sub>—Xiaotangzi Formation; T<sub>3x</sub>—Xujiuhe Formation; T<sub>1</sub>—the Early  
 336 Triassic; T<sub>2</sub>—the Middle Triassic; T<sub>3</sub>—the Late Triassic. Time scale is from the Gradstein *et al.* (2012).

337

### 338 Zircon U-Pb isotopic results

339 In total, 1132 detrital zircons from nine detrital samples analyzed in this study. The U–Pb data for  
 340 each sample are presented in [supplementary Table](#). Below, we discuss only ages that are concordant in  
 341 the range of +5% to -15%. The data are visualized as kernel density estimate (KDE, Vermeesch, 2012)  
 342 plots (Fig. 7).

### 343 Altered tuff

344 Sample SZ02 (102°51'42.92" E, 29°40'47.12"N) of the altered tuff was collected from the  
 345 boundary between the Leikoupo and Jialingjiang formations in the Longcanggou section. 30 of 34  
 346 analyses yielded concordant ages (in the range of +5% to -15%). The data are concordant within  
 347 analytical error and define a weighted mean <sup>206</sup>Pb/<sup>238</sup>Pb age of 246.5 ± 1.7 Ma (n=26) (Fig. 7), which is  
 348 similar to the previous studies in other sites of the Yangtze Block (Ovtcharova *et al.*, 2006; Xie *et al.*,  
 349 2013; Lehrmann *et al.*, 2015). The complete U–Pb isotopic data and calculated dates are presented in  
 350 [supplementary Table 1](#).



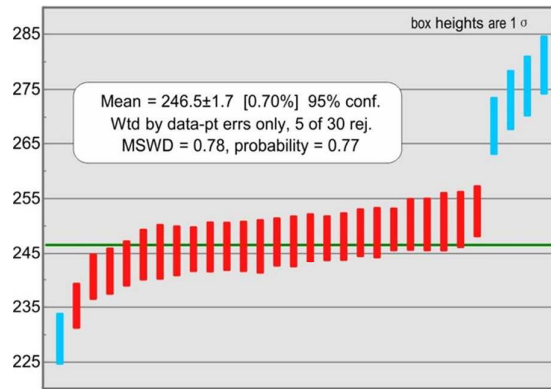


**Fig. 7.** U–Pb zircon ages of the altered tuff (sample SZ02 this study). Blue dates are rejected by ISOPLOT for calculating the weighted mean age.

351  
352  
353  
354

### 355 *Lower Triassic Feixianguan and Jialingjiang Formations*

356 Sample LCG01 (102°51'42.92" E, 29°40'47.12"N), a grey-green fine sandstone, was collected  
357 from the Feixianguan Formation in the Longcanggou section. 99 of 156 analyses yielded concordant  
358 ages (in the range of +5% to -15%), which exhibit a wide spectrum from ca. 243±3Ma to 2.4Ga, 92%  
359 of which are between 240 - 1050 Ma, the KDE plot of this sample shows a major peak at ~800Ma, and  
360 three minor peaks at ~248Ma, ~510Ma and ~950Ma (Fig. 8a).

361 Sample LMD02 (103°25'5.73" E, 29°34'46.76"N), a grey-purple coarse sandstone, was collected  
362 from the Jialingjiang Formation in Longmendong section. Among 129 analyses, 123 analyses yield  
363 concordant ages (in the range of +5% to -15%). Nearly all ages are between 730 - 880 Ma, showing a  
364 dominant peak at ~800 Ma in the KDE plot (Fig. 8b).

### 365 *Middle Triassic Leikoupo Formation*

366 Two samples (grey coarse sandstone), LCG03 (102°51'35.19" E, 29°40'51.35"N) and LCG04  
367 (102°51'35.05" E, 29°40'51.18"N), were collected from the Leikoupo Formation in Longcanggou  
368 section (Fig. 6). 136 out of 153 single zircon dates of the sample LCG03 are concordant. The ages  
369 exhibit a wide range from ca. 242±3Ma to 2.5Ga, with 74% lying between 730 Ma and 880 Ma,  
370 showing a dominant mode at ~800Ma (Fig. 8c), similar to the lower sample LMD02 from Jialingjiang  
371 Formation.

372 152 out of 157 single zircon dates of the sample LCG04 are concordant. The ages exhibit a wide  
373 range from ca. 233±3Ma to 3.0Ga; but most of them fall between 230 Ma to 1050 Ma (89%). The KDE  
374 plot of the sample shows a mode at ~800Ma, and three minor peaks at ~248Ma, ~510Ma and ~950Ma  
375 (Fig. 8d).

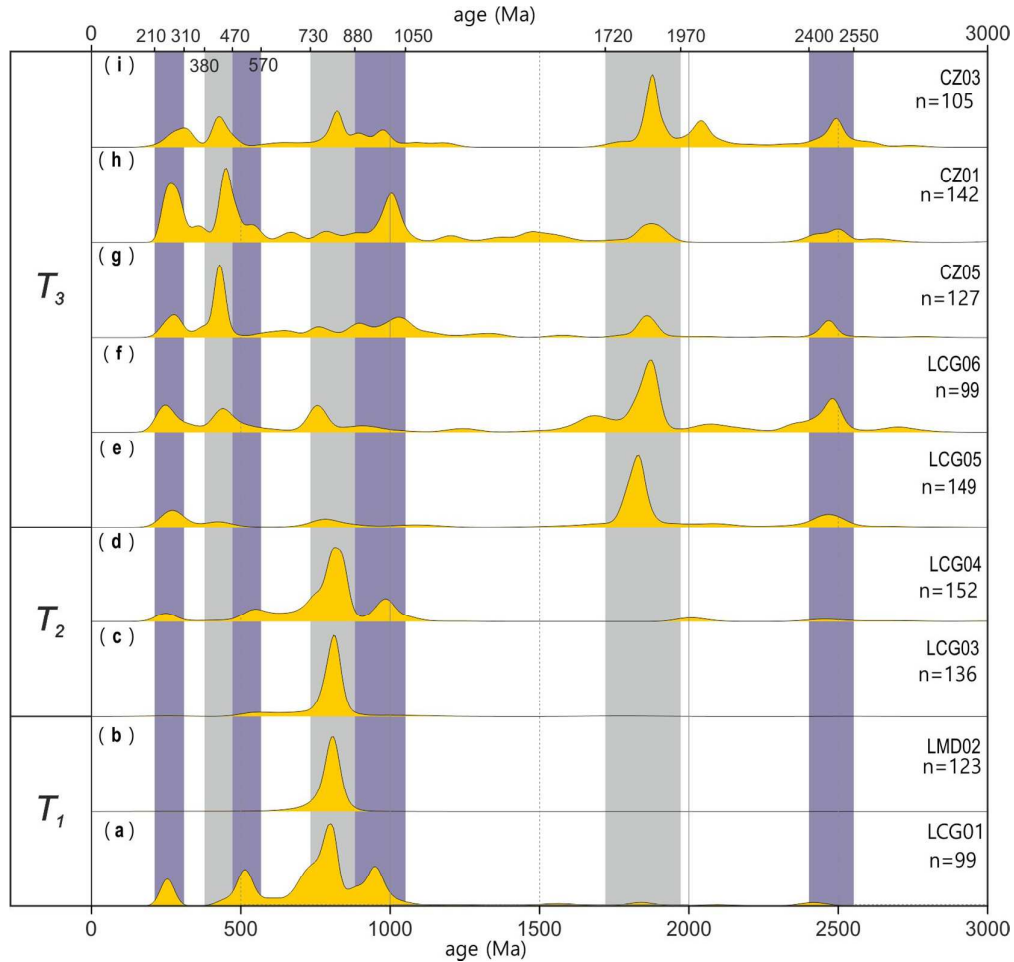
### 376 *Upper Triassic Maantang and Xujiache Formation*

377 Two samples (grey sandstone), LCG05 (102°51'34.05"E, 29°40'51.18"N) and LCG06  
378 (102°51'34.05"E, 29°40'51.18"N), were collected from the Maantang Formation and the upper part of  
379 Xujiache Formation in the Longcanggou section (Fig. 6). 149 of 154 single zircon dates of the sample



380 LCG05 are concordant. Most ages cluster at ~1800 Ma, with minor peaks at ~250 Ma, ~800 Ma and  
 381 ~2500 Ma (Fig. 8e). Their age spectra are significantly different from the lower ones (Fig. 8a-d). 99 of  
 382 110 single zircon dates of the upper Triassic sample LCG06 are concordant. The KDE plot shows five  
 383 peaks at ~246 Ma, ~440 Ma, ~758 Ma, ~1870 Ma and ~2480 Ma, respectively (Fig. 8f).

384 Three samples (grey sandstone), CZ05 (103°24'6"E, 29°37'23"N), CZ01 (103°24'22"E,  
 385 29°37'20"N), and CZ03 (103°24'43.2"E, 29°37'27"N), were collected from the upper part of the  
 386 Xujiahe Formation in the Chuanzhu section (Fig. 6). The KDE plots of these samples are similar,  
 387 showing peaks at ~276 Ma, ~429 Ma, ~1030 Ma, ~1860 Ma and ~2470 Ma (Fig. 8g-i).  
 388



389  
 390 **Fig. 8.** Kernel Density Estimation (KDE) plots of the detrital zircon U-Pb data for samples LCG01,  
 391 LMD02, LCG03, LCG04, LCG05, LCG06, CZ05, CZ01 and CZ03, respectively.  $T_1$ ,  $T_2$  and  $T_3$  are  
 392 Early, Middle and Late Triassic, respectively.  
 393

## 394 DISCUSSION

### 395 Detrital sources

#### 396 *Zircon spectra of potential sources*

397 As suggested by previous detrital zircon studies of the Sichuan Basin (Deng *et al.*, 2008;  
398 Weislogel *et al.*, 2010; Chen, 2011; Luo *et al.*, 2014; Zhang *et al.*, 2015; Shao *et al.*, 2016; Zhu *et al.*,  
399 2017), potential source terrains for the Triassic strata include southeastern Songpan-Ganzi terrane  
400 (SE-SGT), northern Kangdian Oldland (N-KDO), southern Kangdian Oldland (S-KDO), Longmen  
401 Shan thrust belt (LMS), Qinling orogen (QL), southeastern Yangtze Block (SE - YZB) (Figs. 9 and 10).  
402 We compiled zircon U-Pb ages of the crystalline and clastic rocks exposed in these potential source  
403 areas (Fig. 9). The detrital zircon U-Pb age spectrum of the southeastern Songpan-Ganzi terrane shows  
404 four major peaks at ~255Ma, ~435Ma, ~760Ma, ~1860Ma, and two minor peaks at ~1020Ma,  
405 ~2450Ma (Fig. 9f). The northern Kangdian Oldland is characterised by two major peaks at ~800Ma  
406 and ~930Ma, and a minor peak at ~260Ma (Fig. 9g); whereas the southern Kangdian Oldland is more  
407 complex, with peaks at ~810Ma, ~1840Ma, and three minor peaks at ~265Ma, ~2310Ma and ~2430Ma  
408 (Fig. 9h). The Longmen Shan thrust belt produces three major peaks at ~520Ma, ~760Ma and, ~945Ma  
409 (Fig. 9i). The Qinling orogen is characterised by three major peaks at ~440Ma, ~815Ma and ~1995Ma,  
410 and three minor peaks at ~260Ma, ~1830Ma and ~2465Ma (Fig. 9j). The southeastern Yangtze Block  
411 yields a dominant peak at ~815Ma (Fig. 9k).

#### 412 *Detrital sources of the Lower and Middle Triassic strata*

413 Detrital zircon age spectra of four Lower and Middle Triassic samples (LCG01, LCG03, LCG04,  
414 LMD02) is similar and characterized by a mode at ~810 Ma, with three minor peaks at ~255Ma,  
415 ~535Ma and ~970Ma (Fig. 8). To facilitate data interpretation, the ages are combined into a single  
416 KDE plot as Fig. 8a.

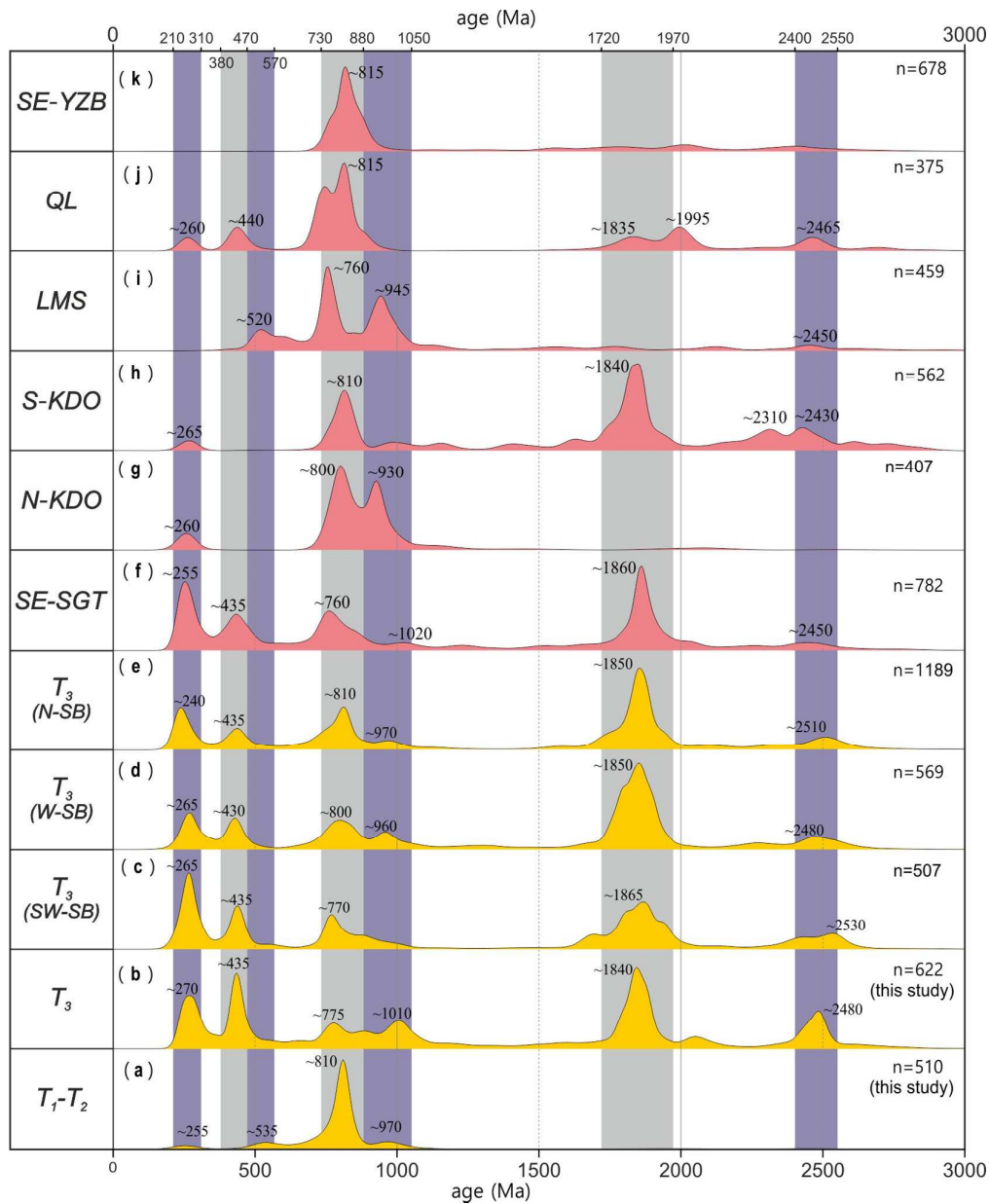
417 The KDE plots of the Lower - Middle Triassic samples are very similar to the northern Kangdian  
418 Oldland and the southeastern Yangtze Block (Figs. 9a, g, k). In addition, detrital zircon age spectra of  
419 Lower and Middle Triassic samples include a minor peak at ~535 Ma which only occurs in the  
420 Longmen Shan (Fig. 9a, i), indicating the Longmen Shan was possibly a source of sediments for the  
421 lower - middle Triassic deposits. Considering the eastward paleocurrent directions of these strata (Fig.  
422 5), we infer that the northern Kangdian Oldland was the main source of the Lower and Middle Triassic  
423 sandstones during the Lower to - Middle Triassic. However, we cannot rule out the southeastern  
424 Yangtze Block as a possible source. This explanation would require a long drainage system to deliver  
425 the sediments into the southwestern Sichuan Basin via the northern Kangdian Oldland, because the  
426 southeastern Yangtze Block and the southwestern Sichuan Basin is separated by deep waters, as  
427 indicated by coeval deposits composed mainly of carbonate, shale and mudstone, with a minor amount  
428 of siltstone (Hu *et al.*, 2010; Tan *et al.*, 2014; Sun *et al.*, 2015).

#### 429 *Detrital sources of the Upper Triassic*

430 In contrast to the Lower - Middle Triassic samples, detrital zircons from the Upper Triassic

1  
2  
3 431 samples (LCG05, LCG06, CZ05, CZ01, CZ03), which exhibit southeastward paleocurrent directions  
4 432 (Fig. 5), are characterized by multiple age peaks at ~270 Ma, ~435 Ma, ~775Ma and ~1010 Ma,  
5 433 ~1840Ma and 2480 Ma (Fig. 9b). Detrital zircon data of the coeval sediments in the southwestern,  
6 434 western and northern Sichuan Basin, as reported in previous studies, yield similar age spectra (Figs. 9c,  
7 435 d, e), indicating that they may have the same or similar sources, including the Qinling orogen,  
8 436 Longmen Shan thrust belt, and eastern Songpan-Ganzi terrane (Chen, 2011; Luo *et al.*, 2014; Zhang *et*  
9 437 *al.*, 2015; Shao *et al.*, 2016).

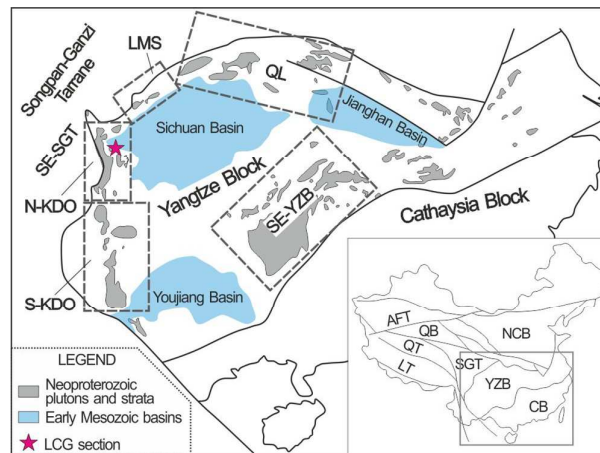
10  
11 438 Similar age spectra are shown by the Triassic turbidites of the southeastern Songpan-Ganzi terrane,  
12 439 which may have experienced marine deposition (Weislogel *et al.*, 2010; Ding *et al.*, 2013; Zhang,  
13 440 2014), and share the similar sources as the Sichuan Basin. Alternatively, the eastern Songpan-Ganzi  
14 441 terrane may have experienced a phase of shortening in response to the Upper Triassic intracontinental  
15 442 orogeny along the Longmen Shan thrust belt (Li *et al.*, 2003a; Yan *et al.*, 2011; Zheng *et al.*, 2016).  
16 443 From this perspective, it is speculated that the eastern Songpan-Ganzi terrane might also be a source  
17 444 region for the Upper Triassic detritus of the Sichuan Basin.  
18  
19  
20  
21  
22  
23  
24  
25  
26  
27  
28  
29  
30  
31  
32  
33  
34  
35  
36  
37  
38  
39  
40  
41  
42  
43  
44  
45  
46  
47  
48  
49  
50  
51  
52  
53  
54  
55  
56  
57  
58  
59  
60



446

447 **Fig. 9.** KDE plots for the detrital zircon ages of the Triassic sediments of the Sichuan Basin and  
 448 potential source areas. (a-b) Age spectra of the Lower-Middle and Upper Triassic sediments in the  
 449 southwestern Sichuan Basin. (c-e) Spectra of the Upper Triassic sediments in the southwestern, western  
 450 and northern Sichuan Basin, reported in previous studies (Deng *et al.*, 2008; Weislogel *et al.*, 2010;  
 451 Chen, 2011; Luo *et al.*, 2014; Zhang *et al.*, 2015; Shao *et al.*, 2016; Zhu *et al.*, 2017). Spectra of  
 452 potential areas, including (f) SE-SGT (southeastern Songpan-Ganzi terrane), compiled from  
 453 sedimentary rocks (Weislogel *et al.*, 2010; Ding *et al.*, 2013; Zhang, 2014), (g) N-KDO (northern  
 454 Kangdian Oldland), compiled from both crystalline (Roger & Calassou, 1997; Guo *et al.*, 1998; Shen  
 455 *et al.*, 2000; Li *et al.*, 2001; Li *et al.*, 2002; Zhou *et al.*, 2002b; Shen *et al.*, 2003; Li *et al.*, 2003b; Zhou  
 456 *et al.*, 2006a; Lin *et al.*, 2006b; Yan *et al.*, 2006; Zhao *et al.*, 2006; Geng *et al.*, 2007; Huang *et al.*, 2009;  
 457 Lin, 2010; Ruan, 2013; Meng *et al.*, 2015) and sedimentary rocks (Zhou *et al.*, 2006a; He *et al.*, 2007;  
 458 Sun *et al.*, 2009), (h) S-KDO (southern Kangdian Oldland), compiled from sedimentary rocks (He *et*

1  
2  
3 459 *al.*, 2007; Wang *et al.*, 2012), (i) LMS (Longmen Shan thrust belt), compiled from both crystalline  
4 460 (Zhou *et al.*, 2006b; Meng *et al.*, 2015) and sedimentary rocks (Duan *et al.*, 2011; Chen *et al.*, 2016), (j)  
5 461 QL (Qinling orogen), compiled from both crystalline and (Li *et al.*, 2016) and sedimentary rocks (He  
6 462 *et al.*, 2007; Wang *et al.*, 2013a), (k) SE-YZB (southeastern Yangtze Block), compiled from sedimentary  
7 463 rocks (Wang *et al.*, 2010; Wang & Zhou, 2012).  
8  
9 464



10  
11  
12  
13  
14  
15  
16  
17  
18  
19  
20  
21  
22  
23  
24  
25 465  
26 466 **Fig. 10.** Map of potential source areas for sediments of the Sichuan Basin, modified after (Li *et al.*,  
27 467 2003b; Sun *et al.*, 2009). ATF—Altyn Tagh fault; CB—Cathaysia Block; LMS—Longmen Shan thrust  
28 468 belt; LT—Lhasa terrane; NCB—north China Block; YZB—Yangtze Block; N-KDO—Northern  
29 469 Kangdian Oldland; QB—Qaidam basin; QL—Qinling orogen; QT—Qiangtang terrane;  
30 470 SE-YZB—southeastern Yangtze Block; S-KDO—southern Kangdian Oldland; SE-SGT—southeastern  
31 471 Songpan-Ganzi terrane.  
32  
33  
34  
35

### 36 473 Palaeographic and tectonic implications

37  
38 474 The Upper Triassic change in detrital zircon age spectrum probably resulted from the impacts of  
39 475 tectonic transition from a passive continental margin to a foreland basin in response to the  
40 476 intra-continental shortening in the upper Yangtze Block.

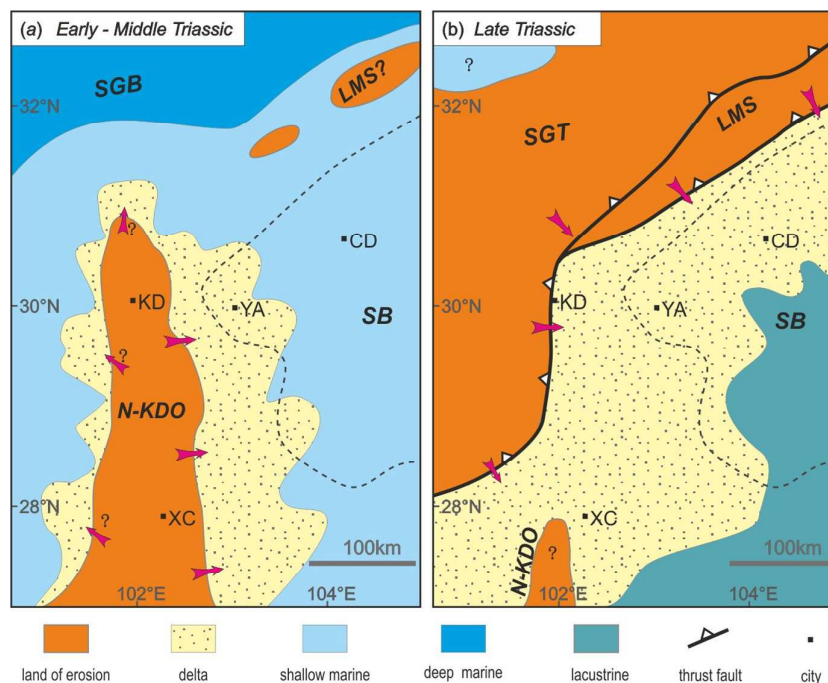
41  
42 477 Lower - Middle Triassic detritus mainly sourced from the northern Kangdian Oldland, as shown  
43 478 by the detrital zircon age and paleocurrent data (Fig. 11a). The uplift and erosion of the northern  
44 479 Kangdian Oldland is a response to the dynamic topography of the eruption of the Emeishan large  
45 480 igneous province, constrained to ~260 Ma by Ar-Ar and zircon U-Pb data (Ali *et al.*, 2002; Zheng *et al.*,  
46 481 2010; Huang *et al.*, 2016). Erosion of the northern Kangdian Oldland might trace back to the latest  
47 482 Permian, as indicated by the Emeishan basalt detritus in the Permian Xuanwei Formation (Xu *et al.*,  
48 483 2004; He *et al.*, 2007; He *et al.*, 2010; Luo *et al.*, 2012).

49  
50 484 Upper Triassic sediments in the Sichuan Basin was mainly sourced from the coeval orogens and  
51 485 fold-and-thrust belts surrounding the basin, as suggested by previous studies (Fig. 11b) (Deng *et al.*,  
52 486 2008; Chen, 2011; Luo *et al.*, 2014; Zhang *et al.*, 2015; Shao *et al.*, 2016; Zhu *et al.*, 2017). The eastern  
53 487 Songpan-Ganzi terrane might also have been significantly shortened and unroofed, providing detritus  
54 488 for the western and southern Sichuan Basin. This inference is supported by the similar age spectra  
55 489 between the terrane and the basin sediments. The Late Triassic shortening of the Songpan-Ganzi  
56 490 turbidites might relate to several factors, (1) westward subduction of the Ganzi-Litang Ocean during



the Late Triassic (Hou *et al.*, 2004), (2) collision between Yidun arc and the Songpan-Ganzi terrane at the end of the Triassic (Hou *et al.*, 2004; Wang *et al.*, 2013b), and (3) intra-continental shortening between the eastern Songpan-Ganzi terrane and the Sichuan Basin, forming the Longmen Shan thrust belt (e.g., Li *et al.*, 2003a).

Late Triassic crustal shorting in the Longmen Shan thrust belt and adjacent regions has been intensively studied. First, the presence of klippen of Paleozoic and Precambrian rocks over Triassic sediments in the Longmen Shan thrust belt front indicate that these structures were formed during the Late Triassic or later. Second, the oldest U–Th–Pb monazite and Sm–Nd garnet ages (204–190 Ma), derived from metamorphosed rocks in the Danba Antiform, immediately south of the Longmen Shan thrust belt, were interpreted as dating the timing of Barrovian metamorphism associated with the deformation (Huang *et al.*, 2003; Weller *et al.*, 2013). Third, muscovite  $^{40}\text{Ar}/^{39}\text{Ar}$  dating of early Paleozoic schist from the northern Longmen Shan thrust belt and Neoproterozoic Pengguan complex from the middle Longmen Shan thrust belt yielded ages between 237–208 Ma and 235–226 Ma, respectively, which were interpreted as minimum age constraints for Mesozoic crustal shortening (Yan *et al.*, 2011; Zheng *et al.*, 2016).



506

507

**Fig. 11.** A schematic map showing the different source areas and directions for the Triassic sediments of the southwestern Sichuan Basin. (a) Detritus was shed into the southwestern Sichuan Basin from the northern Kangdian Oldland to the southwest during Lower – Middle Triassic time. (b) The Longmen Shan thrust belt and possibly the eastern Songpan-Ganzi terrane to the west provided the bulk of clastic sediment flux to the southwestern Sichuan Basin during late Triassic time. CD — Chengdu, SGT — Songpan-Ganzi terrane, KD — Kangding, LMS — Longmen Shan thrust belt, N-KDO — northern Kangdian Oldland, SGB — Songpan-Ganzi basin, SB — Sichuan Basin, XC — Xichang, YA — Ya'an.

515

## 516 CONCLUSIONS

517 Triassic sediments in the southwestern Sichuan Basin record different detrital zircon  
518 geochronology signals. Detrital zircon age spectra of Lower and Middle Triassic samples are similar  
519 and characterized by a dominant age mode at ~810 Ma, with three minor peaks at ~255Ma, ~535Ma  
520 and ~970Ma. In contrast to the Lower - Middle Triassic samples, detrital zircon spectra of Upper  
521 Triassic samples are characterized by multiple age peaks at ~270 Ma, ~435 Ma, ~775Ma and ~1010  
522 Ma, ~1840Ma and ~2480 Ma.

523 Our data reveal a major change of provenance during the Upper Triassic in response to multiple  
524 tectonic events. The uplift and erosion of the northern Kangdian Oldland, triggered by the eruption of  
525 the Emeishan Plume, provided the main detritus for the southwestern Sichuan Basin during the Lower  
526 – Middle Triassic. During the Upper Triassic, the Sichuan Basin was inverted into a foreland basin and  
527 the Longmen Shan thrust belt and possibly the eastern Songpan-Ganzi terrane was uplifted in response  
528 to the closure of the Paleo-Tethys Ocean and intra-continental shortening along the Longmen Shan  
529 thrust belt, becoming the main source areas of the southwestern and western Sichuan Basin. This study  
530 highlights the importance of tectonic events in reorganizing drainage and sediment supply in foreland  
531 basins.

## 532 ACKNOWLEDGEMENTS

533 We thank Yan Liang, Yun Kun, Chen Bin, Wang Weiming, Lu Yanqi and Zhou Qiwei for their  
534 help in the field. This work benefited from discussions with Profs. Hu Xiumian and Dr. Dong Shunli.  
535 Funding for this research was provided by Chinese 1000 Young Talents Program, National Natural  
536 Science Foundation of China (Grant No. 41772211, 41502116, 41372114 and 41340005) and the  
537 National Key Laboratory of Oil and Gas Reservoir Geology and Exploitation (Grant No. PLC201604).

## 538 REFERENCES

- 539 ALI, J.R., FITTON, J.G. & HERZBERG, C. (2010) Emeishan large igneous province (SW China) and the  
540 mantle-plume up-doming hypothesis. *Journal of the Geological Society*, **167**, 953-959.
- 541 ALI, J.R., THOMPSON, G.M., SONG, X. & WANG, Y. (2002) Emeishan Basalts (SW China) and the  
542 'end-Guadalupian' crisis: magnetobiostratigraphic constraints. *Journal of the Geological Society*,  
543 **159**, 21-29.
- 544 BGMRSP (Bureau of Geology and Mineral Resources, Sichuan Province), 1991. Regional Geology of  
545 Sichuan Province. Geological Publishing House, Beijing, in Chinese.
- 546 BGMRSP (Bureau of Geology and Mineral Resources, Sichuan Province), 1997. Multiple stratigraphic  
547 division research in China: lithostratigraphy in Sichuan Province. China University of  
548 Geosciences Press, Wuhan, 1-417 pp, in Chinese.
- 549 BGSP (Bureau of Geology, Sichuan Province), 1974. Bureau of Geology and Mineral Resources of  
550 Sichuan Province. Regional Geological Report of Yingjing Sheet (1:200000). Geological  
551 Publishing House, Beijing, 1-143 pp, in Chinese.
- 552 BURCHFIEL, B.C., CHEN, Z., LIU, Y. & ROYDEN, L.H. (1995) Tectonics of the Longmen Shan and  
553 adjacent regions, central China. *International Geology Review*, **37**, 661-735.
- 554 BUREAU OF GEOLOGY AND MINERAL RESOURCES, S.P.B. (1997). *Multiple stratigraphic division*  
555 *research in China: lithostratigraphy in Sichuan Province*. China University of Geosciences  
556 Press, Wuhan.
- 557 BURGESS, S.D., BOWRING, S.A. & SHEN, S. (2014) High-precision timeline for Earth' s most severe  
558 extinction. *Proceedings of the National Academy of Sciences of the United States of America*, **111**,  
559 3316-3321.
- 560 CHANG, E.Z. (2000) Geology and Tectonics of the Songpan-Ganzi Fold Belt, Southwestern China.
- 561 CHEN, H., HU, J., QU, H. & WU, G. (2011) Early Mesozoic structural deformation in the Chuandian N-S

- 1  
2  
3 562 Tectonic Belt, China. *Sci China Earth Sci*, **41**, 1281-1294.
- 4 563 CHEN, Q., SUN, M., LONG, X., ZHAO, G. & YUAN, C. (2016) U - Pb ages and Hf isotopic record of  
5 564 zircons from the late Neoproterozoic and Silurian - Devonian sedimentary rocks of the western  
6 565 Yangtze Block: Implications for its tectonic evolution and continental affinity. *Gondwana*  
7 566 *Research*.
- 8 567 CHEN, Y. (2011) The Formation of Wesatern Sichuan Foreland Basin and Its Significance in Oil-gas  
9 568 Exploration During Late Triassic, Chengdu University of Technology, Chengdu.
- 10 569 DAI, S., REN, D., CHOU, C., FINKELMAN, R.B., SEREDIN, V.V. & ZHOU, Y. (2012) Geochemistry of  
11 570 trace elements in Chinese coals: A review of abundances, genetic types, impacts on human health,  
12 571 and industrial utilization. *International Journal of Coal Geology*, **94**, 3-21.
- 13 572 DECELLES, P.G., LANGFORD, R.P. & SCHWARTZ R. K. (1983) Two new methods of paleocurrent  
14 573 determination from trough cross-stratification. *Journal of Sedimentary Research*, **53**: 629-642
- 15 574 DENG, F., JIA, D., LUO, L., LI, H., LI, Y. & WU, L. (2008) The contrast between provenances of  
16 575 Songpan-Ganze and Western Sichuan foreland basin in the Late Triassic: clues to the tectonics  
17 576 and palaeogeography. *Geological Review*, **54**, 561-573.
- 18 577 DENG, K., HE, L., QIN, D. & HE, Z. (1982) The earlier Late Triassic sequence and its sedimentary  
19 578 environment in western Sichuan Basin. *Oil & Gas Geology*, **3**, 204-210.
- 20 579 DING, L., YANG, D., CAI, F.L., PULLEN, A., KAPP, P., GEHRELS, G.E., ZHANG, L.Y., ZHANG, Q.H., LAI,  
21 580 Q.Z., YUE, Y.H. & SHI, R.D. (2013) Provenance analysis of the Mesozoic  
22 581 Hoh-Xil-Songpan-Ganzi turbidites in northern Tibet: Implications for the tectonic evolution of the  
23 582 eastern Paleo-Tethys Ocean. *Tectonics*, **32**, 34-48.
- 24 583 DUAN, L., MENG, Q., ZHANG, C. & LIU, X. (2011) Tracing the position of the South China block in  
25 584 Gondwana: U - Pb ages and Hf isotopes of Devonian detrital zircons. *Gondwana Research*, **19**,  
26 585 141-149.
- 27 586 ENKELMANN, E., WEISLOGEL, A., RATSCHBACHER, L., EIDE, E., RENNO, A. & WOODEN, J. (2007) How  
28 587 was the Triassic Songpan-Ganzi basin filled? A provenance study. *Tectonics*, **26**, n/a-n/a.
- 29 588 FENG, Z., BAO, Z. & LI, S. (1997) Potential of oil and gas of the Middle and Lower Triassic of south  
30 589 China from the viewpoint of lithofacies paleogeography. *Journal of the University of Petroleum* ,  
31 590 *China*, **21**, 1-6.
- 32 591 FENG, Z., JIN, Z., HE, Y., BAO, Z. & XIN, W. (1994) *Lithofacies paleogeography of Permian of*  
33 592 *Yunnan-Guizhou-Guangxi Region*. Geological Publishing House, Beijing.
- 34 593 FU, B., KITA, N.T., WILDE, S.A., LIU, X., CLIFF, J. & GREIG, A. (2013) Origin of the  
35 594 Tongbai-Dabie-Sulu Neoproterozoic low-  $\delta$  18O igneous province, east-central China.  
36 595 *Contributions to Mineralogy and Petrology*, **165**, 641-662.
- 37 596 GENG, Y., YANG, C., WANG, X. & LIUDONG, R. (2007) Age of Crystalline Basement in Western  
38 597 Margin of Yangtze Terrane. *Geological Journal of China Universities*, **13**, 429-441.
- 39 598 GRADSTEIN, F.M., OGG, J.G., SCHMITZ, M. & OGG, G. (2012) The Geologic Time Scale 2012  
40 599 2-Volume Set.
- 41 600 GRIFFIN, W.L., POWELL, W.J., PEARSON, N.J., O'REILLY, S.Y. & A, E.M. (2008) GLITTER: data  
42 601 reduction software for laser ablation ICP-MS. In: *Laser Ablation-ICP-MS in the earth sciences*  
43 602 (Ed. by P. S. ED.), **40**, 204-207. Mineralogical association of Canada short course series.
- 44 603 GUO, J., YOU, Z., YANG, J., SHEN, W., XU, S. & WANG, R. (1998) Studying on the U-Pb dating of  
45 604 zircon in Tianwan and Pianlugang bodies from Shimian area, west Sichuan. *Journal of*  
46 605 *Mineralogy and Petrology*, **18**, 92-95.
- 47 606 HE, B., XU, Y., GUAN, J. & ZHONG, Y. (2010) Paleokarst on the top of the Maokou Formation: Further  
48 607 evidence for domal crustal uplift prior to the Emeishan flood volcanism. *Lithos*, **119**, 1-9.
- 49 608 HE, B., XU, Y., HUANG, X., LUO, Z., SHI, Y., YANG, Q. & YU, S. (2007) Age and duration of the  
50 609 Emeishan flood volcanism, SW China: Geochemistry and SHRIMP zircon U - Pb dating of silicic  
51 610 ignimbrites, post-volcanic Xuanwei Formation and clay tuff at the Chaotian section. *Earth and*  
52 611 *Planetary Science Letters*, **255**, 306-323.
- 53 612 HE, B., XU, Y., XIAO, L. & WANG, Y. (2003) Does the Panzhihua-Xichang Rift Exist? *地质论评*, **49**,  
54 613 572-582.
- 55 614 HOU, Z., YANG, Y., QU, X., HUANG, D., LU, Q., WANG, H., YU, J. & TANG, S. (2004) Tectonic  
56 615 evolution and mineralization systems of the Yidun Arc orogen in Sanjiang region, China. *Acta*  
57 616 *Geologica Sinica*, **78**, 109-120.
- 58 617 HU, M., WEI, G., LI, S., YANG, W., ZHU, L. & YANG, Y. (2010) Characteristics of Sequence-based  
59 618 Lithofacies and Paleogeography, and Reservoir Prediction of the Jialingjiang Formation in  
60 619 Sichuan Basin. *Acta Sedimentologica Sinica*, **28**, 1145-1152.
- 60 620 HUANG, H., CAWOOD, P.A., HOU, M., YANG, J., NI, S., DU, Y., YAN, Z. & WANG, J. (2016) Silicic ash

- 1  
2  
3 621 beds bracket Emeishan Large Igneous province to <1m.y. at ~260Ma. *Lithos*, **264**, 17-27.
- 4 622 HUANG, M., BUICK, I.S. & HOU, L.W. (2003) Tectonometamorphic Evolution of the Eastern Tibet  
5 623 Plateau: Evidence from the Central Songpan - Garzê Orogenic Belt, Western China. *Journal of*  
6 624 *Petrology*, **44**, 255-278.
- 7 625 HUANG, S., HUANG, K., ZHONG, Y., LI, X., MAO, X., HU, Z., LIU, S., ZHANG, M. & WU, W. (2017)  
8 626 Carbon isotope composition and comparison of Lower Triassic marine carbonate rocks from  
9 627 Southern Longmenxia section in Guang'an, Sichuan Basin. *Science China Earth Sciences*, 57-71.
- 10 628 HUANG, X., XU, Y., LAN, J., YANG, Q. & LUO, Z. (2009) Neoproterozoic adakitic rocks from  
11 629 Mopanshan in the western Yangtze Craton: Partial melts of a thickened lower crust. *Lithos*, **112**,  
12 630 367-381.
- 13 631 JACKSON, S.E., PEARSON, N.J., GRIFFIN, W.L. & BELOUSOVA, E.A. (2004) The application of laser  
14 632 ablation-inductively coupled plasma-mass spectrometry to in situ U - Pb zircon geochronology.  
15 633 *Chemical Geology*, **211**, 47-69.
- 16 634 JIA, D., WEI, G., CHEN, Z., LI, B., ZENG, Q. & YANG, G. (2006) Longmen Shan fold-thrust belt and its  
17 635 relation to the western Sichuan Basin in central China: New insights from hydrocarbon  
18 636 exploration. *Bulletin*, **90**, 1425-1447.
- 19 637 JIANG, Z., TIAN, J., CHEN, G., LI, X. & ZHANG, M. (2007) Sedimentary characteristics of the Upper  
20 638 Triassic in western Sichuan foreland basin. *JOURNAL OF PALAEOGEOGRAPHY*, **9**, 143-154.
- 21 639 JOCHUM, K.P., WEIS, U., STOLL, B., KUZMIN, D., YANG, Q., RACZEK, I., JACOB, D.E., STRACKE, A.,  
22 640 BIRBAUM, K., FRICK, D.A., GÜNTHER, D. & ENZWEILER, J. (2011) Determination of Reference  
23 641 Values for NIST SRM 610-617 Glasses Following ISO Guidelines. *Geostandards and*  
24 642 *Geoanalytical Research*, **35**, 397-429.
- 25 643 LEHRMANN, D.J., STEPCHINSKI, L., ALTINER, D., ORCHARD, M.J., MONTGOMERY, P., ENOS, P.,  
26 644 ELLWOOD, B.B., BOWRING, S.A., RAMEZANI, J. & WANG, H. (2015) An integrated biostratigraphy  
27 645 (conodonts and foraminifers) and chronostratigraphy (paleomagnetic reversals, magnetic  
28 646 susceptibility, elemental chemistry, carbon isotopes and geochronology) for the Permian - Upper  
29 647 Triassic strata of Guandao section, Nanpanjiang Basin, south China. *Journal of Asian Earth*  
30 648 *Sciences*, **108**, 117-135.
- 31 649 LI, C. (1963) A preliminary study of the tectonic development of the "Kang-Dian Axis". *Acta*  
32 650 *Geologica Sinica*, **43**, 214-229.
- 33 651 LI, X., LI, Z., ZHOU, H., LIU, Y. & KINNY, P.D. (2002) U - Pb zircon geochronology, geochemistry and  
34 652 Nd isotopic study of Neoproterozoic bimodal volcanic rocks in the Kangdian Rift of South China:  
35 653 implications for the initial rifting of Rodinia. *Precambrian Research*, **113**, 135-154.
- 36 654 LI, X., ZHOU, H., LI, Z., LIU, Y. & P., K. (2001) Zircon U-Pb age and petrochemical characteristics of  
37 655 the Neoproterozoic bimodal volcanics from western Yangtze block. *Geochimica*, **30**, 315-322.
- 38 656 LI, Y., ALLEN, P.A., DENSMORE, A.L. & QIANG, X. (2003a) Evolution of the Longmen Shan foreland  
39 657 basin (western Sichuan, China) during the Late Triassic Indosinian orogeny. *Basin Research*, **15**,  
40 658 117-138.
- 41 659 LI, Y., HE, D., LI, D., WEN, Z., MEI, Q., LI, C. & SUN, Y. (2016) Detrital zircon U-Pb geochronology  
42 660 and provenance of Lower Cretaceous sediments: Constraints for the northwestern Sichuan  
43 661 pro-foreland basin. *Palaeogeography, Palaeoclimatology, Palaeoecology*, **453**, 52-72.
- 44 662 LI, Y., SHAO, L., ERIKSSON, K.A., TONG, X., GAO, C. & CHEN, Z. (2014) Linked sequence stratigraphy  
45 663 and tectonics in the Sichuan continental foreland basin, Upper Triassic Xujiahe Formation,  
46 664 southwest China. *Journal of Asian Earth Sciences*, **88**, 116-136.
- 47 665 LI, Y., YAN, Z., LIU, S., LI, H., CAO, J., SU, D., DONG, S., SUN, W., YANG, R. & YAN, L. (2014)  
48 666 Migration of the carbonate ramp and sponge buildup driven by the orogenic wedge advance in the  
49 667 early stage (Carnian) of the Longmen Shan foreland basin, China. *Tectonophysics*, **619-620**,  
50 668 179-193.
- 51 669 LI, Z.X., LI, X.H., KINNY, P.D., WANG, J., ZHANG, S. & ZHOU, H. (2003b) Geochronology of  
52 670 Neoproterozoic syn-rift magmatism in the Yangtze Craton, South China and correlations with  
53 671 other continents: evidence for a mantle superplume that broke up Rodinia. *Precambrian Research*,  
54 672 **122**, 85-109.
- 55 673 LIN, G. (2010) Zircon U-Pb age and petrochemical characteristics of Shimian granite in western  
56 674 Sichuan: petrogenesis and tectonic significance. *Earth Science-Journal of China University of*  
57 675 *Geoscience*, **35**, 611-620.
- 58 676 LIN, G., LI, X. & LI, W. (2006b) SHRIMP U-Pb zircon age, geochemistry and Nd-Hf isotope of  
59 677 Neoproterozoic mafic dyke swarms in western Sichuan: Petrogenesis and tectonic significance.  
60 678 *SCIENCE CHINA: Earth Sciences*, **36**, 630-645.
- 679 LIN, L., CHEN, H., ZHAI, C., XIAOQIANG, H. & JUNWEN, L. (2006a) Sandstone compositions and  
680 paleogeographic evolution of the Upper Triassic Xujiahe formation in the western Sichuan basin,

- 1  
2  
3 681 China. *Petroleum Geology and Experiment*, **28**, 511-517.
- 4 682 LIN, W., WANG, H. & SONG, H. (1982) Upper Permian to Lower-middle Triassic Strata and  
5 683 Sedimentary Environments in Longmendong, Emei, Sichuan. *Journal of Mineralogy and*  
6 684 *Petrology*, 53-58.
- 7 685 LIU, Z. & TONG, J. (2001) The Middle Triassic Stratigraphy and Sedimentary Paleogeography of South  
8 686 China. *ACTA SEDIMENTOLOGICA SINICA*, **19**, 327-332.
- 9 687 LONG, S., WU, S., LI, H., BAI, Z., MA, J. & ZHANG, H. (2011) Hybrid sedimentation in Late  
10 688 Permian-Early Triassic in western Sichuan basin, China. *J. Earth Sci.*, **22**, 340-350.
- 11 689 LUO, L., QI, J., ZHANG, M., WANG, K. & HAN, Y. (2014) Detrital zircon U - Pb ages of Late Triassic -  
12 690 Late Jurassic deposits in the western and northern Sichuan Basin margin: constraints on the  
13 691 foreland basin provenance and tectonic implications. *Int J Earth Sci (Geol Rundsch)*, **103**,  
14 692 1553-1568.
- 15 693 LUO, Y. (1983) The evolution of paleoplates in the Kang-Dian tectonic zone. *Earth Science-Journal of*  
16 694 *Wuhan College of Geology*, **22**, 93-102.
- 17 695 LUO, Z., SUN, W., HAN, J. & WANG, R. (2012) Effect of Emei mantle plume on the conditions of  
18 696 Permian accumulation in middle-upper Yangtze area. *Earth Science Frontiers*, **19**, 144-154.
- 19 697 MENG, E., LIU, F., DU, L., LIU, P. & LIU, J. (2015) Petrogenesis and tectonic significance of the  
20 698 Baoxing granitic and mafic intrusions, southwestern China: Evidence from zircon U - Pb dating  
21 699 and Lu - Hf isotopes, and whole-rock geochemistry. *Gondwana Research*, **28**, 800-815.
- 22 700 MENG, Q. & ZHANG, G. (2000) Geologic framework and tectonic evolution of the Qinling orogen,  
23 701 central China. *Tectonophysics*, **323**, 183-196.
- 24 702 MENG, Q., WANG, E. & HU, J. (2005) Mesozoic sedimentary evolution of the northwest Sichuan basin:  
25 703 Implication for continued clockwise rotation of the South China block. *Geol Soc America Bull*,  
26 704 **117**, 396.
- 27 705 OVTCHAROVA, M., BUCHER, H., SCHALTEGGER, U., GALFETTI, T., BRAYARD, A. & GUEx, J. (2006)  
28 706 New Early to Middle Triassic U - Pb ages from South China: Calibration with ammonoid  
29 707 biochronozones and implications for the timing of the Triassic biotic recovery. *Earth and*  
30 708 *Planetary Science Letters*, **243**, 463-475.
- 31 709 REID, A.J., WILSON, C.J.L. & LIU, S. (2005) Structural evidence for the Permo-Triassic tectonic  
32 710 evolution of the Yidun Arc, eastern Tibetan Plateau. *Journal of Structural Geology*, **27**, 119-137.
- 33 711 ROGER, F. & CALASSOU, S. (1997) Géochronologie U-Pb sur zircons et géochimie (Pb, Sr et Nd) du  
34 712 socle de la chaîne de Songpan-Garze (Chine). *Comptes Rendus de l'Académie des Sciences-Series*  
35 713 *IIA-Earth and Planetary Science*, **324**, 819-826.
- 36 714 ROGER, F., JOLIVET, M., CATTIN, R. & MALAVIEILLE, J. (2011) Mesozoic-Cenozoic tectonothermal  
37 715 evolution of the eastern part of the Tibetan Plateau (Songpan-Garze, Longmen Shan area):  
38 716 insights from thermochronological data and simple thermal modelling. *Geological Society,*  
39 717 *London, Special Publications*, **353**, 9-25.
- 40 718 RUAN, L. (2013) The Metallogenic Regularity of Dashuigou Tellurium Deposit ,Shimian,Sichuan  
41 719 Province and the Origination of Prospecting, China University of Geosciences, Wuhan.
- 42 720 SHAO, T., CHENG, N. & SONG, M. (2016a) Provenance and tectonic-paleogeographic evolution:  
43 721 Constraints from detrital zircon U - Pb ages of Late Triassic-Early Jurassic deposits in the  
44 722 northern Sichuan basin, central China. *Journal of Asian Earth Sciences*, **127**, 12-31.
- 45 723 SHAO, T., CHENG, N. & SONG, M. (2016b) Provenance and tectonic-paleogeographic evolution:  
46 724 Constraints from detrital zircon U - Pb ages of Late Triassic-Early Jurassic deposits in the  
47 725 northern Sichuan basin, central China. *Journal of Asian Earth Sciences*, **127**, 12-31.
- 48 726 SHEN, W., GAO, J., XU, S., LI, H., ZHOU, G., YANG, Z. & YANG, Q. (2003) Geochemical Characteristics  
49 727 of the Shimian Ophiolite, Sichuan Province and Its Tectonic Significance. *Geological Review*, **49**,  
50 728 17-27.
- 51 729 SHEN, W., LI, H., XU, S. & WANG, R. (2000) U-Pb Chronological Study of Zircons from the  
52 730 Huangcaoshan and Xiasuozi Granites in the Western Margin of Yangtze Plate. *Geological Journal*  
53 731 *of China Universities*, **6**, 412-416.
- 54 732 SHI, Z., PRETO, N., JIANG, H., KRYSSTYN, L., ZHANG, Y., OGG, J.G., JIN, X., YUAN, J., YANG, X. & DU,  
55 733 Y. (2016) Demise of Late Triassic sponge mounds along the northwestern margin of the Yangtze  
56 734 Block, South China: Related to the Carnian Pluvial Phase? *Palaeogeography Palaeoclimatology*  
57 735 *Palaeoecology*.
- 58 736 SHI, Z., WANG, Z., HAO, C., GUO, Z. & MO, W. (2015) Sedimentary Facies of the Upper Triassic  
59 737 Maantang Formation in Sichuan Basin. *Journal of Palaeogeography*, **17**, 771-786.
- 60 738 SHI, Z., YANG, W., XIE, Z., JIN, H. & XIE, W. (2010) Upper Triassic Clastic Composition in Sichuan  
739 Basin, Southwest China: Implication for Provenance Analysis and the Indosinian Orogeny. *ACTA*



- 1  
2  
3 740 *GEOLOGICA SINICA*, **84**, 387-397.
- 4 741 SLÁMA, J., KOŠLER, J., CONDON, D.J., CROWLEY, J.L., GERDES, A., HANCHAR, J.M., HORSTWOOD,  
5 742 M.S.A., MORRIS, G.A., NASDALA, L., NORBERG, N., SCHALTEGGER, U., SCHOENE, B., TUBRETT,  
6 743 M.N. & WHITEHOUSE, M.J. (2008) Plešovice zircon — A new natural reference material for U -  
7 744 Pb and Hf isotopic microanalysis. *Chemical Geology*, **249**, 1-35.
- 8 745 SUN, C., HU, M., HU, Z., XUE, D. & WANG, Z. (2015) Sequence-based Lithofacies and Paleogeography  
9 746 of Lower Triassic Feixianguan Formation in Sichuan Basin. *Marine Origin Petroleum Geology*,  
10 747 1-9.
- 11 748 SUN, W., ZHOU, M., GAO, J., YANG, Y., ZHAO, X. & ZHAO, J. (2009) Detrital zircon U - Pb  
12 749 geochronological and Lu - Hf isotopic constraints on the Precambrian magmatic and crustal  
13 750 evolution of the western Yangtze Block, SW China. *Precambrian Research*, **172**, 99-126.
- 14 751 TAN, X., LI, L., LIU, H., CAO, J., WU, X., ZHOU, S. & SHI, X. (2014) Mega-shoaling in carbonate  
15 752 platform of the Middle Triassic Leikoupo Formation, Sichuan Basin, southwest China. *Sci. China*  
16 753 *Earth Sci.*, **57**, 465-479.
- 17 754 TAN, X., XIA, Q., CHEN, J., LI, L., LIU, H., LUO, B., XIA, J. & YANG, J. (2013) Basin-scale sand  
18 755 deposition in the Upper Triassic Xujiage formation of the Sichuan Basin, Southwest China:  
19 756 Sedimentary framework and conceptual model. *Journal of Earth Science*, **24**, 89-103.
- 20 757 TIAN, Y., KOHN, B.P., GLEADOW, A.J.W. & HU, S. (2013) Constructing the Longmen Shan eastern  
21 758 Tibetan Plateau margin: Insights from low-temperature thermochronology. *Tectonics*, **32**,  
22 759 576-592.
- 23 760 TIAN, Y., KOHN, B.P., PHILLIPS, D., HU, S., GLEADOW, A.J.W. & CARTER, A. (2016) Late  
24 761 Cretaceous-earliest Paleogene deformation in the Longmen Shan fold-and-thrust belt, eastern  
25 762 Tibetan Plateau margin: Pre-Cenozoic thickened crust? *Tectonics*, **35**, 2293-2312.
- 26 763 TIAN, Y., KOHN, B.P., ZHU, C., XU, M., HU, S. & GLEADOW, A.J.W. (2012a) Post-orogenic evolution  
27 764 of the Mesozoic Micang Shan Foreland Basin system, central China. *Basin Research*, **24**, 70-90.
- 28 765 TIAN, Y., QIU, N., KOHN, B.P., ZHU, C., HU, S., GLEADOW, A.J.W. & MCINNES, B.I.A. (2012b) Detrital  
29 766 zircon (U - Th)/He thermochronometry of the Mesozoic Daba Shan Foreland Basin, central China:  
30 767 Evidence for timing of post-orogenic denudation. *Tectonophysics*, **570-571**, 65-77.
- 31 768 XU, Y., HE, B., CHUNG, S., MENZIES, M.A. & FREY, F.A. (2004) Geologic, geochemical, and  
32 769 geophysical consequences of plume involvement in the Emeishan flood-basalt province. *Geology*,  
33 770 **32**, 917.
- 34 771 VERMEESCH, P. (2012) On the visualisation of detrital age distributions. *Chemical Geology*, **312-313**,  
35 772 190-194.
- 36 773 WANG, B., WANG, W., CHEN, W.T., GAO, J., ZHAO, X., YAN, D. & ZHOU, M. (2013b) Constraints of  
37 774 detrital zircon U - Pb ages and Hf isotopes on the provenance of the Triassic Yidun Group and  
38 775 tectonic evolution of the Yidun Terrane, Eastern Tibet. *Sedimentary Geology*, **289**, 74-98.
- 39 776 WANG, B., ZHOU, M., LI, J. & YAN, D. (2011) Late Triassic porphyritic intrusions and associated  
40 777 volcanic rocks from the Shangri-La region, Yidun terrane, Eastern Tibetan Plateau: adakitic  
41 778 magmatism and porphyry copper mineralization. *Lithos*, **127**, 24-38.
- 42 779 WANG, H., YANG, S. & LI, S. (1983) Mesozoic and Cenozoic basin formation in east China and  
43 780 adjacent regions and development of the continental margin. *Acta Geologica Sinica*, 213-223.
- 44 781 WANG, L. & PAN, G. (2013) *Geological Map of the Qinghai-Tibet plateau and adjacent areas*.  
45 782 Geologied Publishing House, Beijing.
- 46 783 WANG, L., GRIFFIN, W.L., YU, J. & O'REILLY, S.Y. (2010) Precambrian crustal evolution of the  
47 784 Yangtze Block tracked by detrital zircons from Neoproterozoic sedimentary rocks. *Precambrian*  
48 785 *Research*, **177**, 131-144.
- 49 786 WANG, L., GRIFFIN, W.L., YU, J. & O'REILLY, S.Y. (2013a) U - Pb and Lu - Hf isotopes in detrital  
50 787 zircon from Neoproterozoic sedimentary rocks in the northern Yangtze Block: implications for  
51 788 Precambrian crustal evolution. *Gondwana Research*, **23**, 1261-1272.
- 52 789 WANG, L., LU, Y., ZHAO, S. & LUO, J. (1994) *Permian Lithofacies, Paleogeography and*  
53 790 *Mineralization in South China*. Geological Publishing House, Beijing.
- 54 791 WANG, L., YU, J., GRIFFIN, W.L. & O'REILLY, S.Y. (2012) Early crustal evolution in the western  
55 792 Yangtze Block: evidence from U - Pb and Lu - Hf isotopes on detrital zircons from sedimentary  
56 793 rocks. *Precambrian Research*, **222**, 368-385.
- 57 794 WANG, W. & CENG, C. (1982) The characteristics of alluvial facies of the Lower Triassic Feixianguan  
58 795 formation in the Longmendong, Emei, Sichuan. *Journal of Mineralogy and Petrology*, 71-82.
- 59 796 WANG, W. & ZHOU, M. (2012) Sedimentary records of the Yangtze Block (South China) and their  
60 797 correlation with equivalent Neoproterozoic sequences on adjacent continents. *Sedimentary*  
61 798 *Geology*, **265-266**, 126-142.

- 1  
2  
3 799 WANG, Y., ZHANG, Y., FAN, W. & PENG, T. (2005) Structural signatures and 40 Ar/ 39 Ar  
4 800 geochronology of the Indosinian Xuefengshan tectonic belt, South China Block. *Journal of*  
5 801 *Structural Geology*, **27**, 985-998.
- 6 802 WEI, Y., ZHANG, Z., HE, W., WU, N. & YANG, B. (2014) Evolution of Sedimentary Basins in the Upper  
7 803 Yangtze during Mesozoic. *Editorial Committee of Earth Science-Journal of China University of*  
8 804 *Geosciences*, 1065-1078 in Chinese with English abstract.
- 9 805 WEISLOGEL, A.L. (2008) Tectonostratigraphic and geochronologic constraints on evolution of the  
10 806 northeast Paleotethys from the Songpan-Ganzi complex, central China. *Tectonophysics*, **451**,  
11 807 331-345.
- 12 808 WEISLOGEL, A.L., GRAHAM, S.A., CHANG, E.Z., WOODEN, J.L. & GEHRELS, G.E. (2010) Detrital  
13 809 zircon provenance from three turbidite depocenters of the Middle-Upper Triassic Songpan-Ganzi  
14 810 complex, central China: Record of collisional tectonics, erosional exhumation, and sediment  
15 811 production. *Geological Society of America Bulletin*, **122**, 2041-2062.
- 16 812 WELLER, O.M., STONGE, M.R., WATERS, D.J., RAYNER, N., SEARLE, M.P., CHUNG, S.L., PALIN, R.M.,  
17 813 LEE, Y. & XU, X. (2013) Quantifying Barrovian metamorphism in the Danba Structural  
18 814 Culmination of eastern Tibet. *Journal of Metamorphic Geology*, **31**, 909-935.
- 19 815 WGCMSPIB (Write Group of Continental Mesozoic Stratigraphy and Paleontology in Sichuan Basin  
20 816 of China) (1984) *Continental Mesozoic Stratigraphy and Paleontology in Sichuan Basin of China*.  
21 817 People's Publishing House of Sichuan, Chengdu.
- 22 818 WIEDENBECK, M., HANCHAR, J.M., PECK, W.H., SYLVESTER, P., VALLEY, J., WHITEHOUSE, M., KRONZ,  
23 819 A., MORISHITA, Y., NASDALA, L., FIEBIG, J., FRANCHI, I., GIRARD, J.P., GREENWOOD, R.C.,  
24 820 HINTON, R., KITA, N., MASON, P.R.D., NORMAN, M., OGASAWARA, M., PICCOLI, P.M., RHEDE, D.,  
25 821 SATOH, H., SCHULZ DOBRICK, B., SK R, O., SPICUZZA, M.J., TERADA, K., TINDLE, A., TOGASHI, S.,  
26 822 VENNEMANN, T., XIE, Q. & ZHENG, Y.F. (2004) Further Characterisation of the 91500 Zircon  
27 823 Crystal., **28**, 9-39.
- 28 824 XIE, J., LI, G. & TANG, D. (2006) Analysis on provenance-supply system of Upper Triassic Xujiahe  
29 825 formation, Sichuan Basin. *Natural Gas Exploration and Development*, **29**, 1-3, 13.
- 30 826 XIE, T., ZHOU, Z., ZHANG, Q., HU, S., HUANG, J., WEN, W. & CONG, F. (2013) Zircon U-Pb age for the  
31 827 tuff before the Luoping biota and its geological implication. *Geological Review*, **59**, 159-164.
- 32 828 XU, X., LIU, B. & ZHAO, Y. (1996) Sequence Boundary Genesis and Basin-Mountain Transformation  
33 829 on the Western Margin of the Upper Yangtze Platform during the Permian to Triassic.  
34 830 *Sedimentary Geology and Tethyan Geology*, 1-30.
- 35 831 XU, X., LIU, B., ZHAO, Y. & LU, Y. (1997) *Sequence Stratigraphy and Basin- Mountain*  
36 832 *Transformation in the Western Margin of Upper Yangtze Lnadmass during the Permian to*  
37 833 *Triassic*. Geological Publishing House, Beijing.
- 38 834 XU, Y., HE, B., CHUNG, S., MENZIES, M.A. & FREY, F.A. (2004) Geologic, geochemical, and  
39 835 geophysical consequences of plume involvement in the Emeishan flood-basalt province. *Geol*, **32**,  
40 836 917.
- 41 837 XU, Y., LUO, Z., HUANG, X., HE, B., XIAO, L., XIE, L. & SHI, Y. (2008) Zircon U - Pb and Hf isotope  
42 838 constraints on crustal melting associated with the Emeishan mantle plume. *Geochimica et*  
43 839 *Cosmochimica Acta*, **72**, 3084-3104.
- 44 840 XU, Z., HOU, L. & WANG, Z. (1992) *Orogenic Processes of the Songpan- Garze Orogenic Belt of*  
45 841 *China*. Geol. Publ. House, Beijing.
- 46 842 YAN, D., ZHOU, M., LI, S. & WEI, G. (2011) Structural and geochronological constraints on the  
47 843 Mesozoic-Cenozoic tectonic evolution of the Longmen Shan thrust belt, eastern Tibetan Plateau.  
48 844 *Tectonics*, **30**, n/a-n/a.
- 49 845 YAN, Q., WANG, Z., LIU, S., SHI, Y., LI, Q., YAN, Z., WANG, T., WANG, J., ZHANG, D. & ZHANG, H.  
50 846 (2006) Eastern Margin of the Tibetan Plateau A Window to Probe the Complex Geological  
51 847 History from the Proterozoic to the Cenozoic Revealed by SHRIMP Analyses. *Acta Geologica*  
52 848 *Sinica*, **80**, 1285-1294.
- 53 849 YIN, A. (1996) A Phanerozoic palinspastic reconstruction of China and its neighboring regions, in:  
54 850 Tectonic Evolution of Asia.
- 55 851 ZHANG, G.W., MENG, Q.R. & LAI, S.C. (1995) Tectonics and structure of Qinling orogenic belt.  
56 852 *Science in China*, **38**, 1379-1394.
- 57 853 ZHANG, Y. (2014) U Pb and Lu Hf isotope systematics of detrital zircons from the Songpan Ganzi  
58 854 Triassic flysch NE Tibetan Plateau implications for provenance and (1).
- 59 855 ZHANG, Y., JIA, D., SHEN, L., YIN, H., CHEN, Z., LI, H., LI, Z. & SUN, C. (2015) Provenance of detrital  
60 856 zircons in the Late Triassic Sichuan foreland basin: constraints on the evolution of the Qinling  
857 Orogen and Longmen Shan thrust-fold belt in central China. *International Geology Review*, **57**,  
858 1806-1824.

- 1  
2  
3 859 ZHAO, J. & ZHOU, M. (2007) Geochemistry of Neoproterozoic mafic intrusions in the Panzhihua  
4 860 district (Sichuan Province, SW China): Implications for subduction-related metasomatism in the  
5 861 upper mantle. *Precambrian Research*, **152**, 27-47.
- 6 862 ZHAO, J., CHEN, Y. & LI, Z. (2006) Zircon U-Pb SHRIMP Dating for the Kangding Complex and Its  
7 863 Geological Significance. *GEOSCIENCE*, **20**, 378-385.
- 8 864 ZHAO, Y., XU, X. & LIU, B. (1996) High-frequency sequences and sea-level oscillations in the Emei  
9 865 area on the western margin of the Upper Yangtze Platform. *Lithofacies Paleogeography*, **16**, 1-18.
- 10 866 ZHAO, Z., ZHOU, H., CHEN, X., LIU, Y., ZHANG, Y., LIU, Y. & YANG, Y. (2012) Sequence lithofacies  
11 867 paleogeography and favorable exploration zones of the Permian in Sichuan Basin and adjacent  
12 868 areas, China. *Acta Petrolei Sinica*, **33**, 35-51.
- 13 869 ZHENG, L., YANG, Z., TONG, Y. & YUAN, W. (2010) Magnetostratigraphic constraints on two - stage  
14 870 eruptions of the Emeishan continental flood basalts. *Geochemistry Geophysics Geosystems*, **11**.
- 15 871 ZHENG, Y., LI, H., SUN, Z., WANG, H., ZHANG, J., LI, C. & CAO, Y. (2016) New geochronology  
16 872 constraints on timing and depth of the ancient earthquakes along the Longmen Shan fault belt,  
17 873 eastern Tibet. *Tectonics*.
- 18 874 ZHOU, M., MA, Y., YAN, D., XIA, X., ZHAO, J. & SUN, M. (2006a) The Yanbian Terrane (Southern  
19 875 Sichuan Province, SW China): A Neoproterozoic arc assemblage in the western margin of the  
20 876 Yangtze Block. *Precambrian Research*, **144**, 19-38.
- 21 877 ZHOU, M., YAN, D., KENNEDY, A.K., LI, Y. & DING, J. (2002b) SHRIMP U - Pb zircon  
22 878 geochronological and geochemical evidence for Neoproterozoic arc-magmatism along the western  
23 879 margin of the Yangtze Block, South China. *Earth and Planetary Science Letters*, **196**, 51-67.
- 24 880 ZHOU, M., YAN, D., WANG, C., QI, L. & KENNEDY, A. (2006b) Subduction-related origin of the 750  
25 881 Ma Xuelongbao adakitic complex (Sichuan Province, China): implications for the tectonic setting  
26 882 of the giant Neoproterozoic magmatic event in South China. *Earth and Planetary Science Letters*,  
27 883 **248**, 286-300.
- 28 884 ZHOU, M.F., KENNEDY, A.K., SUN, M., MALPAS, J. & LESHER, C.M. (2002a) Neoproterozoic arc -  
29 885 related mafic intrusions along the northern margin of South China: implications for the accretion  
30 886 of Rodinia. *The Journal of geology*, **110**, 611-618.
- 31 887 ZHU, H., ZHOU, B., WANG, S., LUO, M., LIAO, Z. & GUO, Y. (2011) Detrital zircon U-Pb dating by  
32 888 LA-ICP-MS and its geological significance in western margin of Yangtze terrane. *JOURNAL OF*  
33 889 *MINERALOGY AND PETROLOGY*, **31**, 70-74.
- 34 890 ZHU, M., CHEN, H., ZHOU, J. & YANG, S. (2017) Provenance change from the Middle to Late Triassic  
35 891 of the southwestern Sichuan basin, Southwest China: Constraints from the sedimentary record and  
36 892 its tectonic significance. *Tectonophysics*, **700-701**, 92-107.
- 37 893 ZHU, Z. & WANG, G. (1986) Paleogeography of before and after deposition of green-bean rock (altered  
38 894 tuff) between the early and middle Triassic in the upper Yangtze platform and its adjacent areas.  
39 895 *Oil & Gas Geology*, **7**, 344-355.
- 40  
41  
42  
43  
44  
45  
46  
47  
48  
49  
50  
51  
52  
53  
54  
55  
56  
57  
58  
59  
60

Grains	SZ02														discordance		preferred ages			
	ratios							ages							%discor d.68-75	%discor d.68-76	preferr ed age	1 sigma		
	Pb207/ Pb206	1 sigma	Pb206/ U238	1 sigma	Pb207/ U235	1 sigma	Pb208/ Th232	1 sigma	Pb207/ Pb206	1 sigma	Pb206/ U238	1 sigma	Pb207/ U235	1 sigma					Pb208/ Th232	1 sigma
1	0.0513	0.002	0.0391	0.0007	0.2761	0.0106	0.0125	0.0015	254.5	85.68	247.2	4.62	247.6	8.46	251.8	29.64	0.16	2.95	247.2	4.62
2	0.0511	0.0014	0.0393	0.0007	0.2759	0.0079	0.0109	0.0012	243.8	61.59	248.2	4.2	247.4	6.29	219.9	24.3	-0.32	-1.77	248.2	4.2
3	0.0515	0.0028	0.0397	0.0008	0.2812	0.0153	0.0104	0.0014	261.4	121.47	250.9	5.18	251.6	12.13	209.1	27.98	0.28	4.18	250.9	5.18
4	0.0512	0.0017	0.039	0.0007	0.2743	0.0094	0.0085	0.001	247.9	75.11	246.3	4.38	246.1	7.46	171.4	19.63	-0.08	0.65	246.3	4.38
5	0.0604	0.0029	0.0384	0.0008	0.3189	0.015	0.0121	0.0014	617.8	99.96	242.6	5.05	281	11.57	243	28.29	15.83	154.66		
6	0.0508	0.0015	0.0394	0.0007	0.2754	0.0083	0.0116	0.0013	232.8	65.22	248.9	4.22	247	6.61	233.5	25.61	-0.76	-6.47	248.9	4.22
7	0.0516	0.0017	0.0392	0.0007	0.2786	0.0093	0.0116	0.0013	269.5	72.43	247.9	4.32	249.6	7.36	233.5	25.86	0.69	8.71	247.9	4.32
8	0.0511	0.0021	0.0387	0.0007	0.272	0.011	0.0119	0.0014	242.9	90.02	244.8	4.61	244.3	8.76	239.2	27.79	-0.20	-0.78	244.8	4.61
9	0.0885	0.0056	0.0473	0.0013	0.5759	0.035	0.0199	0.0024	1393.2	116.61	297.8	7.67	461.8	22.56	399.1	46.87	55.07	367.83		
10	0.0513	0.0025	0.0388	0.0008	0.2737	0.0131	0.0104	0.0013	252.3	107.22	245.3	4.98	245.6	10.42	209.3	25.87	0.12	2.85	245.3	4.98
11	0.0509	0.0016	0.0372	0.0006	0.2611	0.0085	0.0093	0.0009	236.9	72.59	235.4	3.97	235.5	6.87	186.6	16.93	0.04	0.64	235.4	3.97
12	0.0512	0.0021	0.0394	0.0007	0.2779	0.0116	0.0115	0.001	249.1	93.08	248.9	4.46	249	9.18	231.5	20.29	0.04	0.08	248.9	4.46
13	0.0511	0.0022	0.0389	0.0007	0.2742	0.0116	0.0118	0.0011	243.7	95.43	246.3	4.56	246	9.26	236.5	21.62	-0.12	-1.06	246.3	4.56
14	0.0765	0.0021	0.0358	0.0006	0.3773	0.0108	0.0117	0.001	1108	54.89	226.6	3.84	325	7.93	234.5	20.05	43.42	388.97		
15	0.0508	0.0026	0.0362	0.0007	0.254	0.0127	0.0098	0.001	233.5	113.11	229.4	4.51	229.8	10.3	196.7	19.82	0.17	1.79	229.4	4.51
16	0.0513	0.0022	0.0396	0.0007	0.2802	0.0118	0.0105	0.001	254.4	94.14	250.4	4.57	250.8	9.33	211.8	20.84	0.16	1.60	250.4	4.57
17	0.0509	0.0017	0.0384	0.0007	0.2699	0.0091	0.0104	0.001	237.1	74.49	243.2	4.1	242.6	7.24	209.7	19.4	-0.25	-2.51	243.2	4.1
18	0.0508	0.0013	0.0392	0.0006	0.2747	0.0075	0.0105	0.0009	232.8	59.2	247.9	3.96	246.4	5.97	211.9	18.59	-0.61	-6.09	247.9	3.96
19	0.051	0.0017	0.0381	0.0007	0.2676	0.009	0.0101	0.0009	240.6	74.53	240.8	4.12	240.8	7.17	203.9	17.03	0.00	-0.08	240.8	4.12
20	0.0509	0.0021	0.0391	0.0007	0.2744	0.0111	0.0106	0.0009	237.5	90.2	247.1	4.37	246.2	8.81	213.1	18.4	-0.36	-3.89	247.1	4.37
21	0.0514	0.0009	0.0395	0.0006	0.2797	0.0056	0.0105	0.0009	259.4	40.4	249.5	3.75	250.4	4.47	211.7	17.89	0.36	3.97	249.5	3.75
22	0.051	0.0019	0.0382	0.0007	0.2685	0.01	0.0109	0.001	238.4	82.94	241.8	4.19	241.5	7.98	219.3	20.29	-0.12	-1.41	241.8	4.19
23	0.0511	0.0016	0.0389	0.0007	0.2738	0.0087	0.0101	0.0009	245.5	70.07	245.8	4.07	245.7	6.93	203	18.1	-0.04	-0.12	245.8	4.07
24	0.051	0.0023	0.0388	0.0007	0.2732	0.012	0.0105	0.001	241.9	98.57	245.5	4.52	245.2	9.56	210.3	18.95	-0.12	-1.47	245.5	4.52
25	0.0512	0.0016	0.04	0.0007	0.2825	0.0089	0.0121	0.0017	251.8	68.41	252.8	4.5	252.6	7.08	242.6	33.1	-0.08	-0.40	252.8	4.5
26	0.0517	0.0021	0.0425	0.0008	0.3031	0.0124	0.0139	0.0018	274	90.54	268.4	5.15	268.8	9.69	278	36.63	0.15	2.09	268.4	5.15
27	0.0554	0.0015	0.028	0.0005	0.2136	0.0061	0.0051	0.0007	426.7	58.88	178	3.12	196.5	5.13	103.2	13.6	10.39	139.72		
28	0.0518	0.0018	0.0443	0.0008	0.3165	0.0113	0.0134	0.0018	277.6	77.5	279.5	5.11	279.2	8.68	269.9	36.3	-0.11	-0.68	279.5	5.11
29	0.052	0.0021	0.0437	0.0009	0.3128	0.0128	0.0137	0.0019	283.6	89.83	275.7	5.28	276.4	9.87	274.5	37.8	0.25	2.87	275.7	5.28
30	0.0512	0.0018	0.0389	0.0007	0.2747	0.0101	0.0118	0.0016	249.7	80.46	246.2	4.54	246.4	8.02	237.1	31.97	0.08	1.42	246.2	4.54
31	0.0513	0.0019	0.0396	0.0008	0.28	0.0105	0.0122	0.0017	254.8	82.43	250.4	4.67	250.7	8.32	245.5	32.95	0.12	1.76	250.4	4.67
32	0.0512	0.0023	0.0398	0.0008	0.2805	0.0127	0.0126	0.0017	250.7	100.67	251.3	4.98	251.1	10.06	252.4	33.81	-0.08	-0.24	251.3	4.98
33	0.0519	0.0021	0.0433	0.0008	0.3093	0.0127	0.0126	0.0018	278.6	90.04	273.2	5.2	273.6	9.81	252.8	35.88	0.15	1.98	273.2	5.2
34	0.0513	0.0022	0.0389	0.0008	0.2755	0.0119	0.0125	0.0017	255.6	96.03	246.3	4.85	247	9.47	250.3	34.45	0.28	3.78	246.3	4.85

LCG01																			
sample	concentrations				ratios					ages					discordance		preferred ages		
	ppm U	ppm Pb	atomic Th/U	Pb207/Pb206	1 sigma	Pb207/U235	1 sigma	Pb206/U238	1 sigma	age 206/238	1 sigma	age 207/235	1 sigma	age 207/206	1 sigma	%disc ord.68-75	%disc ord.68-76	preferr ed age	1 sigma
LCG01-1	461.5	60.4	0.4704	0.06392	0.00089	1.09301	0.01631	0.12406	0.00153	753.9	8.8	750	9.9	739	7.3	0.5	2.0	753.9	8.8
LCG01-2	126.4	15.4	17.2335	0.76611	0.04149	25.3903	1.14056	0.24046	0.01266	1389.1	65.8	3323.3	73.8	4860	54.5	-58.2	-71.4		
LCG01-3	397.2	36.8	0.6721	0.05743	0.00092	0.65781	0.01094	0.08311	0.00105	514.7	6.2	513.3	8.2	508.1	6.4	0.3	1.3	514.7	6.2
LCG01-4	338.8	47	0.7184	0.06478	0.00093	1.09125	0.01658	0.12223	0.00152	743.4	8.7	749.1	10.1	767.2	7.7	-0.8	-3.1	743.4	8.7
LCG01-5	214.5	30.6	0.9181	0.06253	0.00102	1.03251	0.01746	0.11981	0.00153	729.5	8.8	720.2	10.7	692.3	8.2	1.3	5.4	729.5	8.8
LCG01-6	618.7	61.6	3.0869	0.4505	0.0466	4.86727	0.39114	0.07839	0.00575	486.5	34.4	1796.6	106.8	4086.9	103.2	-72.9	-88.1		
LCG01-7	97.2	111.3	3.8597	0.41269	0.01979	23.5561	1.10363	0.41414	0.01886	2233.8	86	3250.2	64.4	3956	47.7	-31.3	-43.5		
LCG01-8	179.5	22.8	1.91	0.05722	0.00105	0.66716	0.01252	0.08459	0.0011	523.5	6.5	519	9.1	500	7.2	0.9	4.7	523.5	6.5
LCG01-9	490.2	78.8	0.3145	0.07047	#####	1.53197	0.02135	0.15773	0.00192	944.1	10.7	943.3	10.8	942.1	7.8	0.1	0.2	944.1	10.7
LCG01-10	297.9	42.5	5.3816	0.5917	0.02612	10.3657	0.35961	0.1271	0.00486	771.3	27.8	2468	54.1	4487.7	44.3	-68.7	-82.8		
LCG01-11	128.5	21.4	5.8637	0.37978	0.0447	4.04795	0.38964	0.07733	0.00612	480.2	36.6	1643.9	115.5	3830.9	116.8	-70.8	-87.5		
LCG01-12	47.3	12.1	37.9446	0.65851	0.06096	23.1159	1.72528	0.25469	0.02219	1462.6	114	3231.8	123.7	4642.7	93	-54.7	-68.5		
LCG01-13	268.7	40.4	0.8222	0.06721	0.00103	1.19401	0.01915	0.1289	0.00163	781.6	9.3	797.8	11	844.3	8.8	-2.0	-7.4	781.6	9.3
LCG01-14	2129.5	97.2	0.3733	0.06919	#####	0.42769	0.006	0.04485	0.00054	282.8	3.3	361.5	5.4	904.4	7.8	-21.8	-68.7		
LCG01-15	390.3	63.9	0.4734	0.06964	0.00095	1.47469	0.02164	0.15363	0.00189	921.3	10.6	920.1	11.1	917.8	8.2	0.1	0.4	921.3	10.6
LCG01-16	43.5	21.9	16.7334	0.72278	0.02698	107.53	5.21479	1.07941	0.05584	4719.3	173.1	4759.1	64.2	4776.7	37.6	-0.8	-1.2		
LCG01-17	1120	96.8	0.7693	0.06745	0.00089	0.68784	0.00977	0.07399	#####	460.1	5.4	531.5	7.4	851.7	7.6	-13.4	-46.0	460.1	5.4
LCG01-18	439.7	21.2	0.9287	0.05211	0.00105	0.29008	0.00589	0.04039	0.00053	255.2	3.3	258.6	5.5	290.2	5.1	-1.3	-12.1	255.2	3.3
LCG01-19	102.5	26.2	32.8291	0.51699	0.03517	7.06961	0.36651	0.09922	0.00543	609.8	31.8	2120.2	77.7	4290.4	68.1	-71.2	-85.8		
LCG01-20	166.2	49.6	1.3349	0.09543	0.00133	3.15391	0.04699	0.23978	0.00303	1385.6	15.8	1446	14.5	1536.6	11	-4.2	-9.8	1536.6	11
LCG01-21	987.2	90.2	0.669	0.05929	0.00077	0.67	0.00947	0.08199	0.00099	508	5.9	520.7	7.2	577.8	5.7	-2.4	-12.1	508	5.9
LCG01-22	204.5	32.7	0.9054	0.06721	0.00101	1.23997	0.01964	0.13386	0.00168	809.8	9.6	818.9	11	844.3	8.6	-1.1	-4.1	809.8	9.6
LCG01-23	82.8	11.9	0.5862	0.06765	0.00134	1.2201	0.02434	0.13086	0.00179	792.8	10.2	809.8	13.4	857.8	11.5	-2.1	-7.6	792.8	10.2
LCG01-24	1011.1	522.9	0.1878	0.29354	0.00337	21.5297	0.27708	0.53215	0.00636	2750.5	26.8	3162.8	16.1	3436.5	11.3	-13.0	-20.0		
LCG01-25	244.3	73.5	4.2865	0.53956	0.02094	17.1738	0.57271	0.23094	0.00829	1339.4	43.4	2944.6	50.7	4353.1	38.9	-54.5	-69.2		
LCG01-26	262.9	40.9	0.9713	0.0657	0.00099	1.16222	0.01848	0.12834	0.00161	778.4	9.2	783	10.7	796.8	8.3	-0.6	-2.3	778.4	9.2
LCG01-27	218.3	20.7	0.6552	0.05736	0.00102	0.67294	0.01225	0.08512	0.0011	526.6	6.5	522.5	9	505.4	7.1	0.8	4.2	526.6	6.5
LCG01-28	653.7	94.4	0.3451	0.08589	0.00136	1.73886	0.02861	0.14688	0.00191	883.5	10.7	1023	13.2	1335.7	11.8	-13.6	-33.9	883.5	10.7
LCG01-29	494.9	67.3	0.8765	0.06478	0.00089	1.0281	0.01517	0.11515	0.00142	702.6	8.2	718	9.5	767.2	7.4	-2.1	-8.4	702.6	8.2
LCG01-30	339.9	151.7	0.6353	0.12972	0.00156	6.92008	0.09213	0.38704	0.00469	2109.1	21.8	2101.2	15.1	2094.2	10.7	0.4	0.7	2094.2	10.7
LCG01-31	508.7	79.1	0.2811	0.06958	#####	1.47699	0.02077	0.15402	0.00188	923.5	10.5	921	10.8	916	7.8	0.3	0.8	923.5	10.5
LCG01-32	1235.2	77.9	0.1015	0.09489	0.00131	0.8731	0.0128	0.06676	0.00083	416.6	5	637.2	8.8	1525.9	10.9	-34.6	-72.7		
LCG01-33	67.4	-1.9	32.2749	0.93858	0.05693	27.2271	1.26761	0.21047	0.01259	1231.3	67	3391.7	83.4	5148.1	61.2	-63.7	-76.1		
LCG01-34	154	13.1	6.1232	0.6502	0.04268	12.3191	0.61373	0.13747	0.0079	830.3	44.8	2629	81.9	4624.4	65.9	-68.4	-82.0		
LCG01-35	119.5	21	17.4689	0.57601	0.03565	10.8164	0.51875	0.13624	0.00724	823.4	41.1	2507.5	75.8	4448.6	62.1	-67.2	-81.5		
LCG01-36	1120.5	86.3	0.1557	0.06018	#####	0.66443	0.00949	0.0801	0.00097	496.7	5.8	517.3	7.3	610.1	6.1	-4.0	-18.6	496.7	5.8
LCG01-37	133.8	20.5	0.6927	0.06795	0.00113	1.26313	0.02175	0.13487	0.00175	815.6	9.9	829.3	12	867	9.7	-1.7	-5.9	815.6	9.9
LCG01-38	1058.4	106.2	0.3215	0.06847	0.00087	0.92689	0.01286	0.09822	0.00119	604	7	666	8.6	882.8	7.5	-9.3	-31.6	604	7
LCG01-39	68	36.3	0.83	0.15571	0.0021	9.39194	0.13746	0.43762	0.00566	2340	25.4	2377	17.1	2409.6	12.4	-1.6	-2.9	2409.6	12.4
LCG01-40	43.5	9.9	22.2698	0.58325	0.03136	13.9274	0.60303	0.17325	0.00824	1030	45.3	2744.8	68	4466.8	53.9	-62.5	-76.9		
LCG01-41	353.7	33.7	0.6346	0.06967	0.00107	0.83734	0.01343	0.0872	0.0011	539	6.5	617.7	9.2	918.6	9.3	-12.7	-41.3	539	6.5
LCG01-42	492.8	182	1.0193	0.15866	0.00189	6.98954	0.09251	0.31963	0.00386	1787.9	18.9	2110.1	15.1	2441.4	11	-15.3	-26.8		
LCG01-43	422.2	64.6	3.665	0.58069	0.0266	11.3783	0.41335	0.14217	0.00566	856.9	31.9	2554.6	56.6	4460.4	45.9	-66.5	-80.8		
LCG01-44	159.8	24.6	0.9238	0.07282	0.00117	1.28356	0.02144	0.12789	0.00165	775.8	9.4	838.4	11.8	1008.9	10.3	-7.5	-23.1	775.8	9.4





1  
2  
3  
4  
5  
6  
7  
8  
9  
10  
11  
12  
13  
14  
15  
16  
17  
18  
19  
20  
21  
22  
23  
24  
25  
26  
27  
28  
29  
30  
31  
32  
33  
34  
35  
36  
37  
38  
39  
40  
41  
42  
43  
44  
45  
46  
47  
48  
49  
50  
51  
52  
53  
54  
55  
56  
57  
58  
59  
60

LCG01-94	225.2	32.2	5.5265	0.42084	0.03512	4.87718	0.32109	0.08409	0.00516	520.5	30.7	1798.3	87.3	3985.3	83.1	-71.1	-86.9		
LCG01-95	245.3	42	0.4173	0.07178	0.00109	1.61118	0.02576	0.16287	0.00207	972.7	11.5	974.6	12.4	979.7	9.5	-0.2	-0.7	972.7	11.5
LCG01-96	213.5	18.4	5.3471	0.4199	0.04997	3.42518	0.32304	0.05918	0.00479	370.6	29.2	1510.2	113.1	3981.9	118.4	-75.5	-90.7		
LCG01-97	578.8	90.6	0.1811	0.07845	0.00104	1.74791	0.02505	0.16166	0.00198	966	11	1026.4	11.7	1158.3	9.2	-5.9	-16.6	966	11
LCG01-98	124.3	19.9	0.6708	0.06447	0.00128	1.26262	0.02538	0.14211	0.00193	856.6	10.9	829.1	13.6	757.1	10.6	3.3	13.1	856.6	10.9
LCG01-99	177.4	31	0.4102	0.07056	0.00115	1.62057	0.02739	0.16664	0.00215	993.6	11.9	978.2	13.1	944.7	10	1.6	5.2	993.6	11.9
LCG01-100	167.8	15.3	0.6959	0.06406	0.0013	0.71953	0.01471	0.0815	0.00111	505.1	6.6	550.4	10.4	743.6	10.7	-8.2	-32.1	505.1	6.6
LCG01-101	265.5	45.1	0.439	0.07173	0.00104	1.60788	0.0247	0.16264	0.00203	971.4	11.3	973.3	12	978.3	9.1	-0.2	-0.7	971.4	11.3
LCG01-102	688.2	220.5	0.3419	0.14962	0.00189	6.44365	0.08915	0.31247	0.00383	1752.9	18.8	2038.2	15.5	2341.6	11.5	-14.0	-25.1		
LCG01-103	113.6	21.3	2.0686	0.06475	0.00139	1.08417	0.02326	0.12149	0.0017	739.1	9.8	745.7	13.5	766.2	11.5	-0.9	-3.5	739.1	9.8
LCG01-104	593.7	29	0.921	0.05218	0.00096	0.29519	0.00553	0.04105	0.00053	259.3	3.3	262.6	5.2	293.3	4.7	-1.3	-11.6	259.3	3.3
LCG01-105	25	8.1	19.9876	0.68115	0.06073	41.1922	3.37665	0.43879	0.04048	2345.2	181.4	3799.8	127.2	4691.5	89.6	-38.3	-50.0		
LCG01-106	155.6	15	3.1385	0.20944	0.00442	1.69304	0.03345	0.05865	0.00094	367.4	5.7	1005.9	16.9	2901.2	20.2	-63.5	-87.3		
LCG01-107	676	145.3	0.5374	0.49286	0.01136	17.7713	0.3854	0.26163	0.00565	1498.2	28.9	2977.4	30.4	4220	23	-49.7	-64.5		
LCG01-108	182.7	18.7	0.6173	0.05869	0.00118	0.75512	0.01537	0.09335	0.00126	575.3	7.4	571.2	10.6	555.6	8.6	0.7	3.5	575.3	7.4
LCG01-109	305.3	46.7	0.3898	0.06817	0.00107	1.3853	0.02267	0.14746	0.00188	886.7	10.6	882.7	11.9	873.7	9.2	0.5	1.5	886.7	10.6
LCG01-110	349.4	67.9	1.3825	0.06888	0.00105	1.37578	0.02198	0.14493	0.00183	872.5	10.3	878.6	11.6	895.1	9.1	-0.7	-2.5	872.5	10.3
LCG01-111	51.5	7.6	26.728	0.75205	0.05353	30.1204	1.83277	0.2906	0.02043	1644.5	102	3490.7	98.3	4833.5	71.7	-52.9	-66.0		
LCG01-112	166.2	27.8	0.3839	0.06803	0.00118	1.50609	0.02685	0.16062	0.00211	960.2	11.7	932.9	13.3	869.5	10.1	2.9	10.4	960.2	11.7
LCG01-113	222	33.1	4.9563	0.63888	0.03071	14.3191	0.54567	0.16262	0.00705	971.3	39.1	2771.1	61.4	4599	48.3	-64.9	-78.9		
LCG01-114	13.8	3.3	24.08	0.55256	0.10661	40.8606	8.05413	0.53655	0.09899	2769	415.3	3791.8	264.6	4387.9	193.3	-27.0	-36.9		
LCG01-115	274.5	37	0.7899	0.06562	0.00105	1.06658	0.01772	0.11793	0.0015	718.6	8.6	737.1	10.7	794.3	8.8	-2.5	-9.5	718.6	8.6
LCG01-116	279.9	23.9	0.5466	0.06999	0.00171	0.78541	0.01885	0.08142	0.00121	504.6	7.2	588.6	12.8	928.1	14.9	-14.3	-45.6	504.6	7.2
LCG01-117	166.7	21.2	8.5248	0.70831	0.02636	20.1164	0.62478	0.20607	0.00728	1207.8	38.9	3097	49.6	4747.7	37.4	-61.0	-74.6		
LCG01-118	354.2	108.8	0.5881	0.15651	0.00213	6.1332	0.08961	0.28433	0.0036	1613.1	18.1	1995	16.2	2418.3	12.5	-19.1	-33.3		
LCG01-119	261.8	33.6	1.117	0.07203	0.00154	1.0758	0.02294	0.10837	0.00153	663.3	8.9	741.6	13.5	986.8	13.5	-10.6	-32.8	663.3	8.9
LCG01-120	142.3	16.9	0.4313	0.06351	0.00138	0.99055	0.02155	0.11317	0.00158	691.1	9.1	699	13.1	725.4	11.3	-1.1	-4.7	691.1	9.1
LCG01-121	234.2	54.7	1.3843	0.07065	0.00113	1.72112	0.02877	0.17676	0.00228	1049.2	12.5	1016.4	13.2	947.3	9.9	3.2	10.8	1049.2	12.5
LCG01-122	271.9	36.2	1.022	0.07239	0.0012	1.10772	0.01894	0.11103	0.00144	678.7	8.4	757.1	11.2	996.9	10.5	-10.3	-31.9	678.7	8.4
LCG01-123	256.5	37	1.1714	0.06809	0.00118	1.08493	0.01939	0.11561	0.00151	705.2	8.7	746	11.5	871.3	10.1	-5.5	-19.1	705.2	8.7
LCG01-124	58.9	9.9	0.9271	0.07573	0.0028	1.49064	0.05313	0.14282	0.00279	860.6	15.7	926.6	25.4	1087.9	24.7	-7.1	-20.9	860.6	15.7
LCG01-125	37.7	9.2	36.9501	0.68196	0.04876	29.8492	1.86458	0.31758	0.02259	1777.9	110.5	3481.9	99.1	4693.2	71.9	-48.9	-62.1		
LCG01-126	85	15.8	0.4889	0.08406	0.00174	2.01391	0.04183	0.17384	0.00251	1033.2	13.8	1120.2	17.1	1293.9	15.1	-7.8	-20.1	1033.2	13.8
LCG01-127	145	29.8	5.5999	0.72666	0.03117	23.2894	0.83875	0.23255	0.00962	1347.8	50.3	3239.1	58	4784.4	43.2	-58.4	-71.8		
LCG01-128	396.7	80.5	4.4014	0.65332	0.02693	18.5247	0.63454	0.20574	0.0079	1206.1	42.2	3017.4	54.3	4631.3	41.4	-60.0	-74.0		
LCG01-129	25	6.1	23.3359	0.73522	0.06052	43.2383	3.34303	0.42671	0.03666	2290.9	165.6	3847.9	118.1	4801.1	82.8	-40.5	-52.3		
LCG01-130	556	50	4.0201	0.48271	0.02834	4.88748	0.21891	0.07347	0.00338	457	20.3	1800.1	62.9	4189.3	58.7	-74.6	-89.1		
LCG01-131	257	41.6	0.849	0.07128	0.00115	1.34529	0.02261	0.13694	0.00176	827.3	10	865.5	12	965.5	10.1	-4.4	-14.3	827.3	10
LCG01-132	301.6	46.3	0.7823	0.06416	0.00099	1.17577	0.01898	0.13296	0.00168	804.7	9.6	789.3	10.9	746.9	8.2	1.9	7.7	804.7	9.6
LCG01-133	134.4	6.4	0.7648	0.05612	0.00166	0.32159	0.00926	0.04158	0.00063	262.6	3.9	283.1	8.2	457.1	10.9	-7.2	-42.5	262.6	3.9
LCG01-134	219.3	40.9	0.8714	0.0716	0.00112	1.5506	0.02541	0.15714	0.00201	940.9	11.2	950.7	12.5	974.6	9.8	-1.0	-3.5	940.9	11.2
LCG01-135	176.3	35.6	1.2067	0.07094	0.00115	1.54124	0.02602	0.15764	0.00203	943.6	11.3	947	12.8	955.7	10	-0.4	-1.3	943.6	11.3
LCG01-136	120	9	0.3973	0.06244	0.00153	0.62379	0.01509	0.07249	0.00105	451.1	6.3	492.2	11.1	689.2	12.3	-8.3	-34.5	451.1	6.3
LCG01-137	147.6	6.2	0.5132	0.0479	0.00154	0.25974	0.00817	0.03935	0.00061	248.8	3.8	234.5	7.5	94.3	2.9	6.1	163.7		
LCG01-138	2.7	NaN	20.2447	0.83112	0.01297		492.407	38.0458	4.2966	23624	709.4	NA	115.7	4976	15.7	NA	374.8		
LCG01-139	130.1	18.9	0.8079	0.06634	0.00127	1.14244	0.02215	0.12496	0.00168	759	9.6	773.7	12.7	817.1	10.7	-1.9	-7.1	759	9.6
LCG01-140	561.8	90.7	0.574	0.0709	0.00098	1.45911	0.02159	0.14932	0.00184	897.2	10.3	913.6	11.2	954.5	8.6	-1.8	-6.0	897.2	10.3
LCG01-141	368.5	34.1	0.5255	0.05827	0.00095	0.69374	0.01177	0.08639	0.0011	534.2	6.5	535	8.6	539.9	6.8	-0.2	-1.1	534.2	6.5
LCG01-142	593.2	29.2	1.0825	0.06154	0.00109	0.33296	0.00602	0.03926	0.00051	248.2	3.2	291.8	5.6	658.2	8.6	-14.9	-62.3	248.2	3.2

1																				
2	LCG01-143	121.1	18.2	0.677	0.06593	0.00125	1.21333	0.02335	0.13353	0.00179	808	10.2	806.7	12.9	804.2	10.5	0.2	0.5	808	10.2
3	LCG01-144	224.6	44.2	1.2895	0.07147	0.00111	1.48706	0.02428	0.15097	0.00192	906.4	10.8	925.1	12.2	970.9	9.7	-2.0	-6.6	906.4	10.8
4	LCG01-145	114.7	18.3	0.9137	0.06521	0.00128	1.19748	0.0238	0.13324	0.00181	806.3	10.3	799.4	13.2	781.1	10.7	0.9	3.2	806.3	10.3
5	LCG01-146	232.6	NaN	1.8313	0.78774	0.02277	133.056	5.26535	1.22558	0.05074	5157.2	147	4973.6	50.9	4899.7	29.1	3.7	5.3		
6	LCG01-147	95.6	15.3	0.9926	0.06476	0.00137	1.17186	0.02486	0.13131	0.00183	795.3	10.4	787.5	13.9	766.5	11.4	1.0	3.8	795.3	10.4
7	LCG01-148	116.8	44.2	0.5827	0.11229	0.00166	5.19313	0.08155	0.33557	0.00435	1865.3	21	1851.5	16.7	1836.8	12.6	0.7	1.6	1836.8	12.6
8	LCG01-149	207.6	31.9	0.731	0.06566	0.00112	1.21896	0.02149	0.1347	0.00175	814.6	9.9	809.3	12	795.6	9.4	0.7	2.4	814.6	9.9
9	LCG01-150	107.3	16.3	0.9244	0.06466	0.00135	1.12554	0.02359	0.12631	0.00175	766.8	10	765.6	13.5	763.3	11.2	0.2	0.5	766.8	10
10	LCG01-151	94	20.5	0.6905	0.08098	0.00146	2.13688	0.03948	0.19146	0.0026	1129.3	14.1	1160.8	15.6	1221	12.8	-2.7	-7.5	1221	12.8
11	LCG01-152	813	64.5	0.5512	0.05893	0.00089	0.59881	0.00952	0.07373	0.00092	458.6	5.5	476.5	7.5	564.5	6.5	-3.8	-18.8	458.6	5.5
12	LCG01-153	3112.4	327.4	0.0002	0.0568	0.00816	0.89633	0.12783	0.1145	0.00294	698.8	17	649.8	70.1	483.8	55.3	7.6	44.5		
13	LCG01-154	188	17.8	0.6603	0.05564	0.00103	0.64808	0.01229	0.08452	0.00111	523	6.6	507.3	9.1	438	6.6	3.1	19.4	523	6.6
14	LCG01-155	177.4	32.7	0.6126	0.07067	0.0012	1.62651	0.02854	0.167	0.00219	995.6	12.1	980.5	13.5	947.9	10.5	1.5	5.0	995.6	12.1
15	LCG01-156	158.8	20.6	0.7574	0.06302	0.00129	0.98503	0.02032	0.1134	0.00155	692.5	9	696.2	12.4	708.9	10.4	-0.5	-2.3	692.5	9

**LMD02**

sample	concentrations			ratios				ages				discordance		preferred ages					
	ppm U	ppm Pb	atomic Th/U	Pb207/Pb206	1 sigma	Pb207/U235	1 sigma	Pb206/U238	1 sigma	age 206/238	1 sigma	age 207/235	1 sigma	age 207/206	1 sigma	%disc ord.68-75	%disc ord.68-76	preferr ed age	1 sigma
LMD02_001	255.6	38.6	0.6336	0.06529	0.00106	1.22089	0.02062	0.13568	0.00175	820.2	9.9	810.2	11.6	783.7	34.1	1.2	4.7	820.2	9.9
LMD02_002	179.7	25.7	0.6288	0.06661	0.00129	1.18357	0.02325	0.12892	0.00176	781.7	10.1	793	13	825.6	40.4	-1.4	-5.3	781.7	10.1
LMD02_003	107.8	15.5	0.5158	0.06453	0.00132	1.18716	0.02458	0.13348	0.00186	807.7	10.6	794.6	13.6	759	43.1	1.6	6.4	807.7	10.6
LMD02_004	243.1	30.7	0.2979	0.06335	0.00116	1.08604	0.02032	0.12438	0.00166	755.7	9.5	746.6	12	720	38.9	1.2	5.0	755.7	9.5
LMD02_005	102.6	15.2	0.6498	0.06667	0.00147	1.2185	0.02694	0.13261	0.0019	802.7	10.8	809.1	14.7	827.5	46	-0.8	-3.0	802.7	10.8
LMD02_006	164.1	26.1	0.8027	0.0691	0.00138	1.30422	0.02637	0.13694	0.0019	827.3	10.8	847.6	14	901.7	41.2	-2.4	-8.2	827.3	10.8
LMD02_007	192.2	31	1.0616	0.06648	0.00115	1.19916	0.02143	0.13087	0.00172	792.8	9.8	800.2	12	821.5	36.1	-0.9	-3.5	792.8	9.8
LMD02_008	313.7	48.5	0.8102	0.06446	0.00099	1.18322	0.0191	0.13317	0.00169	805.9	9.6	792.8	11	756.8	32.4	1.7	6.5	805.9	9.6
LMD02_009	111.8	17.1	0.74	0.06482	0.00144	1.18985	0.02641	0.13318	0.00191	806	10.9	795.9	14.6	768.5	46.8	1.3	4.9	806	10.9
LMD02_010	138.6	18.8	0.6391	0.06417	0.00131	1.08053	0.02221	0.12217	0.00169	743	9.7	743.9	13	747.2	43.1	-0.1	-0.6	743	9.7
LMD02_011	115.7	16.7	0.5805	0.06293	0.00139	1.14409	0.02542	0.1319	0.00188	798.7	10.7	774.4	14.2	705.9	47	3.1	13.2	798.7	10.7
LMD02_012	505.2	67.4	0.7793	0.06379	0.001	1.02237	0.01688	0.11629	0.00149	709.2	8.6	715.1	10.4	734.7	33.2	-0.8	-3.5	709.2	8.6
LMD02_013	390.8	57.3	0.6168	0.06482	0.00107	1.1908	0.0204	0.13329	0.00173	806.6	9.8	796.3	11.6	768.5	34.8	1.3	5.0	806.6	9.8
LMD02_014	67.3	9.2	0.868	0.06458	0.00206	1.03964	0.03231	0.11681	0.00198	712.2	11.4	723.7	18.7	760.7	67.3	-1.6	-6.4	712.2	11.4
LMD02_015	297.4	41.3	0.9426	0.06502	0.00114	1.05939	0.01911	0.11822	0.00156	720.3	9	733.5	11.5	775	36.9	-1.8	-7.1	720.3	9
LMD02_016	351	49.4	0.4556	0.06462	0.00101	1.18283	0.01944	0.13281	0.0017	803.9	9.7	792.6	11.1	762	32.9	1.4	5.5	803.9	9.7
LMD02_017	247.7	36.5	0.5585	0.06623	0.00105	1.22978	0.0205	0.13472	0.00174	814.7	9.9	814.2	11.5	813.7	33.1	0.1	0.1	814.7	9.9
LMD02_018	579.7	66.6	0.499	0.06484	0.00096	0.96805	0.01516	0.10832	0.00137	663	8	687.5	9.7	769.1	31.2	-3.6	-13.8	663	8
LMD02_019	209.1	27.4	0.5906	0.06444	0.00145	1.0689	0.02398	0.12035	0.00173	732.6	10	738.2	14	756.1	47.5	-0.8	-3.1	732.6	10
LMD02_020	238.6	36	0.6406	0.0662	0.00107	1.23171	0.02078	0.13499	0.00175	816.3	9.9	815.1	11.6	812.7	33.8	0.1	0.4	816.3	9.9
LMD02_021	235.9	36.9	0.8462	0.06452	0.00102	1.18049	0.01953	0.13274	0.00171	803.5	9.7	791.5	11.2	758.7	33.3	1.5	5.9	803.5	9.7
LMD02_022	339.9	49.8	0.459	0.0654	0.00111	1.23592	0.02177	0.13711	0.0018	828.3	10.2	817	12	787.2	35.6	1.4	5.2	828.3	10.2
LMD02_023	81.7	12.2	0.559	0.06522	0.00148	1.23094	0.02797	0.13693	0.00199	827.3	11.3	814.8	15.1	781.4	47.7	1.5	5.9	827.3	11.3
LMD02_024	232.7	33.6	0.6181	0.06516	0.00103	1.16351	0.01931	0.12955	0.00167	785.3	9.5	783.6	11.1	779.5	33.2	0.2	0.7	785.3	9.5
LMD02_025	180.4	26.4	0.6683	0.06572	0.00109	1.1816	0.0204	0.13045	0.0017	790.4	9.7	792.1	11.6	797.5	34.8	-0.2	-0.9	790.4	9.7
LMD02_026	446.4	65.1	0.6762	0.06481	#####	1.16184	0.01748	0.13007	0.00163	788.3	9.3	782.8	10.2	768.2	29.2	0.7	2.6	788.3	9.3
LMD02_027	102.6	15.3	0.6737	0.07139	0.00143	1.30176	0.02643	0.1323	0.00185	801	10.5	846.5	14	968.6	40.9	-5.4	-17.3	801	10.5
LMD02_028	337.9	52.8	0.8675	0.06536	0.00096	1.19072	0.01869	0.13217	0.00167	800.2	9.5	796.3	10.7	785.9	30.8	0.5	1.8	800.2	9.5
LMD02_029	245.1	37.5	0.6453	0.06484	0.00107	1.22456	0.02108	0.13702	0.00179	827.8	10.1	811.9	11.8	769.1	34.7	2.0	7.6	827.8	10.1

1  
2  
3  
4  
5  
6  
7  
8  
9  
10  
11  
12  
13  
14  
15  
16  
17  
18  
19  
20  
21  
22  
23  
24  
25  
26  
27  
28  
29  
30  
31  
32  
33  
34  
35  
36  
37  
38  
39  
40  
41  
42  
43  
44  
45  
46  
47  
48  
49  
50  
51  
52  
53  
54  
55  
56  
57  
58  
59  
60

LMD02_03c	185.6	28.3	0.798	0.0651	0.00122	1.17595	0.02262	0.13106	0.00178	793.9	10.1	789.4	12.7	777.6	39.4	0.6	2.1	793.9	10.1
LMD02_03i	112.4	16.8	0.7878	0.06506	0.00174	1.15744	0.0305	0.12907	0.00202	782.6	11.5	780.8	16.9	776.3	56.3	0.2	0.8	782.6	11.5
LMD02_03e	227.4	37.4	0.9332	0.06552	0.00128	1.23291	0.02457	0.13653	0.00188	825	10.7	815.7	13.4	791.1	41	1.1	4.3	825	10.7
LMD02_03s	112.4	16.8	0.7341	0.06461	0.00175	1.17174	0.03123	0.13158	0.00207	796.9	11.8	787.5	17.2	761.7	57.1	1.2	4.6	796.9	11.8
LMD02_03a	46.4	6.6	0.6876	0.0633	0.00239	1.08908	0.03994	0.12482	0.00233	758.2	13.4	748.1	22.3	718.3	80.2	1.4	5.6	758.2	13.4
LMD02_03f	130.1	19.2	1.0983	0.06349	0.00154	1.1034	0.02664	0.12609	0.00188	765.5	10.8	755	15.2	724.7	51.4	1.4	5.6	765.5	10.8
LMD02_03c	182.4	26.9	0.7583	0.06475	0.00131	1.14715	0.02353	0.12855	0.00179	779.6	10.2	775.9	13.3	766.2	42.6	0.5	1.7	779.6	10.2
LMD02_03j	332.7	48.9	0.6338	0.06539	0.00108	1.19402	0.02056	0.13248	0.00173	802	9.8	797.8	11.6	786.9	34.7	0.5	1.9	802	9.8
LMD02_03h	113.1	18.5	1.1832	0.06533	0.00155	1.15004	0.02715	0.12772	0.00189	774.8	10.8	777.3	15.2	785	49.8	-0.3	-1.3	774.8	10.8
LMD02_03s	305.9	46.5	0.8023	0.06427	0.00111	1.15997	0.02083	0.13094	0.00173	793.2	9.9	781.9	11.9	750.5	36.5	1.4	5.7	793.2	9.9
LMD02_04c	63.4	8.4	0.8568	0.06596	0.0019	1.02937	0.02902	0.11322	0.00183	691.4	10.6	718.6	17	805.1	60.3	-3.8	-14.1	691.4	10.6
LMD02_04i	477.8	69.9	0.7728	0.06611	0.00103	1.17021	0.01922	0.12843	0.00165	778.9	9.4	786.7	11.1	809.9	32.6	-1.0	-3.8	778.9	9.4
LMD02_04e	89.5	14.5	1.0273	0.06506	0.00166	1.21066	0.03069	0.13501	0.00206	816.4	11.7	805.5	16.5	776.3	53.7	1.4	5.2	816.4	11.7
LMD02_04a	157.5	24.3	0.8499	0.06532	0.00136	1.18312	0.02487	0.13142	0.00185	796	10.5	792.8	13.8	784.7	43.7	0.4	1.4	796	10.5
LMD02_04a	105.2	16.1	0.7417	0.06461	0.00157	1.18969	0.02873	0.13359	0.002	808.3	11.4	795.8	15.7	761.7	51.2	1.6	6.1	808.3	11.4
LMD02_04f	38.6	5.8	0.8642	0.06527	0.00249	1.15712	0.04279	0.12862	0.00246	780	14.1	780.6	23.2	783.1	80.2	-0.1	-0.4	780	14.1
LMD02_04c	234.6	34.9	0.5921	0.06617	0.0012	1.23092	0.02306	0.13497	0.00182	816.2	10.3	814.8	12.7	811.8	37.9	0.2	0.5	816.2	10.3
LMD02_04j	125.5	19	0.7067	0.06695	0.00138	1.23195	0.02569	0.13351	0.00188	807.9	10.7	815.2	14	836.2	42.9	-0.9	-3.4	807.9	10.7
LMD02_04h	346.4	50.2	0.8304	0.0638	0.00107	1.08942	0.01902	0.12389	0.00162	752.9	9.3	748.2	11.3	735	35.5	0.6	2.4	752.9	9.3
LMD02_04s	346.4	51.7	0.701	0.06703	0.00107	1.21433	0.02042	0.13145	0.00171	796.1	9.7	807.2	11.5	838.7	33.2	-1.4	-5.1	796.1	9.7
LMD02_05c	166.7	26.4	0.805	0.06748	0.0012	1.26236	0.0232	0.13572	0.00182	820.4	10.3	829	12.6	852.6	37	-1.0	-3.8	820.4	10.3
LMD02_05i	139.9	21.6	0.9927	0.06733	0.00152	1.1772	0.02657	0.12685	0.00185	769.9	10.6	790	14.8	848	46.9	-2.5	-9.2	769.9	10.6
LMD02_05e	207.8	33.8	1.501	0.0645	0.00116	1.0602	0.01975	0.11926	0.0016	726.3	9.2	733.9	11.7	758.1	37.9	-1.0	-4.2	726.3	9.2
LMD02_05a	177.8	28.3	0.667	0.06735	0.00125	1.31704	0.02505	0.14188	0.00193	855.3	10.9	853.2	13.3	848.6	38.6	0.2	0.8	855.3	10.9
LMD02_05a	378.4	35.9	0.9917	0.07366	0.00185	0.82419	0.02038	0.08119	0.00124	503.2	7.4	610.4	13.5	1032.2	50.8	-17.6	-51.2		
LMD02_05f	207.2	30.9	0.7842	0.06403	0.00112	1.13808	0.0206	0.12897	0.00171	782	9.8	771.6	11.9	742.6	37	1.3	5.3	782	9.8
LMD02_05c	757.5	71.8	0.7756	0.06704	0.00112	0.77973	0.01356	0.08439	0.00111	522.3	6.6	585.3	9.5	839	34.8	-10.8	-37.8	522.3	6.6
LMD02_05j	180.4	26.9	0.6943	0.06663	0.00138	1.21224	0.02551	0.132	0.00186	799.3	10.6	806.2	13.9	826.2	43.2	-0.9	-3.3	799.3	10.6
LMD02_05h	323.5	51.2	0.7791	0.06488	0.00109	1.22508	0.02157	0.13701	0.00181	827.7	10.3	812.1	12	770.4	35.4	1.9	7.4	827.7	10.3
LMD02_05s	194.8	30.4	0.8385	0.06434	0.00123	1.17867	0.02312	0.13291	0.00182	804.4	10.4	790.7	12.9	752.8	40.4	1.7	6.9	804.4	10.4
LMD02_06c	96.1	14.1	0.5779	0.06627	0.00158	1.21639	0.02897	0.13318	0.00199	806	11.3	808.1	15.7	814.9	49.8	-0.3	-1.1	806	11.3
LMD02_06i	289.5	44.8	0.7083	0.06516	0.00116	1.22889	0.02268	0.13683	0.00183	826.7	10.4	813.8	12.5	779.5	37.4	1.6	6.1	826.7	10.4
LMD02_06e	117.6	19.5	1.1976	0.0653	0.00161	1.17376	0.02885	0.13042	0.00197	790.3	11.2	788.4	15.9	784	51.8	0.2	0.8	790.3	11.2
LMD02_06a	96.1	14.1	0.6036	0.06643	0.00161	1.21335	0.02926	0.13251	0.00199	802.2	11.3	806.7	15.9	820	50.6	-0.6	-2.2	802.2	11.3
LMD02_06a	277.1	40.8	0.5808	0.06448	0.00125	1.19599	0.02379	0.13457	0.00185	813.9	10.5	798.7	13.1	757.4	40.9	1.9	7.5	813.9	10.5
LMD02_06f	261.4	37.7	0.6099	0.06419	0.00122	1.15579	0.02256	0.13064	0.00178	791.5	10.1	780	12.7	747.9	40.2	1.5	5.8	791.5	10.1
LMD02_06c	314.4	49.8	1.2558	0.06438	0.00123	1.09379	0.02147	0.12327	0.00169	749.4	9.7	750.3	12.5	754.1	40.3	-0.1	-0.6	749.4	9.7
LMD02_06j	233.3	36.2	0.7766	0.06734	0.00163	1.25431	0.03031	0.13514	0.00204	817.1	11.6	825.3	16.1	848.3	50.3	-1.0	-3.7	817.1	11.6
LMD02_06h	124.2	18.3	0.5838	0.06595	0.00153	1.21999	0.02834	0.13421	0.00198	811.8	11.3	809.8	15.3	804.8	48.6	0.3	0.9	811.8	11.3
LMD02_06s	394.1	57.1	0.6058	0.06619	0.00126	1.19004	0.0232	0.13044	0.00179	790.4	10.2	796	12.9	812.4	39.8	-0.7	-2.7	790.4	10.2
LMD02_07c	293.5	41.3	0.7705	0.0636	0.00122	1.07719	0.02113	0.12288	0.00168	747.1	9.6	742.3	12.4	728.4	40.7	0.7	2.6	747.1	9.6
LMD02_07i	108.5	18.2	0.8694	0.06669	0.00167	1.29697	0.03242	0.1411	0.00216	850.9	12.2	844.4	16.8	828.1	52.2	0.8	2.7	850.9	12.2
LMD02_07e	314.4	54.2	1.6577	0.06366	0.00124	1.08886	0.02169	0.12409	0.00171	754.1	9.8	747.9	12.6	730.4	41.3	0.8	3.2	754.1	9.8
LMD02_07a	292.8	45.4	0.6989	0.0648	0.00123	1.22376	0.0239	0.13701	0.00188	827.7	10.7	811.5	13.1	767.8	40	2.0	7.8	827.7	10.7
LMD02_07a	165.4	26	1.0265	0.06489	0.00148	1.14472	0.02627	0.128	0.00187	776.4	10.7	774.7	14.7	770.8	48	0.2	0.7	776.4	10.7
LMD02_07f	73.9	10.2	0.485	0.069	0.0024	1.23705	0.04185	0.13008	0.00239	788.3	13.6	817.5	22.1	898.7	71.8	-3.6	-12.3	788.3	13.6
LMD02_07c	190.2	28.9	0.5713	0.06731	0.00149	1.28576	0.02877	0.13859	0.00202	836.7	11.4	839.4	15.1	847.4	46	-0.3	-1.3	836.7	11.4
LMD02_07j	709.8	100.9	0.6332	0.06459	0.00116	1.1408	0.02119	0.12815	0.00172	777.3	9.8	772.9	12.1	761	37.9	0.6	2.1	777.3	9.8
LMD02_07h	417	65.1	0.8635	0.06552	0.00113	1.19814	0.0216	0.13269	0.00177	803.2	10.1	799.7	12.1	791.1	36.2	0.4	1.5	803.2	10.1



LMD02_12f	125.8	20.1	0.7855	0.06614	0.00138	1.2531	0.02637	0.13749	0.00191	830.5	10.8	824.8	14.2	810.8	11.7	0.7	2.4	830.5	10.8
LMD02_12f	243.5	36.8	0.6414	0.06705	0.00117	1.24079	0.02233	0.13429	0.00176	812.3	10	819.2	12.3	839.3	10	-0.8	-3.2	812.3	10

**LCG03**

sample	concentrations		ratios					ages					discordance		preferred ages				
	ppm U	ppm Pb	atomic Th/U	Pb207/Pb206	1 sigma	Pb207/U235	1 sigma	Pb206/U238	1 sigma	age 206/238	1 sigma	age 207/235	1 sigma	age 207/206	1 sigma	%disc ord.68-75	%disc ord.68-76	preferred age	1 sigma
LCG03-1	58.8	9.3	0.6696	0.06699	0.00178	1.29322	0.03392	0.1401	0.00217	845.2	12.3	842.7	17.6	837.5	15.2	0.3	0.9	845.2	12.3
LCG03-2	133.9	22.1	0.9601	0.06702	0.00132	1.24832	0.02494	0.13517	0.00184	817.3	10.4	822.6	13.5	838.4	11.2	-0.7	-2.5	817.3	10.4
LCG03-3	17.2	2.5	0.6536	0.06926	0.00317	1.25261	0.05515	0.13125	0.00285	795	16.2	824.6	28.6	906.5	27.4	-3.6	-12.3	795	16.2
LCG03-4	135.4	24.6	0.7251	0.1136	0.00189	2.41376	0.04118	0.1542	0.00207	924.5	11.6	1246.7	15.4	1857.8	14.2	-25.8	-50.2		
LCG03-5	196.8	31.2	0.9818	0.06666	0.00117	1.18624	0.02137	0.12914	0.00169	783	9.6	794.2	12.1	827.2	9.9	-1.4	-5.3	783	9.6
LCG03-6	75.1	11.6	0.8835	0.07132	0.00169	1.269	0.02974	0.12912	0.00191	782.8	10.9	831.9	15.9	966.6	14.8	-5.9	-19.0	782.8	10.9
LCG03-7	119.2	19	0.8304	0.06916	0.00137	1.28678	0.02582	0.13501	0.00185	816.4	10.5	839.9	13.8	903.5	11.9	-2.8	-9.6	816.4	10.5
LCG03-8	268.3	41	0.8239	0.06601	0.00108	1.18178	0.02008	0.12993	0.00166	787.5	9.5	792.1	11.4	806.7	9.1	-0.6	-2.4	787.5	9.5
LCG03-9	94.4	15.7	1.2788	0.06343	0.00148	1.10029	0.02556	0.12588	0.00182	764.3	10.4	753.5	14.6	722.7	12.1	1.4	5.8	764.3	10.4
LCG03-10	144.1	28.4	1.0877	0.07116	0.00128	1.53508	0.02829	0.15654	0.00208	937.5	11.6	944.5	13.8	962	11.2	-0.7	-2.5	937.5	11.6
LCG03-11	18.3	-0.3	0.8761	0.87223	0.03895	4.24802	0.12479	0.03534	0.00136	223.9	8.5	1683.4	48.5	5044.5	45	-86.7	-95.6		
LCG03-12	349	54.1	0.7727	0.06574	0.00102	1.21344	0.01974	0.13394	0.00169	810.3	9.6	806.8	11.1	798.1	8.6	0.4	1.5	810.3	9.6
LCG03-13	139	23.1	1.0588	0.0662	0.0013	1.21326	0.02412	0.13299	0.0018	804.9	10.2	806.7	13.3	812.7	11	-0.2	-1.0	804.9	10.2
LCG03-14	44.1	6.1	0.6251	0.06663	0.00209	1.14417	0.03498	0.12462	0.0021	757.1	12	774.5	19.3	826.2	17.7	-2.2	-8.4	757.1	12
LCG03-15	190.2	32.9	0.18	0.07448	0.00123	1.8067	0.03096	0.17603	0.00229	1045.2	12.6	1047.9	13.7	1054.5	10.8	-0.3	-0.9	1045.2	12.6
LCG03-16	110.1	17.6	0.9022	0.06468	0.00141	1.18945	0.02593	0.13345	0.00188	807.5	10.7	795.7	14.3	763.9	11.7	1.5	5.7	807.5	10.7
LCG03-17	98.4	16.2	0.8713	0.06649	0.00148	1.27221	0.02832	0.13885	0.00198	838.2	11.2	833.4	15	821.8	12.5	0.6	2.0	838.2	11.2
LCG03-18	377.9	53	0.3136	0.06655	0.00103	1.25971	0.02048	0.13738	0.00174	829.8	9.9	827.8	11.3	823.7	8.7	0.2	0.7	829.8	9.9
LCG03-19	258.2	39.2	0.9032	0.06686	0.00113	1.16996	0.02054	0.12699	0.00164	770.7	9.4	786.6	11.6	833.4	9.6	-2.0	-7.5	770.7	9.4
LCG03-20	70.5	11	0.9682	0.0597	0.00165	1.05135	0.02874	0.12781	0.00198	775.4	11.3	729.6	16.5	592.7	12.4	6.3	30.8		
LCG03-21	222.2	35.2	0.6832	0.06589	0.00115	1.26886	0.02276	0.13974	0.00182	843.2	10.3	831.9	12.4	802.9	9.7	1.4	5.0	843.2	10.3
LCG03-22	302.3	43.4	0.6458	0.06527	0.00105	1.1457	0.01918	0.12738	0.00162	772.9	9.3	775.2	11.1	783.1	8.8	-0.3	-1.3	772.9	9.3
LCG03-23	116.7	18.1	0.8028	0.06601	0.00135	1.20069	0.02484	0.132	0.00182	799.3	10.4	800.9	13.7	806.7	11.4	-0.2	-0.9	799.3	10.4
LCG03-24	45.7	7.1	0.7508	0.06378	0.00188	1.18415	0.03423	0.13474	0.00218	814.8	12.4	793.2	18.5	734.3	15.4	2.7	11.0	814.8	12.4
LCG03-25	141.5	21.8	0.6055	0.06581	0.00126	1.25875	0.02448	0.1388	0.00187	837.9	10.6	827.3	13.3	800.3	10.6	1.3	4.7	837.9	10.6
LCG03-26	140	21	0.7479	0.06545	0.00128	1.17563	0.0234	0.13035	0.00177	789.9	10.1	789.3	13.1	788.8	10.7	0.1	0.1	789.9	10.1
LCG03-27	702.1	191.8	13.3263	0.70131	0.02254	48.1939	1.59021	0.49871	0.01769	2608.2	76.1	3955.7	47.6	4733.4	32.3	-34.1	-44.9		
LCG03-28	119.2	18.3	0.6676	0.06775	0.00135	1.27383	0.02565	0.13646	0.00187	824.6	10.6	834.1	13.8	860.9	11.6	-1.1	-4.2	824.6	10.6
LCG03-29	168.4	25.9	0.7293	0.06569	0.0012	1.20992	0.02265	0.13367	0.00177	808.8	10.1	805.2	12.5	796.5	10.1	0.4	1.5	808.8	10.1
LCG03-30	539.7	55.7	0.2499	0.06179	0.00093	0.8849	0.01411	0.10394	0.0013	637.5	7.6	643.6	9.3	666.8	7.4	-1.0	-4.4	637.5	7.6
LCG03-31	137	24	1.3662	0.0651	0.00129	1.17295	0.0236	0.13075	0.00178	792.1	10.1	788	13.2	777.6	10.8	0.5	1.9	792.1	10.1
LCG03-32	112.1	16.4	0.5734	0.06917	0.00141	1.26845	0.0261	0.13307	0.00184	805.4	10.5	831.7	14	903.8	12.2	-3.2	-10.9	805.4	10.5
LCG03-33	26.4	4.4	1.1888	0.06697	0.00247	1.179	0.04216	0.12776	0.00238	775.1	13.6	790.8	22.7	836.8	21	-2.0	-7.4	775.1	13.6
LCG03-34	2166.5	260.6	0.0012	0.34411	0.01985	6.36752	0.32134	0.13429	0.00539	812.3	30.6	2027.8	61.7	3681.1	57	-59.9	-77.9		
LCG03-35	50.2	8.2	0.975	0.06682	0.00186	1.23746	0.03392	0.1344	0.00213	812.9	12.1	817.7	18	832.2	15.8	-0.6	-2.3	812.9	12.1
LCG03-36	98.4	58	3.3217	0.10831	0.0017	4.58331	0.076	0.30711	0.00408	1726.5	20.1	1746.2	17.1	1771.2	13.2	-1.1	-2.5	1771.2	13.2
LCG03-37	1169.7	232.6	1.0944	0.07955	0.00106	1.69149	0.02449	0.1543	0.00189	925	10.6	1005.3	11.6	1185.9	9.3	-8.0	-22.0	925	10.6
LCG03-38	148.6	23.3	0.6663	0.06984	0.0013	1.3391	0.0255	0.13916	0.00187	839.9	10.6	862.8	13.3	923.7	11.3	-2.7	-9.1	839.9	10.6
LCG03-39	106.5	16.2	0.8184	0.06684	0.00142	1.19607	0.02562	0.12987	0.00182	787.1	10.4	798.8	14.1	832.8	12.1	-1.5	-5.5	787.1	10.4
LCG03-40	205.4	34.9	0.9937	0.06674	0.00115	1.27795	0.0228	0.13896	0.00181	838.8	10.2	835.9	12.3	829.7	9.8	0.3	1.1	838.8	10.2
LCG03-41	136.5	20.4	0.6158	0.06832	0.00133	1.26627	0.02496	0.1345	0.00182	813.5	10.3	830.7	13.5	878.3	11.4	-2.1	-7.4	813.5	10.3









1  
2  
3  
4  
5  
6  
7  
8  
9  
10  
11  
12  
13  
14  
15  
16  
17  
18  
19  
20  
21  
22  
23  
24  
25  
26  
27  
28  
29  
30  
31  
32  
33  
34  
35  
36  
37  
38  
39  
40  
41  
42  
43  
44  
45  
46  
47  
48  
49  
50  
51  
52  
53  
54  
55  
56  
57  
58  
59  
60

LCG04-031	99.6	15.1	0.7798	0.0626	0.00112	1.13326	0.02094	0.13139	0.00177	795.8	10.1	769.3	12.1	694.7	9	3.4	14.6	795.8	10.1
LCG04-032	264.8	38.6	0.5143	0.06522	0.00089	1.21972	0.01807	0.13574	0.00172	820.5	9.8	809.6	10.4	781.4	7.4	1.3	5.0	820.5	9.8
LCG04-033	97.2	54.4	0.9419	0.15658	0.00185	9.63293	0.1288	0.4465	0.00569	2379.7	25.4	2400.3	16	2419.1	10.9	-0.9	-1.6	2419.1	10.9
LCG04-034	213.4	96.1	1.9333	0.12269	0.00141	5.13888	0.06705	0.304	0.00378	1711.1	18.7	1842.6	14.4	1995.7	10	-7.1	-14.3	1995.7	10
LCG04-035	42.7	6.8	0.9375	0.06252	0.0016	1.14137	0.02898	0.13249	0.00202	802.1	11.5	773.2	16.1	691.9	12.8	3.7	15.9	802.1	11.5
LCG04-036	307.5	44.9	0.5436	0.06541	0.00086	1.21354	0.01746	0.13465	0.00169	814.3	9.6	806.8	10.1	787.6	7.2	0.9	3.4	814.3	9.6
LCG04-037	154.9	32	0.5385	0.07518	0.00104	1.96186	0.02933	0.18939	0.00242	1118.1	13.1	1102.5	12.7	1073.3	9.2	1.4	4.2	1073.3	9.2
LCG04-038	234	42	0.4228	0.07163	0.00094	1.68024	0.02403	0.17023	0.00214	1013.4	11.8	1001.1	11.6	975.4	8.2	1.2	3.9	1013.4	11.8
LCG04-039	98	14.6	0.6374	0.06583	0.00116	1.21748	0.02214	0.13422	0.0018	811.9	10.2	808.6	12.3	801	9.8	0.4	1.4	811.9	10.2
LCG04-040	217.4	33.8	0.2898	0.07008	0.00095	1.51262	0.02215	0.15664	0.00198	938.1	11	935.5	11.3	930.7	8.3	0.3	0.8	938.1	11
LCG04-041	193.6	29.1	1.1225	0.067	0.001	1.16133	0.01834	0.12578	0.00162	763.7	9.3	782.6	10.8	837.8	8.5	-2.4	-8.8	763.7	9.3
LCG04-042	292.4	42.8	0.6406	0.06694	0.00089	1.22852	0.01775	0.13318	0.00167	806	9.5	813.7	10.2	835.9	7.6	-0.9	-3.6	806	9.5
LCG04-043	30	4.7	0.6113	0.06644	0.00193	1.29732	0.03708	0.1417	0.00232	854.3	13.1	844.5	19.1	820.3	16.3	1.2	4.1	854.3	13.1
LCG04-044	114.6	17.4	0.5947	0.06558	0.00112	1.24746	0.02207	0.13805	0.00184	833.6	10.4	822.3	12.2	793	9.4	1.4	5.1	833.6	10.4
LCG04-045	246.6	31.6	0.9045	0.06694	0.00097	1.06174	0.01641	0.1151	0.00147	702.3	8.5	734.7	10.1	835.9	8.3	-4.4	-16.0	702.3	8.5
LCG04-046	309	50	0.3215	0.0697	0.00089	1.51944	0.02135	0.1582	0.00197	946.8	11	938.3	10.9	919.5	7.7	0.9	3.0	946.8	11
LCG04-047	362	62.2	0.5282	0.07052	0.00088	1.55871	0.02145	0.1604	0.00199	959	11.1	954	10.9	943.5	7.7	0.5	1.6	959	11.1
LCG04-048	77.5	10	1.6918	0.06058	0.00139	0.76612	0.01748	0.09177	0.00132	566	7.8	577.5	11.9	624.4	10.7	-2.0	-9.3	566	7.8
LCG04-049	264	42.8	0.2561	0.07277	0.00095	1.65508	0.02351	0.16505	0.00206	984.8	11.4	991.5	11.4	1007.6	8.3	-0.7	-2.3	984.8	11.4
LCG04-050	355.7	68.2	0.9557	0.06777	0.00085	1.47221	0.02034	0.15763	0.00195	943.6	10.9	919	10.7	861.5	7.3	2.7	9.5	943.6	10.9
LCG04-051	578.6	101.7	0.4945	0.07302	0.00085	1.65182	0.02171	0.16415	0.00201	979.8	11.1	990.2	10.7	1014.5	7.5	-1.1	-3.4	979.8	11.1
LCG04-052	286.9	41.7	0.715	0.06427	0.00087	1.13954	0.01676	0.12866	0.00161	780.2	9.2	772.3	10	750.5	7.2	1.0	4.0	780.2	9.2
LCG04-053	162	23.3	0.6363	0.06442	0.001	1.15493	0.01891	0.1301	0.00168	788.4	9.6	779.6	11	755.4	8.3	1.1	4.4	788.4	9.6
LCG04-054	255.3	38.1	0.63	0.06527	0.00092	1.21877	0.01841	0.13549	0.00171	819.1	9.7	809.2	10.6	783.1	7.7	1.2	4.6	819.1	9.7
LCG04-055	150.2	23.5	0.6927	0.0658	0.00105	1.25946	0.021	0.13888	0.00181	838.3	10.2	827.7	11.7	800	8.8	1.3	4.8	838.3	10.2
LCG04-056	372.3	152.2	0.5005	0.12587	0.00141	6.40439	0.08198	0.36921	0.00452	2025.7	21.3	2032.9	14.6	2041.1	9.9	-0.4	-0.8	2041.1	9.9
LCG04-057	60.9	9.3	0.5715	0.06637	0.00148	1.27303	0.0284	0.13918	0.00203	840	11.5	833.7	15.2	818.1	12.5	0.8	2.7	840	11.5
LCG04-058	130.4	20.5	0.6698	0.06445	0.00105	1.23898	0.02103	0.13949	0.00182	841.8	10.3	818.4	11.7	756.4	8.7	2.9	11.3	841.8	10.3
LCG04-059	198.4	18.8	0.632	0.05626	0.00097	0.66234	0.01178	0.08543	0.00111	528.5	6.6	516	8.7	462.6	6.4	2.4	14.2	528.5	6.6
LCG04-060	360.4	63.1	0.3605	0.07042	0.00088	1.63746	0.02252	0.16873	0.00208	1005.1	11.5	984.7	11.1	940.6	7.7	2.1	6.9	1005.1	11.5
LCG04-061	384.9	56.8	0.8938	0.06887	#####	1.21168	0.01724	0.12766	0.00159	774.5	9.1	806	10	894.8	7.8	-3.9	-13.4	774.5	9.1
LCG04-062	236.3	24.5	0.2116	0.05909	0.00093	0.85621	0.01412	0.10515	0.00135	644.5	7.9	628.1	9.5	570.4	6.9	2.6	13.0	644.5	7.9
LCG04-063	283.7	42.2	0.5179	0.06472	0.00087	1.22879	0.01797	0.13776	0.00172	832	9.7	813.8	10.3	765.2	7.2	2.2	8.7	832	9.7
LCG04-064	88.5	3.9	0.598	0.0541	0.00181	0.2984	0.00971	0.04003	0.00065	253	4	265.1	8.7	375.2	10.5	-4.6	-32.6	253	4
LCG04-065	180.2	27.3	0.6337	0.06629	0.00105	1.2531	0.02086	0.13717	0.00178	828.6	10.1	824.8	11.6	815.5	8.9	0.5	1.6	828.6	10.1
LCG04-066	158.9	64.8	0.3231	0.12252	0.00146	6.4245	0.08595	0.38046	0.00474	2078.4	22.1	2035.6	15.1	1993.2	10.4	2.1	4.3	1993.2	10.4
LCG04-067	550.9	103.1	0.091	0.08083	0.00094	2.18237	0.02863	0.19592	0.00239	1153.4	12.9	1175.4	11.7	1217.3	8.2	-1.9	-5.3	1217.3	8.2
LCG04-068	315.4	41	0.633	0.06893	0.00101	1.13261	0.01754	0.11922	0.00152	726.1	8.8	769	10.5	896.6	8.7	-5.6	-19.0	726.1	8.8
LCG04-069	176.3	25.7	0.5128	0.06681	0.00103	1.25135	0.02023	0.1359	0.00175	821.4	9.9	824	11.3	831.9	8.8	-0.3	-1.3	821.4	9.9
LCG04-070	349.4	43.3	0.3524	0.06366	0.00086	1.05799	0.01546	0.12059	0.0015	734	8.6	732.8	9.6	730.4	7	0.2	0.5	734	8.6
LCG04-071	302.7	43.9	0.5469	0.06593	0.00089	1.22096	0.01783	0.13438	0.00168	812.8	9.5	810.2	10.3	804.2	7.5	0.3	1.1	812.8	9.5
LCG04-072	117	13.7	0.7387	0.05795	0.00114	0.80079	0.01601	0.10026	0.00136	615.9	8	597.3	10.8	527.9	8.1	3.1	16.7	615.9	8
LCG04-073	1123.1	239.2	0.0742	0.10132	0.00114	3.11656	0.03982	0.22317	0.0027	1298.6	14.2	1436.8	12.7	1648.4	9.2	-9.6	-21.2		
LCG04-074	377.8	56.8	1.0013	0.06823	0.00091	1.1708	0.01695	0.12451	0.00155	756.5	8.9	787	10	875.5	7.8	-3.9	-13.6	756.5	8.9
LCG04-075	153.3	6.6	0.5352	0.0504	0.00134	0.2777	0.00727	0.03998	0.00058	252.7	3.6	248.8	6.7	213.5	5.1	1.6	18.4	252.7	3.6
LCG04-076	627.6	126.9	0.3824	0.07535	0.00088	2.00544	0.02636	0.1931	0.00235	1138.1	12.7	1117.4	11.4	1077.9	7.8	1.9	5.6		
LCG04-077	190.5	87.6	0.9152	0.15946	0.00195	8.66668	0.11807	0.39434	0.00499	2142.9	23.1	2303.6	16	2449.9	11.3	-7.0	-12.5	2449.9	11.3
LCG04-078	275.1	44.8	0.7731	0.06539	0.00089	1.2719	0.0187	0.14113	0.00176	851	9.9	833.2	10.5	786.9	7.5	2.1	8.2	851	9.9
LCG04-079	85.4	12.8	0.4302	0.06496	0.00121	1.27363	0.02432	0.14226	0.00193	857.4	10.9	834	13.1	773	10.1	2.8	10.9	857.4	10.9









1  
2  
3  
4  
5  
6  
7  
8  
9  
10  
11  
12  
13  
14  
15  
16  
17  
18  
19  
20  
21  
22  
23  
24  
25  
26  
27  
28  
29  
30  
31  
32  
33  
34  
35  
36  
37  
38  
39  
40  
41  
42  
43  
44  
45  
46  
47  
48  
49  
50  
51  
52  
53  
54  
55  
56  
57  
58  
59  
60

LCG05_064	1032.87	1285.41	1.2445	0.25635	0.00521	0.0366	0.00049	0.05079	0.00101	231.7	4.21	231.5	45.48	231.8	3.07	-0.1	0.0	231.8	3.07
LCG05_065	161.30	106.74	0.6618	6.86711	0.10429	0.39334	0.00535	0.12662	0.00175	2094.4	13.46	2051.6	24.21	2138.3	24.74	-4.1	-2.1	2051.6	24.21
LCG05_066	546.15	130.47	0.2389	5.11992	0.06832	0.33419	0.00422	0.11112	0.0013	1839.4	11.33	1817.7	21.07	1858.7	20.4	-2.2	-1.0	1817.7	21.07
LCG05_067	2476.06	601.41	0.2429	0.4985	0.00714	0.06665	0.00083	0.05424	7.00E-04	410.7	4.83	381	28.95	416	5.04	-8.4	-1.3	416	5.04
LCG05_068	1672.40	822.36	0.4917	0.26684	0.00469	0.03984	0.00052	0.04857	0.00082	240.2	3.76	127.2	39.03	251.9	3.21	-49.5	-4.6	251.9	3.21
LCG05_069	2391.17	1351.28	0.5651	0.50539	0.00728	0.06717	0.00084	0.05457	0.00071	415.3	4.91	394.5	28.85	419.1	5.09	-5.9	-0.9	419.1	5.09
LCG05_070	2102.53	1134.20	0.5394	0.51699	0.00783	0.0658	0.00084	0.05698	8.00E-04	423.1	5.24	490.2	30.95	410.8	5.05	19.3	3.0	410.8	5.05
LCG05_071	614.06	538.21	0.8765	4.08684	0.05535	0.28179	0.00357	0.10519	0.00126	1651.7	11.05	1717.6	21.82	1600.4	17.96	7.3	3.2	1717.6	21.82
LCG05_072	254.68	72.76	0.2857	9.83227	0.13486	0.44849	0.00584	0.15901	0.00192	2419.2	12.64	2445.1	20.27	2388.5	25.99	2.4	1.3	2445.1	20.27
LCG05_073	2040.28	1456.64	0.7139	0.31229	0.00506	0.0438	0.00056	0.05172	0.00079	276	3.92	272.8	34.52	276.3	3.46	-1.3	-0.1	276.3	3.46
LCG05_074	973.45	332.90	0.3420	0.53665	0.00956	0.07078	0.00093	0.05499	0.00094	436.2	6.32	411.8	37.51	440.9	5.62	-6.6	-1.1	440.9	5.62
LCG05_075	1403.57	812.15	0.5786	0.3356	0.00588	0.04544	0.00059	0.05357	9.00E-04	293.8	4.47	353	37.54	286.4	3.66	23.3	2.6	286.4	3.66
LCG05_076	90.55	138.09	1.5250	6.79137	0.12399	0.37636	0.00573	0.13088	0.00227	2084.6	16.16	2109.8	30.08	2059.3	26.81	2.5	1.2	2109.8	30.08
LCG05_077	1788.43	1144.84	0.6401	0.26606	0.0056	0.03983	0.00054	0.04845	0.00101	239.5	4.49	121.1	48.19	251.8	3.36	-51.9	-4.9	251.8	3.36
LCG05_078	2524.17	814.07	0.3225	6.12181	0.07655	0.36592	0.0045	0.12134	0.00129	1993.4	10.91	1976.1	18.82	2010.2	21.24	-1.7	-0.8	1976.1	18.82
LCG05_079	546.15	243.76	0.4463	7.09284	0.09346	0.40378	0.0051	0.12741	0.00146	2123.1	11.73	2062.5	20.04	2186.4	23.4	-5.7	-2.9	2062.5	20.04
LCG05_080	1018.72	652.79	0.6408	4.95906	0.06531	0.32489	0.00408	0.11071	0.00127	1812.4	11.13	1811.1	20.69	1813.6	19.84	-0.1	-0.1	1811.1	20.69
LCG05_081	469.74	324.95	0.6918	5.04866	0.07096	0.33125	0.00428	0.11054	0.00139	1827.5	11.91	1808.4	22.61	1844.5	20.72	-2.0	-0.9	1808.4	22.61
LCG05_082	1208.32	150.38	0.1245	10.0165	0.13084	0.47153	0.00596	0.15407	0.00174	2436.3	12.06	2391.6	19.06	2490.3	26.09	-4.0	-2.2	2391.6	19.06
LCG05_083	404.66	263.66	0.6516	10.9212	0.14467	0.48736	0.00622	0.16253	0.00187	2516.4	12.32	2482.2	19.23	2559.3	26.95	-3.0	-1.7	2482.2	19.23
LCG05_084	2328.92	1290.31	0.5540	5.12435	0.06484	0.33872	0.00418	0.10973	0.00119	1840.2	10.75	1794.9	19.58	1880.5	20.13	-4.6	-2.1	1794.9	19.58
LCG05_085	376.36	181.20	0.4815	4.81912	0.0691	0.32125	0.00418	0.10881	0.0014	1788.2	12.06	1779.4	23.35	1795.8	20.4	-0.9	-0.4	1779.4	23.35
LCG05_086	755.55	566.97	0.7504	0.36891	0.00886	0.05126	0.00074	0.0522	0.00126	318.8	6.57	294.3	53.95	322.2	4.51	-8.7	-1.1	322.2	4.51
LCG05_087	5031.36	909.03	0.1807	3.99514	0.04999	0.25965	0.00319	0.1116	0.00119	1633.2	10.16	1825.7	19.18	1488	16.32	22.7	9.8	1825.7	19.18
LCG05_088	4278.64	506.94	0.1185	10.3591	0.12913	0.45189	0.00556	0.16627	0.00176	2467.4	11.54	2520.5	17.64	2403.7	24.67	4.9	2.7	2520.5	17.64
LCG05_089	673.49	441.88	0.6561	11.4191	0.14695	0.4161	0.00523	0.19905	0.0022	2558	12.01	2818.4	17.96	2242.7	23.8	25.7	14.1	2818.4	17.96
LCG05_090	367.87	317.27	0.8624	9.71064	0.13034	0.44128	0.00566	0.15961	0.00187	2407.7	12.36	2451.5	19.67	2356.4	25.33	4.0	2.2	2451.5	19.67
LCG05_091	362.21	484.10	1.3365	0.64511	0.01393	0.08254	0.00116	0.05669	0.00121	505.5	8.6	478.8	46.97	511.3	6.9	-6.4	-1.1	511.3	6.9
LCG05_092	820.64	310.99	0.3790	10.3718	0.1326	0.46126	0.00575	0.1631	0.00178	2468.5	11.84	2488	18.32	2445.1	25.38	1.8	1.0	2488	18.32
LCG05_093	1547.89	91.32	0.0590	1.25326	0.01828	0.14032	0.00178	0.06478	0.00086	824.9	8.24	767.2	27.65	846.5	10.07	-9.4	-2.6	846.5	10.07
LCG05_094	752.72	617.42	0.8202	1.16921	0.01793	0.12893	0.00166	0.06578	0.00093	786.3	8.39	799.3	29.39	781.8	9.46	2.2	0.6	781.8	9.46
LCG05_095	257.51	109.12	0.4238	5.34905	0.07869	0.33858	0.00447	0.11459	0.00152	1876.7	12.58	1873.4	23.8	1879.9	21.55	-0.3	-0.2	1873.4	23.8
LCG05_096	189.60	116.28	0.6133	5.3093	0.08157	0.3309	0.00447	0.11638	0.00164	1870.4	13.13	1901.3	25.1	1842.7	21.65	3.2	1.5	1901.3	25.1
LCG05_097	648.02	232.01	0.3580	0.51705	0.0106	0.06911	0.00095	0.05426	0.00109	423.2	7.1	381.8	44.55	430.8	5.72	-11.4	-1.8	430.8	5.72
LCG05_098	1881.81	419.78	0.2231	5.18073	0.0658	0.33538	0.00414	0.11205	0.00122	1849.5	10.81	1832.9	19.55	1864.4	20	-1.7	-0.8	1832.9	19.55
LCG05_099	1089.47	429.60	0.3943	5.35106	0.07008	0.34464	0.00431	0.11262	0.00128	1877.1	11.2	1842.1	20.4	1909	20.68	-3.5	-1.7	1842.1	20.4
LCG05_100	1126.26	640.18	0.5684	5.25063	0.0679	0.3383	0.00421	0.11258	0.00125	1860.9	11.03	1841.4	20.04	1878.5	20.29	-2.0	-0.9	1841.4	20.04
LCG05_101	1477.15	701.87	0.4752	5.34823	0.06842	0.344	0.00426	0.11277	0.00124	1876.6	10.94	1844.5	19.71	1905.9	20.44	-3.2	-1.5	1844.5	19.71
LCG05_102	599.92	174.66	0.2911	9.87196	0.1286	0.45244	0.00569	0.15827	0.00178	2422.9	12.01	2437.2	18.89	2406.1	25.28	1.3	0.7	2437.2	18.89
LCG05_103	322.60	193.18	0.5988	6.68289	0.09341	0.37336	0.00484	0.12983	0.00161	2070.4	12.34	2095.7	21.62	2045.2	22.74	2.5	1.2	2095.7	21.62
LCG05_104	2238.36	1235.35	0.5519	9.24985	0.11645	0.43275	0.00534	0.15504	0.00166	2363.1	11.54	2402.3	18.08	2318.1	24.01	3.6	1.9	2402.3	18.08
LCG05_105	2988.26	1623.36	0.5432	5.18534	0.06598	0.33627	0.00416	0.11185	0.00122	1850.2	10.83	1829.7	19.59	1868.7	20.05	-2.1	-1.0	1829.7	19.59
LCG05_106	1129.09	169.90	0.1505	5.14796	0.06745	0.33213	0.00416	0.11243	0.00128	1844.1	11.14	1839.1	20.41	1848.7	20.11	-0.5	-0.2	1839.1	20.41
LCG05_107	2011.98	679.22	0.3376	1.79608	0.02446	0.10555	0.00134	0.12343	0.0015	1044	8.88	2006.4	21.47	646.8	7.8	210.2	61.4	646.8	7.8
LCG05_108	178.28	279.86	1.5698	10.3658	0.1685	0.4595	0.00668	0.16363	0.00244	2468	15.05	2493.6	24.87	2437.3	29.52	2.3	1.3	2493.6	24.87
LCG05_109	390.51	260.03	0.6659	10.9466	0.15057	0.47572	0.0062	0.16691	0.00201	2518.6	12.8	2526.9	20.09	2508.6	27.08	0.7	0.4	2526.9	20.09
LCG05_110	449.94	254.66	0.5660	7.36464	0.10241	0.40813	0.00529	0.13089	0.00161	2156.7	12.43	2109.9	21.38	2206.4	24.2	-4.4	-2.3	2109.9	21.38
LCG05_111	551.81	166.49	0.3017	10.4524	0.1604	0.47901	0.00669	0.15828	0.00219	2475.7	14.22	2437.4	23.26	2522.9	29.15	-3.4	-1.9	2437.4	23.26
LCG05_112	899.87	593.94	0.6600	3.90089	0.05364	0.28529	0.00362	0.09918	0.00121	1613.9	11.11	1608.8	22.49	1617.9	18.18	-0.6	-0.2	1608.8	22.49



1  
2  
3  
4  
5  
6  
7  
8  
9  
10  
11  
12  
13  
14  
15  
16  
17  
18  
19  
20  
21  
22  
23  
24  
25  
26  
27  
28  
29  
30  
31  
32  
33  
34  
35  
36  
37  
38  
39  
40  
41  
42  
43  
44  
45  
46  
47  
48  
49  
50  
51  
52  
53  
54  
55  
56  
57  
58  
59  
60

LCG06_002	788.65	699.51	0.8870	1.0925	0.02021	0.12234	0.00155	0.06479	0.00121	749.7	9.81	767.5	38.71	744	8.9	3.2	0.8	744	8.9
LCG06_003	501.47	267.30	0.5330	5.09132	0.07387	0.32564	0.00401	0.11343	0.00159	1834.7	12.31	1855.1	25.15	1817.2	19.49	2.1	1.0	1855.1	25.15
LCG06_004	427.13	157.89	0.3697	1.10812	0.02703	0.12669	0.00181	0.06346	0.00158	757.3	13.02	723.7	52.06	768.9	10.37	-5.9	-1.5	768.9	10.37
LCG06_005	179.31	81.45	0.4542	4.19653	0.08677	0.29953	0.00447	0.10165	0.0021	1673.3	16.95	1654.4	37.88	1689	22.18	-2.0	-0.9	1654.4	37.88
LCG06_006	4004.49	1293.09	0.3229	0.5249	0.00766	0.06775	0.00078	0.05621	8.00E-04	428.4	5.1	459.9	31.5	422.6	4.73	8.8	1.4	422.6	4.73
LCG06_007	3247.91	1202.45	0.3702	2.22221	0.03787	0.08203	0.00116	0.19655	0.00355	1188.1	11.94	2797.8	29.28	508.2	6.94	450.5	133.8	508.2	6.94
LCG06_008	1141.43	259.87	0.2277	1.54022	0.0233	0.15643	0.00187	0.07143	0.00106	946.6	9.31	969.8	30	936.9	10.4	3.5	1.0	936.9	10.4
LCG06_009	276.98	275.14	0.9934	0.43915	0.01858	0.05428	0.00101	0.0587	0.00259	369.7	13.11	555.9	93.53	340.7	6.2	63.2	8.5	340.7	6.2
LCG06_010	96.21	131.64	1.3683	1.19888	0.0523	0.12212	0.00255	0.07123	0.00324	800.1	24.15	963.9	89.79	742.7	14.66	29.8	7.7	742.7	14.66
LCG06_011	432.96	591.72	1.3667	5.15275	0.07706	0.32637	0.00409	0.11454	0.00166	1844.8	12.72	1872.7	25.95	1820.8	19.87	2.9	1.3	1872.7	25.95
LCG06_012	833.84	324.45	0.3891	4.67527	0.06419	0.3054	0.00364	0.11106	0.00147	1762.8	11.48	1816.9	23.76	1718	17.98	5.8	2.6	1816.9	23.76
LCG06_013	362.98	349.40	0.9626	5.07489	0.08005	0.31926	0.00413	0.11532	0.00178	1831.9	13.38	1884.9	27.52	1786.1	20.16	5.5	2.6	1884.9	27.52
LCG06_014	269.69	256.84	0.9524	5.66583	0.1039	0.36656	0.00521	0.11214	0.00202	1926.2	15.83	1834.3	32.33	2013.2	24.57	-8.9	-4.3	1834.3	32.33
LCG06_015	329.46	158.87	0.4822	0.26719	0.01367	0.0358	0.00072	0.05415	0.00289	240.4	10.95	377.2	115.2	226.7	4.49	66.4	6.0	226.7	4.49
LCG06_016	1247.85	300.70	0.2410	4.89079	0.06352	0.31087	0.00361	0.11414	0.00141	1800.7	10.95	1866.4	22.14	1745	17.77	7.0	3.2	1866.4	22.14
LCG06_017	654.54	916.01	1.3995	0.28766	0.0095	0.03361	0.00055	0.0621	0.00215	256.7	7.49	677.6	72.22	213.1	3.41	218.0	20.5	213.1	3.41
LCG06_018	71.43	65.27	0.9137	4.35103	0.12176	0.30349	0.00565	0.10401	0.00295	1703.1	23.1	1696.9	51.43	1708.6	27.97	-0.7	-0.3	1696.9	51.43
LCG06_019	505.85	297.83	0.5888	8.27073	0.11253	0.38698	0.00471	0.15506	0.00201	2261.1	12.32	2402.5	21.91	2108.8	21.89	13.9	7.2	2402.5	21.91
LCG06_020	647.25	220.68	0.3409	4.97842	0.06893	0.31089	0.00374	0.11618	0.00155	1815.7	11.71	1898.2	23.75	1745.1	18.37	8.8	4.0	1898.2	23.75
LCG06_021	2428.64	835.11	0.3439	0.5368	0.00839	0.06839	0.00081	0.05694	0.00088	436.3	5.54	488.6	34.1	426.5	4.86	14.6	2.3	426.5	4.86
LCG06_022	263.86	120.94	0.4583	0.79303	0.02357	0.10042	0.00155	0.05729	0.00175	592.9	13.35	502.3	66.49	616.9	9.06	-18.6	-3.9	616.9	9.06
LCG06_023	1995.69	371.69	0.1862	5.05009	0.06253	0.31851	0.00362	0.11503	0.00134	1827.8	10.49	1880.3	20.88	1782.4	17.7	5.5	2.5	1880.3	20.88
LCG06_024	387.77	187.75	0.4842	4.91579	0.07396	0.31882	0.004	0.11186	0.00164	1805	12.69	1829.9	26.27	1784	19.54	2.6	1.2	1829.9	26.27
LCG06_025	415.46	182.86	0.4401	5.45198	0.07951	0.3323	0.00412	0.11903	0.00168	1893.1	12.51	1941.7	25.01	1849.5	19.95	5.0	2.4	1941.7	25.01
LCG06_026	141.40	94.72	0.6699	0.62573	0.029	0.05175	0.00117	0.08773	0.00433	493.4	18.11	1376.5	91.91	325.2	7.15	323.3	51.7	325.2	7.15
LCG06_027	84.55	58.25	0.6889	9.59807	0.19038	0.43136	0.00701	0.16143	0.00313	2397	18.24	2470.7	32.4	2311.9	31.56	6.9	3.7	2470.7	32.4
LCG06_028	1010.23	505.01	0.4999	4.45851	0.05909	0.25824	0.00304	0.12526	0.00159	1723.3	10.99	2032.4	22.32	1480.8	15.57	37.3	16.4	2032.4	22.32
LCG06_029	294.47	235.48	0.7997	0.61739	0.02027	0.0759	0.00124	0.05901	0.00201	488.2	12.73	567.5	72.48	471.6	7.4	20.3	3.5	471.6	7.4
LCG06_030	195.34	237.56	1.2161	4.17524	0.07874	0.29146	0.00412	0.10393	0.00195	1669.2	15.45	1695.4	34.23	1648.8	20.55	2.8	1.2	1695.4	34.23
LCG06_031	1774.11	440.02	0.2480	0.74242	0.01169	0.09183	0.00109	0.05865	0.00091	563.8	6.81	554.2	33.56	566.4	6.43	-2.2	-0.5	566.4	6.43
LCG06_032	693.90	99.24	0.1430	3.42881	0.04959	0.25205	0.00305	0.09869	0.00139	1511	11.37	1599.6	25.99	1449	15.7	10.4	4.3	1599.6	25.99
LCG06_033	507.30	278.81	0.5496	13.9204	0.18118	0.52272	0.00628	0.1932	0.00236	2744.3	12.33	2769.6	19.9	2710.7	26.58	2.2	1.2	2769.6	19.9
LCG06_034	214.29	347.66	1.6224	6.56048	0.10733	0.36518	0.00492	0.13034	0.00208	2054.1	14.41	2102.5	27.76	2006.7	23.25	4.8	2.4	2102.5	27.76
LCG06_035	1078.75	566.05	0.5247	1.12157	0.01806	0.12296	0.00149	0.06618	0.00106	763.7	8.64	812	32.99	747.6	8.54	8.6	2.2	747.6	8.54
LCG06_036	431.50	351.53	0.8147	0.56907	0.01618	0.06754	0.00102	0.06113	0.0018	457.4	10.47	643.7	62.07	421.3	6.15	52.8	8.6	421.3	6.15
LCG06_037	521.88	302.41	0.5795	5.22587	0.07486	0.32473	0.00398	0.11675	0.00161	1856.8	12.21	1907.1	24.61	1812.8	19.38	5.2	2.4	1907.1	24.61
LCG06_038	578.73	244.43	0.4224	5.48329	0.0763	0.34506	0.00417	0.11529	0.00154	1898	11.95	1884.4	23.84	1910.9	19.97	-1.4	-0.7	1884.4	23.84
LCG06_039	724.51	479.76	0.6622	1.15194	0.02037	0.12763	0.0016	0.06548	0.00116	778.2	9.61	789.8	36.7	774.3	9.13	2.0	0.5	774.3	9.13
LCG06_040	2193.94	1105.56	0.5039	2.91007	0.03692	0.19727	0.00226	0.10702	0.00129	1384.5	9.59	1749.3	21.86	1160.7	12.15	50.7	19.3	1749.3	21.86
LCG06_041	803.23	274.79	0.3421	5.01646	0.0677	0.32089	0.00381	0.11342	0.00146	1822.1	11.43	1854.8	23.14	1794.1	18.57	3.4	1.6	1854.8	23.14
LCG06_042	476.69	391.07	0.8204	10.9578	0.14775	0.47899	0.00585	0.16597	0.00211	2519.6	12.55	2517.4	21.25	2522.9	25.48	-0.2	-0.1	2517.4	21.25
LCG06_043	1224.53	339.51	0.2773	5.20432	0.06736	0.33267	0.00387	0.11349	0.00139	1853.3	11.02	1856.1	22.03	1851.3	18.7	0.3	0.1	1856.1	22.03
LCG06_044	80.18	85.94	1.0719	6.19465	0.21321	0.29426	0.00734	0.15273	0.00544	2003.7	30.09	2376.7	59.42	1662.8	36.58	42.9	20.5	2376.7	59.42
LCG06_045	1332.40	744.40	0.5587	0.27378	0.00667	0.03596	0.00049	0.05523	0.00138	245.7	5.32	421.4	54.45	227.7	3.05	85.1	7.9	227.7	3.05
LCG06_046	586.02	361.21	0.6164	11.4717	0.15028	0.48519	0.00581	0.17153	0.00212	2562.3	12.24	2572.6	20.47	2549.8	25.24	0.9	0.5	2572.6	20.47
LCG06_047	846.96	295.74	0.3492	13.0319	0.16367	0.51347	0.00599	0.18413	0.00216	2682	11.84	2690.4	19.3	2671.4	25.51	0.7	0.4	2690.4	19.3
LCG06_048	424.21	221.61	0.5224	4.66627	0.07166	0.30845	0.0039	0.10975	0.00164	1761.2	12.84	1795.3	27.01	1733.1	19.23	3.6	1.6	1795.3	27.01
LCG06_049	469.40	178.26	0.3798	3.34809	0.05574	0.25974	0.00335	0.09352	0.00154	1492.3	13.02	1498.4	30.75	1488.5	17.17	0.7	0.3	1498.4	30.75
LCG06_050	53.94	44.63	0.8274	4.33611	0.15041	0.31577	0.00688	0.09962	0.00351	1700.3	28.62	1617	64.29	1769	33.72	-8.6	-3.9	1617	64.29



LCG06_100	137.03	78.92	0.5760	9.6487	0.16292	0.44108	0.0063	0.1587	0.00259	2401.8	15.53	2441.8	27.37	2355.5	28.18	3.7	2.0	2441.8	27.37
LCG06_101	137.03	71.84	0.5243	4.38412	0.09638	0.29919	0.00469	0.1063	0.00235	1709.3	18.18	1737	39.89	1687.3	23.28	2.9	1.3	1737	39.89
LCG06_102	97.67	99.71	1.0208	9.80059	0.19483	0.43956	0.00717	0.16175	0.00314	2416.2	18.32	2474	32.39	2348.7	32.12	5.3	2.9	2474	32.39
LCG06_103	1446.11	346.35	0.2395	1.51228	0.02265	0.15306	0.00183	0.07168	0.00105	935.4	9.15	976.8	29.54	918.1	10.22	6.4	1.9	918.1	10.22
LCG06_104	2575.88	1855.14	0.7202	2.33449	0.0304	0.20529	0.00236	0.0825	0.00102	1222.8	9.26	1257.3	23.86	1203.7	12.62	4.5	1.6	1257.3	23.86
LCG06_105	578.73	609.70	1.0535	4.35858	0.06358	0.29467	0.00362	0.1073	0.00151	1704.5	12.05	1754.1	25.54	1664.8	18.02	5.4	2.4	1754.1	25.54
LCG06_106	247.82	270.90	1.0931	4.96948	0.084	0.31325	0.00422	0.11509	0.00191	1814.1	14.29	1881.2	29.66	1756.7	20.7	7.1	3.3	1881.2	29.66
LCG06_107	756.58	578.91	0.7652	0.33884	0.00943	0.04805	0.00069	0.05116	0.00147	296.3	7.15	248	64.64	302.5	4.24	-18.0	-2.0	302.5	4.24
LCG06_108	596.23	440.06	0.7381	0.42926	0.01561	0.05476	0.00092	0.05687	0.00215	362.7	11.09	485.9	81.94	343.7	5.63	41.4	5.5	343.7	5.63
LCG06_109	129.74	123.94	0.9553	1.10973	0.04251	0.11832	0.00226	0.06804	0.00271	758	20.46	869.9	80.45	720.9	13.01	20.7	5.1	720.9	13.01
LCG06_110	297.39	159.40	0.5360	1.20678	0.03171	0.13782	0.00207	0.06352	0.00171	803.7	14.59	725.8	56.07	832.3	11.72	-12.8	-3.4	832.3	11.72

CZ05																			
sample	concentrations				ratios				ages				discordance		preferred ages				
	ppm U	ppm Pb	atomic Th/U	Pb207/Pb206	1 sigma	Pb207/U235	1 sigma	Pb206/U238	1 sigma	age 206/238	1 sigma	age 207/235	1 sigma	age 207/206	1 sigma	%disc ord.68-75	%disc ord.68-76	preferr ed age	1 sigma
CZ05-001	518	57	0.11	5.48193	0.08841	0.34499	0.00397	0.11529	0.00181	1897.8	27.7	1910.7	38.1	1884.4	56.1	-0.7	-1.4	1884.4	56.1
CZ05-002	535	509	0.95	0.54017	0.01356	0.06988	0.00086	0.05609	0.00141	438.5	17.88	435.4	10.4	455.4	110.0	0.7	4.4	435.4	10.4
CZ05-003	386	167	0.43	1.77861	0.03865	0.17423	0.00212	0.07406	0.00161	1037.7	28.26	1035.4	23.3	1043.2	86.5	0.2	0.7	1035.4	23.3
CZ05-004	219	182	0.83	1.43275	0.03393	0.14628	0.00181	0.07106	0.00169	902.7	28.32	880.1	20.4	959.2	95.7	2.6	8.2	880.1	20.4
CZ05-005	359	18	0.05	0.79061	0.01817	0.09468	0.00115	0.06059	0.00139	591.5	20.6	583.1	13.5	624.6	97.7	1.4	6.6	583.1	13.5
CZ05-006	321	242	0.75	1.38256	0.03083	0.1541	0.00184	0.06509	0.00145	881.5	26.28	923.9	20.5	777.3	92.1	-4.6	-18.9	923.9	20.5
CZ05-007	323	120	0.37	0.33342	0.01067	0.04699	0.00061	0.05148	0.00167	292.2	16.24	296	7.5	262.1	145.2	-1.3	-12.9	296	7.5
CZ05-008	697	213	0.31	1.52301	0.02918	0.14525	0.00171	0.07607	0.00145	939.7	23.48	874.3	19.3	1097	74.9	7.5	20.3	874.3	19.3
CZ05-009	277	220	0.80	0.53917	0.01678	0.07107	0.00093	0.05504	0.00173	437.9	22.14	442.6	11.2	413.9	136.5	-1.1	-6.9	442.6	11.2
CZ05-010	278	123	0.44	5.5004	0.10316	0.34638	0.00418	0.11521	0.00214	1900.7	32.22	1917.3	40.0	1883.2	66.3	-0.9	-1.8	1883.2	66.3
CZ05-011	136	82	0.60	1.20173	0.03446	0.12978	0.0017	0.06718	0.00195	801.4	31.78	786.6	19.4	843.4	118.5	1.9	6.7	786.6	19.4
CZ05-012	721	361	0.50	1.14435	0.02151	0.12419	0.00145	0.06685	0.00124	774.6	20.36	754.6	16.7	833.2	76.6	2.7	9.4	754.6	16.7
CZ05-013	552	414	0.75	9.19166	0.15408	0.41585	0.00489	0.16036	0.00264	2357.3	30.7	2241.6	44.5	2459.5	55.1	5.2	8.9	2459.5	55.1
CZ05-014	484	215	0.45	0.56628	0.01469	0.07218	0.0009	0.05692	0.00149	455.6	19.06	449.3	10.8	487.7	114.5	1.4	7.9	449.3	10.8
CZ05-015	400	261	0.65	1.66251	0.03238	0.16963	0.002	0.07111	0.00137	994.3	24.7	1010.1	22.1	960.5	78.0	-1.6	-5.2	1010.1	22.1
CZ05-016	389	172	0.44	0.53875	0.01455	0.07091	0.00089	0.05512	0.0015	437.6	19.2	441.6	10.7	417	118.1	-0.9	-5.9	441.6	10.7
CZ05-017	609	97	0.16	5.12799	0.08378	0.32432	0.00373	0.11471	0.00183	1840.8	27.76	1810.8	36.4	1875.4	57.1	1.7	3.4	1875.4	57.1
CZ05-018	969	923	0.95	0.52692	0.0113	0.06762	0.0008	0.05654	0.00121	429.8	15.02	421.8	9.7	472.8	94.3	1.9	10.8	421.8	9.7
CZ05-019	335	167	0.50	0.33323	0.01127	0.04419	0.00059	0.05471	0.00188	292	17.16	278.8	7.3	400.1	148.9	4.7	30.3	278.8	7.3
CZ05-020	1705	421	0.25	4.25282	0.06964	0.28416	0.00327	0.10858	0.00174	1684.3	26.92	1612.3	32.8	1775.7	58.0	4.5	9.2	1775.7	58.0
CZ05-021	59	37	0.62	0.40458	0.02782	0.05787	0.00107	0.05072	0.00355	345	40.22	362.7	13.0	228.2	308.1	-4.9	-58.9	362.7	13.0
CZ05-022	398	382	0.96	2.11797	0.03912	0.19873	0.00233	0.07732	0.00141	1154.7	25.48	1168.5	25.0	1129.5	72.0	-1.2	-3.5	1129.5	72.0
CZ05-023	553	140	0.25	1.86147	0.03331	0.17733	0.00206	0.07616	0.00134	1067.5	23.64	1052.4	22.6	1099.2	69.9	1.4	4.3	1052.4	22.6
CZ05-024	971	360	0.37	0.52755	0.01061	0.06907	0.00081	0.05541	0.00111	430.2	14.1	430.6	9.8	428.5	86.9	-0.1	-0.5	430.6	9.8
CZ05-025	208	186	0.89	0.28677	0.01222	0.03974	0.00057	0.05235	0.00227	256	19.3	251.2	7.1	300.8	191.9	1.9	16.5	251.2	7.1
CZ05-026	902	39	0.04	5.31244	0.08589	0.33848	0.00388	0.11386	0.0018	1870.9	27.64	1879.4	37.4	1862	56.5	-0.5	-0.9	1862	56.5
CZ05-027	198	150	0.75	0.9606	0.03875	0.10836	0.00162	0.06431	0.00265	683.6	40.14	663.2	18.9	751.9	169.1	3.1	11.8	663.2	18.9
CZ05-028	464	135	0.29	0.46144	0.01177	0.06083	0.00075	0.05503	0.00141	385.3	16.36	380.7	9.1	413.5	111.3	1.2	7.9	380.7	9.1
CZ05-029	192	202	1.05	1.77174	0.03975	0.17616	0.00216	0.07297	0.00164	1035.2	29.12	1045.9	23.6	1013.1	89.2	-1.0	-3.2	1045.9	23.6
CZ05-030	134	93	0.69	0.32871	0.01614	0.0433	0.00068	0.05507	0.00276	288.6	24.68	273.3	8.4	415.2	216.1	5.6	34.2	273.3	8.4
CZ05-031	289	194	0.67	4.93917	0.11659	0.30904	0.00407	0.11595	0.00277	1809	39.86	1736	40.1	1894.7	84.6	4.2	8.4	1894.7	84.6
CZ05-032	21	1	0.03	5.36076	0.21517	0.32755	0.00593	0.11873	0.0049	1878.6	68.7	1826.5	57.6	1937.3	144.2	2.9	5.7	1937.3	144.2





CZ05-082	176	138	0.78	2.30096	0.05199	0.20427	0.00252	0.08171	0.00186	1212.6	31.98	1198.2	26.9	1238.6	87.5	1.2	3.3	1238.6	87.5
CZ05-083	443	196	0.44	0.55791	0.01417	0.07396	0.00091	0.05472	0.0014	450.2	18.46	459.9	10.9	400.1	113.5	-2.1	-14.9	459.9	10.9
CZ05-084	163	72	0.44	10.5225	0.19416	0.46568	0.00556	0.16391	0.00301	2481.9	34.22	2464.6	48.9	2496.4	61.2	0.7	1.3	2496.4	61.2
CZ05-085	412	160	0.39	5.04493	0.09144	0.32264	0.00377	0.11343	0.00204	1826.9	30.72	1802.6	36.7	1855	64.3	1.3	2.8	1855	64.3
CZ05-086	159	213	1.33	0.92371	0.02786	0.10871	0.00142	0.06163	0.00188	664.3	29.4	665.3	16.6	661.5	128.4	-0.2	-0.6	665.3	16.6
CZ05-087	102	36	0.36	6.35656	0.13319	0.36388	0.00453	0.12672	0.00267	2026.3	36.76	2000.5	42.8	2052.9	73.4	1.3	2.6	2052.9	73.4
CZ05-088	540	1025	1.90	1.11617	0.02315	0.12344	0.00146	0.06559	0.00136	761.1	22.22	750.3	16.8	793.4	85.8	1.4	5.4	750.3	16.8
CZ05-089	407	194	0.48	1.09332	0.02404	0.12385	0.00149	0.06403	0.00141	750.1	23.32	752.7	17.1	742.8	91.9	-0.3	-1.3	752.7	17.1
CZ05-090	651	636	0.98	1.51035	0.02942	0.152	0.00178	0.07208	0.0014	934.6	23.8	912.1	20.0	987.9	78.5	2.5	7.7	912.1	20.0
CZ05-091	542	474	0.87	0.27429	0.00809	0.03869	0.00049	0.05142	0.00153	246.1	12.88	244.7	6.1	259.7	134.1	0.6	5.8	244.7	6.1
CZ05-092	201	157	0.78	1.34349	0.03398	0.14151	0.00177	0.06886	0.00176	864.7	29.44	853.2	20.0	894.7	103.7	1.3	4.6	853.2	20.0
CZ05-093	829	984	1.19	3.61716	0.06523	0.26737	0.0031	0.09813	0.00176	1553.3	28.7	1527.4	31.5	1589	66.1	1.7	3.9	1589	66.1
CZ05-094	431	251	0.58	0.52961	0.01881	0.06739	0.00093	0.05701	0.00206	431.6	24.98	420.4	11.2	491.2	156.7	2.7	14.4	420.4	11.2
CZ05-095	892	759	0.85	10.3596	0.18405	0.43924	0.00511	0.17108	0.00301	2467.4	32.9	2347.2	45.8	2568.2	58.3	5.1	8.6	2568.2	58.3
CZ05-096	1281	513	0.40	1.59513	0.03066	0.15174	0.00178	0.07625	0.00146	968.3	24	910.7	19.9	1101.8	75.7	6.3	17.3	910.7	19.9
CZ05-097	275	339	1.23	0.45917	0.01578	0.06173	0.00083	0.05395	0.00188	383.7	21.96	386.1	10.1	369	153.2	-0.6	-4.6	386.1	10.1
CZ05-098	847	574	0.68	0.52173	0.01202	0.06804	0.00082	0.05562	0.00129	426.3	16.04	424.3	9.9	437	100.7	0.5	2.9	424.3	9.9
CZ05-099	376	259	0.69	9.87779	0.17921	0.442	0.00517	0.1621	0.00292	2423.4	33.46	2359.6	46.3	2477.7	60.2	2.7	4.8	2477.7	60.2
CZ05-100	494	298	0.60	1.44681	0.03131	0.14793	0.00178	0.07094	0.00154	908.5	25.98	889.4	20.0	955.7	87.6	2.1	6.9	889.4	20.0
CZ05-101	503	273	0.54	4.91864	0.09199	0.31471	0.00369	0.11337	0.00211	1805.5	31.56	1763.8	36.2	1854.1	66.6	2.4	4.9	1854.1	66.6
CZ05-102	261	121	0.46	5.22613	0.10156	0.33722	0.00401	0.11241	0.00218	1856.9	33.12	1873.3	38.7	1838.8	69.5	-0.9	-1.9	1838.8	69.5
CZ05-103	355	128	0.36	7.94485	0.14798	0.39537	0.00466	0.14576	0.0027	2224.8	33.6	2147.7	43.1	2296.7	63.1	3.6	6.5	2296.7	63.1
CZ05-104	222	138	0.62	0.63669	0.01996	0.07712	0.00102	0.05989	0.00191	500.3	24.76	478.9	12.2	599.5	134.9	4.5	20.1	478.9	12.2
CZ05-105	389	226	0.58	0.54787	0.01519	0.07119	0.0009	0.05582	0.00157	443.6	19.92	443.3	10.8	444.9	122.1	0.1	0.4	443.3	10.8
CZ05-106	662	399	0.60	0.33448	0.00908	0.04639	0.00058	0.05229	0.00143	293	13.82	292.3	7.1	298.3	122.6	0.2	2.0	292.3	7.1
CZ05-107	354	150	0.42	10.2741	0.18999	0.46345	0.00545	0.1608	0.00296	2459.8	34.22	2454.8	48.1	2464.1	61.5	0.2	0.4	2464.1	61.5
CZ05-108	509	90	0.18	4.72764	0.09138	0.30588	0.00362	0.11211	0.00216	1772.2	32.4	1720.4	35.8	1833.9	69.2	3.0	6.2	1833.9	69.2
CZ05-109	230	177	0.77	3.53169	0.07713	0.26415	0.00325	0.09698	0.00213	1534.3	34.56	1511	33.1	1566.8	81.3	1.5	3.6	1566.8	81.3
CZ05-110	638	188	0.30	0.73071	0.01708	0.09466	0.00113	0.05599	0.00131	557	20.04	583	13.4	451.7	102.3	-4.5	-29.1	583	13.4
CZ05-111	1156	29	0.03	0.53021	0.01606	0.06846	0.00089	0.05618	0.00173	431.9	21.3	426.9	10.7	458.5	134.4	1.2	6.9	426.9	10.7
CZ05-112	1268	969	0.76	1.89332	0.03548	0.17732	0.00206	0.07744	0.00145	1078.7	24.9	1052.3	22.6	1132.7	73.4	2.5	7.1	1052.3	22.6
CZ05-113	714	373	0.52	2.41555	0.04629	0.20962	0.00245	0.08358	0.0016	1247.2	27.52	1226.8	26.1	1282.7	73.7	1.7	4.4	1282.7	73.7
CZ05-114	293	153	0.52	10.535	0.20988	0.47353	0.00579	0.16137	0.00322	2483	36.94	2499	50.7	2470	66.7	-0.6	-1.2	2470	66.7
CZ05-115	47	9	0.18	10.2523	0.25421	0.46062	0.00645	0.16144	0.00407	2457.8	45.88	2442.3	56.9	2470.8	83.9	0.6	1.2	2470.8	83.9
CZ05-116	423	210	0.50	1.3943	0.03066	0.14448	0.00174	0.07	0.00155	886.5	26	870	19.6	928.2	89.5	1.9	6.3	870	19.6
CZ05-117	137	189	1.38	1.65979	0.04681	0.16104	0.00211	0.07476	0.00214	993.3	35.74	962.6	23.4	1061.9	113.2	3.2	9.4	962.6	23.4
CZ05-118	624	436	0.70	2.66374	0.05257	0.22311	0.00263	0.08659	0.00171	1318.5	29.14	1298.3	27.7	1351.5	75.2	1.6	3.9	1351.5	75.2
CZ05-119	998	193	0.19	5.08479	0.09435	0.32672	0.0038	0.11288	0.00209	1833.6	31.48	1822.5	36.9	1846.3	66.1	0.6	1.3	1846.3	66.1
CZ05-120	648	285	0.44	1.66398	0.03371	0.16711	0.00197	0.07222	0.00146	994.9	25.7	996.1	21.8	992.3	81.4	-0.1	-0.4	996.1	21.8
CZ05-121	598	403	0.67	0.97135	0.02201	0.11303	0.00136	0.06233	0.00142	689.2	22.68	690.3	15.8	685.6	95.8	-0.2	-0.7	690.3	15.8
CZ05-122	1025	634	0.62	0.51145	0.01147	0.06845	0.00082	0.05419	0.00122	419.4	15.4	426.8	9.9	378.8	99.6	-1.7	-12.7	426.8	9.9
CZ05-123	171	164	0.96	1.17261	0.03462	0.13237	0.00173	0.06425	0.00193	787.9	32.36	801.4	19.7	749.9	124.1	-1.7	-6.9	801.4	19.7
CZ05-124	405	265	0.66	0.51282	0.01494	0.06717	0.00086	0.05537	0.00164	420.3	20.06	419.1	10.3	427.1	128.4	0.3	1.9	419.1	10.3
CZ05-125	781	654	0.84	1.74959	0.0362	0.16561	0.00197	0.07662	0.00159	1027	26.74	987.9	21.8	1111.4	81.8	4.0	11.1	987.9	21.8
CZ05-126	642	225	0.35	0.92771	0.0258	0.10353	0.00132	0.06499	0.00183	666.4	27.18	635.1	15.5	774	116.5	4.9	17.9	635.1	15.5
CZ05-127	380	246	0.65	4.97638	0.09702	0.32072	0.00379	0.11254	0.0022	1815.3	32.96	1793.3	37.0	1840.8	69.8	1.2	2.6	1840.8	69.8

CZ01

concentrations

ratios

ages

discordance

preferred ages

sample	ppm U	ppm Pb	atomic Th/U	Pb207/Pb206	1 sigma	Pb207/U235	1 sigma	Pb206/U238	1 sigma	age 206/238	1 sigma	age 207/235	1 sigma	age 207/206	1 sigma	%disc ord.68-75	%disc ord.68-76	preferred age	1 sigma
CZ01-001	429	128	0.30	0.44598	0.0108	0.05945	0.00073	0.05442	0.00132	374.5	15.16	372.3	8.9	388.4	106.2	0.6	4.1	372.3	8.9
CZ01-002	447	386	0.86	0.29797	0.00803	0.04287	0.00053	0.05041	0.00136	264.8	12.56	270.6	6.6	214.1	122.7	-2.1	-26.4	270.6	6.6
CZ01-003	196	82	0.42	0.35134	0.01245	0.04716	0.00064	0.05404	0.00194	305.7	18.7	297.1	7.9	372.4	157.1	2.9	20.2	297.1	7.9
CZ01-004	120	21	0.18	2.26748	0.05019	0.20538	0.00255	0.08008	0.00177	1202.2	31.2	1204.1	27.2	1199.1	85.7	-0.2	-0.4	1199.1	85.7
CZ01-005	392	146	0.37	0.59046	0.0134	0.07646	0.00093	0.05602	0.00126	471.2	17.12	474.9	11.1	452.8	98.4	-0.8	-4.9	474.9	11.1
CZ01-006	147	92	0.63	0.42888	0.01566	0.05709	0.00079	0.05449	0.00202	362.4	22.26	357.9	9.6	391.4	160.4	1.3	8.6	357.9	9.6
CZ01-007	53	56	1.05	0.70965	0.03269	0.09016	0.00139	0.0571	0.00267	544.5	38.82	556.5	16.4	494.7	200.3	-2.2	-12.5	556.5	16.4
CZ01-008	1788	459	0.26	0.30391	0.00568	0.03928	0.00046	0.05612	0.00103	269.5	8.86	248.4	5.7	456.9	79.9	8.5	45.6	248.4	5.7
CZ01-009	653	589	0.90	0.63305	0.01257	0.07913	0.00094	0.05803	0.00113	498	15.62	490.9	11.2	530.5	85.4	1.4	7.5	490.9	11.2
CZ01-010	186	73	0.39	5.65043	0.09784	0.35277	0.00417	0.11619	0.00196	1923.8	29.88	1947.8	39.8	1898.3	60.0	-1.2	-2.6	1898.3	60.0
CZ01-011	1088	155	0.14	0.46081	0.00883	0.06239	0.00073	0.05357	0.00101	384.8	12.28	390.2	8.9	353.1	84.0	-1.4	-10.5	390.2	8.9
CZ01-012	95	128	1.35	1.69196	0.04378	0.17052	0.00219	0.07197	0.00187	1005.5	33.02	1015	24.2	985.2	104.0	-0.9	-3.0	1015	24.2
CZ01-013	572	600	1.05	0.55826	0.01179	0.07338	0.00088	0.05519	0.00115	450.4	15.36	456.5	10.5	419.6	90.7	-1.3	-8.8	456.5	10.5
CZ01-014	305	119	0.39	5.99155	0.09964	0.36597	0.00428	0.11876	0.00191	1974.6	28.94	2010.4	40.4	1937.6	57.0	-1.8	-3.8	1937.6	57.0
CZ01-015	559	258	0.46	0.29526	0.00769	0.04125	0.00051	0.05192	0.00135	262.7	12.06	260.6	6.3	281.8	117.0	0.8	7.5	260.6	6.3
CZ01-016	665	30	0.04	0.92593	0.0171	0.10969	0.00129	0.06123	0.00111	665.5	18.04	670.9	15.0	647.4	76.6	-0.8	-3.6	670.9	15.0
CZ01-017	141	86	0.61	1.36982	0.03365	0.14705	0.00185	0.06757	0.00166	876.1	28.84	884.4	20.8	855.4	100.4	-0.9	-3.4	884.4	20.8
CZ01-018	1517	211	0.14	0.29515	0.00582	0.03835	0.00045	0.05582	0.00108	262.6	9.12	242.6	5.6	445	84.4	8.2	45.5	242.6	5.6
CZ01-019	238	146	0.61	5.03663	0.08672	0.32373	0.00382	0.11286	0.00189	1825.5	29.18	1807.9	37.2	1845.9	59.9	1.0	2.1	1845.9	59.9
CZ01-020	149	120	0.80	2.38057	0.05015	0.21447	0.00263	0.08052	0.00168	1236.8	30.12	1252.6	27.9	1209.6	81.1	-1.3	-3.6	1209.6	81.1
CZ01-021	339	232	0.69	1.75547	0.03331	0.17017	0.00202	0.07483	0.00139	1029.2	24.56	1013	22.3	1064	73.9	1.6	4.8	1013	22.3
CZ01-022	295	293	0.99	0.56365	0.01458	0.07145	0.00089	0.05722	0.00148	453.9	18.94	444.9	10.8	499.7	113.1	2.0	11.0	444.9	10.8
CZ01-023	510	220	0.43	1.76467	0.03143	0.17398	0.00204	0.07357	0.00128	1032.6	23.08	1034	22.4	1029.8	69.3	-0.1	-0.4	1034	22.4
CZ01-024	374	188	0.50	0.35235	0.0097	0.04831	0.00061	0.05291	0.00146	306.5	14.56	304.1	7.5	325	122.9	0.8	6.4	304.1	7.5
CZ01-025	162	80	0.50	0.35455	0.01382	0.04866	0.00069	0.05285	0.00209	308.1	20.72	306.3	8.4	322.3	174.5	0.6	5.0	306.3	8.4
CZ01-026	437	326	0.75	1.59577	0.02956	0.16388	0.00194	0.07064	0.00128	968.6	23.12	978.3	21.5	946.9	73.2	-1.0	-3.3	978.3	21.5
CZ01-027	161	188	1.17	1.64456	0.0373	0.16707	0.00207	0.0714	0.00161	987.5	28.64	996	22.9	969	90.7	-0.9	-2.8	996	22.9
CZ01-028	175	64	0.37	30.4783	0.49114	0.71457	0.0084	0.3094	0.00478	3502.4	31.68	3475.7	63.2	3517.9	47.3	0.8	1.2	3517.9	47.3
CZ01-029	212	130	0.61	0.35273	0.0124	0.04691	0.00064	0.05454	0.00194	306.8	18.62	295.5	7.9	393.5	154.2	3.8	24.9	295.5	7.9
CZ01-030	353	246	0.70	3.72362	0.06432	0.27817	0.00327	0.0971	0.00162	1576.5	27.66	1582.1	33.0	1569.2	62.0	-0.4	-0.8	1569.2	62.0
CZ01-031	1141	512	0.45	0.33691	0.00696	0.04554	0.00054	0.05367	0.00109	294.8	10.56	287.1	6.7	356.9	90.7	2.7	19.6	287.1	6.7
CZ01-032	234	180	0.77	0.32003	0.01109	0.04112	0.00058	0.05645	0.00199	281.9	17.06	259.8	7.2	469.4	153.8	8.5	44.7	259.8	7.2
CZ01-033	858	530	0.62	0.26194	0.00625	0.03765	0.00046	0.05047	0.0012	236.2	10.06	238.2	5.7	216.6	108.0	-0.8	-10.0	238.2	5.7
CZ01-034	154	102	0.66	1.86077	0.04153	0.18289	0.00227	0.07381	0.00163	1067.3	29.48	1082.7	24.7	1036.2	88.2	-1.4	-4.5	1082.7	24.7
CZ01-035	174	290	1.67	0.52838	0.01704	0.07055	0.00094	0.05432	0.00177	430.7	22.64	439.5	11.3	384.4	142.3	-2.0	-14.3	439.5	11.3
CZ01-036	238	293	1.23	4.83352	0.08616	0.32891	0.00391	0.1066	0.00185	1790.7	30	1833.1	38.0	1742.1	62.6	-2.3	-5.2	1742.1	62.6
CZ01-037	313	197	0.63	0.40591	0.01138	0.055	0.0007	0.05353	0.0015	345.9	16.44	345.2	8.6	351.4	124.5	0.2	1.8	345.2	8.6
CZ01-038	149	133	0.89	0.60402	0.01964	0.07777	0.00104	0.05634	0.00185	479.8	24.86	482.8	12.5	465.1	142.5	-0.6	-3.8	482.8	12.5
CZ01-039	134	72	0.54	0.43221	0.01676	0.05765	0.00082	0.05439	0.00214	364.7	23.78	361.3	10.0	387	170.4	0.9	6.6	361.3	10.0
CZ01-040	464	177	0.38	11.1875	0.1838	0.49365	0.00577	0.1644	0.00259	2538.9	30.62	2586.5	49.8	2501.4	52.5	-1.8	-3.4	2501.4	52.5
CZ01-041	1357	454	0.33	0.37098	0.00736	0.05157	0.00061	0.05219	0.00101	320.4	10.9	324.1	7.5	293.6	87.4	-1.1	-10.4	324.1	7.5
CZ01-042	799	357	0.45	0.65398	0.01294	0.08188	0.00098	0.05794	0.00112	510.9	15.9	507.3	11.6	527.2	84.5	0.7	3.8	507.3	11.6
CZ01-043	150	103	0.68	1.67788	0.03936	0.17149	0.00215	0.07098	0.00166	1000.2	29.84	1020.3	23.6	956.8	93.9	-2.0	-6.6	1020.3	23.6
CZ01-044	386	253	0.66	0.30965	0.009	0.04331	0.00056	0.05186	0.00151	273.9	13.96	273.3	6.9	279.2	130.6	0.2	2.1	273.3	6.9
CZ01-045	558	247	0.44	0.54135	0.01201	0.06995	0.00085	0.05614	0.00123	439.3	15.82	435.8	10.2	457.6	95.7	0.8	4.8	435.8	10.2
CZ01-046	334	207	0.62	1.65794	0.03271	0.16747	0.00201	0.07182	0.00139	992.6	25	998.2	22.2	980.7	77.7	-0.6	-1.8	998.2	22.2

1  
2  
3  
4  
5  
6  
7  
8  
9  
10  
11  
12  
13  
14  
15  
16  
17  
18  
19  
20  
21  
22  
23  
24  
25  
26  
27  
28  
29  
30  
31  
32  
33  
34  
35  
36  
37  
38  
39  
40  
41  
42  
43  
44  
45  
46  
47  
48  
49  
50  
51  
52  
53  
54  
55  
56  
57  
58  
59  
60

CZ01-047	250	229	0.92	5.36408	0.09582	0.34348	0.00409	0.11329	0.00196	1879.1	30.58	1903.4	39.3	1852.8	61.9	-1.3	-2.7	1852.8	61.9
CZ01-048	738	434	0.59	0.57977	0.01193	0.07572	0.00091	0.05555	0.00112	464.3	15.34	470.5	10.9	434	87.9	-1.3	-8.4	470.5	10.9
CZ01-049	74	61	0.82	3.43252	0.08047	0.27205	0.0035	0.09153	0.00214	1511.9	36.86	1551.2	35.5	1457.5	87.7	-2.5	-6.4	1457.5	87.7
CZ01-050	311	200	0.64	3.28213	0.06034	0.26596	0.00317	0.08952	0.0016	1476.8	28.62	1520.2	32.3	1415.3	67.4	-2.9	-7.4	1415.3	67.4
CZ01-051	36	33	0.92	1.52797	0.0639	0.15913	0.0025	0.06966	0.00296	941.7	51.32	951.9	27.8	918.2	170.2	-1.1	-3.7	951.9	27.8
CZ01-052	431	24	0.06	5.49545	0.0955	0.34439	0.00407	0.11576	0.00194	1899.9	29.86	1907.8	39.0	1891.7	59.6	-0.4	-0.9	1891.7	59.6
CZ01-053	266	187	0.70	1.782	0.037	0.17705	0.00216	0.07301	0.00149	1038.9	27.02	1050.8	23.6	1014.4	81.1	-1.1	-3.6	1050.8	23.6
CZ01-054	431	126	0.29	0.29777	0.00862	0.04181	0.00054	0.05167	0.0015	264.7	13.48	264	6.6	270.9	130.2	0.3	2.5	264	6.6
CZ01-055	369	236	0.64	0.27029	0.00837	0.03838	0.0005	0.05109	0.00159	242.9	13.38	242.8	6.2	244.7	140.1	0.0	0.8	242.8	6.2
CZ01-056	229	75	0.33	5.53018	0.10065	0.35133	0.00421	0.11419	0.00201	1905.3	31.3	1940.9	40.2	1867.1	63.0	-1.8	-4.0	1867.1	63.0
CZ01-057	584	217	0.37	0.52497	0.01188	0.06865	0.00084	0.05547	0.00124	428.5	15.82	428	10.1	431.1	97.3	0.1	0.7	428	10.1
CZ01-058	291	90	0.31	0.56415	0.01558	0.07333	0.00094	0.05581	0.00154	454.2	20.22	456.2	11.3	444.5	120.2	-0.4	-2.6	456.2	11.3
CZ01-059	35	17	0.49	1.42407	0.06346	0.15257	0.00244	0.06771	0.00307	899.1	53.16	915.3	27.3	859.8	182.6	-1.8	-6.5	915.3	27.3
CZ01-060	177	178	1.00	1.20737	0.0305	0.13206	0.00168	0.06632	0.00167	804	28.06	799.6	19.1	816.6	103.5	0.6	2.1	799.6	19.1
CZ01-061	307	165	0.54	2.19958	0.04341	0.19976	0.00241	0.07988	0.00154	1180.9	27.56	1174	25.9	1194	75.1	0.6	1.7	1194	75.1
CZ01-062	190	164	0.87	0.61937	0.01865	0.07758	0.00102	0.05792	0.00175	489.5	23.38	481.6	12.2	526.4	130.5	1.6	8.5	481.6	12.2
CZ01-063	293	84	0.29	0.29687	0.00976	0.03928	0.00053	0.05483	0.00182	264	15.28	248.4	6.5	405.3	143.5	6.3	38.7	248.4	6.5
CZ01-064	44	20	0.45	1.27777	0.05242	0.14326	0.00219	0.0647	0.00269	835.9	46.74	863.1	24.7	764.7	170.7	-3.2	-12.9	863.1	24.7
CZ01-065	463	278	0.60	3.39671	0.06203	0.25968	0.00309	0.09489	0.00167	1503.6	28.64	1488.2	31.7	1525.9	65.8	1.0	2.5	1525.9	65.8
CZ01-066	657	350	0.53	3.85843	0.06854	0.28769	0.0034	0.0973	0.00166	1605	28.66	1630	34.1	1572.9	63.4	-1.5	-3.6	1572.9	63.4
CZ01-067	891	257	0.29	2.68001	0.04782	0.22263	0.00263	0.08733	0.0015	1323	26.38	1295.7	27.8	1367.8	65.3	2.1	5.3	1367.8	65.3
CZ01-068	103	108	1.05	3.29571	0.07426	0.26016	0.0033	0.0919	0.00205	1480	35.1	1490.7	33.7	1465.2	83.8	-0.7	-1.7	1465.2	83.8
CZ01-069	447	218	0.49	2.72413	0.05101	0.22666	0.00271	0.08719	0.00158	1335.1	27.82	1317	28.5	1364.7	69.0	1.4	3.5	1364.7	69.0
CZ01-070	221	123	0.56	0.54118	0.01646	0.06936	0.00092	0.0566	0.00173	439.2	21.68	432.3	11.0	475.4	132.3	1.6	9.1	432.3	11.0
CZ01-071	297	157	0.53	10.7883	0.19256	0.48172	0.00575	0.16247	0.00279	2505.1	33.18	2534.8	50.0	2481.5	57.3	-1.2	-2.1	2481.5	57.3
CZ01-072	408	181	0.44	0.89021	0.01977	0.10653	0.00131	0.06062	0.00133	646.5	21.24	652.6	15.2	625.9	92.9	-0.9	-4.3	652.6	15.2
CZ01-073	263	193	0.73	8.99398	0.16286	0.41433	0.00497	0.15747	0.00275	2337.4	33.1	2234.7	45.3	2428.7	58.6	4.6	8.0	2428.7	58.6
CZ01-074	239	225	0.94	1.61735	0.03554	0.16489	0.00203	0.07116	0.00154	977	27.58	983.9	22.5	962	87.1	-0.7	-2.3	983.9	22.5
CZ01-075	121	50	0.42	1.70752	0.04437	0.17406	0.00225	0.07117	0.00184	1011.4	33.28	1034.5	24.7	962.2	104.1	-2.2	-7.5	1034.5	24.7
CZ01-076	312	114	0.37	5.17675	0.09649	0.32103	0.00386	0.11698	0.00211	1848.8	31.72	1794.8	37.7	1910.6	64.0	3.0	6.1	1910.6	64.0
CZ01-077	149	92	0.62	2.59901	0.05779	0.22511	0.00282	0.08376	0.00184	1300.4	32.6	1308.8	29.7	1286.8	84.3	-0.6	-1.7	1286.8	84.3
CZ01-078	657	206	0.31	12.3418	0.21845	0.51398	0.00609	0.1742	0.00295	2630.8	33.26	2673.6	51.8	2598.4	56.0	-1.6	-2.9	2598.4	56.0
CZ01-079	1192	323	0.27	0.27577	0.00628	0.03829	0.00047	0.05225	0.00117	247.3	10	242.2	5.8	296.3	100.7	2.1	18.3	242.2	5.8
CZ01-080	174	166	0.95	13.3255	0.24582	0.52877	0.0064	0.18283	0.00325	2703	34.84	2736.3	54.0	2678.7	58.3	-1.2	-2.2	2678.7	58.3
CZ01-081	214	249	1.16	0.55935	0.01686	0.07334	0.00096	0.05533	0.00167	451.1	21.96	456.2	11.6	425.5	131.2	-1.1	-7.2	456.2	11.6
CZ01-082	128	219	1.71	1.77734	0.04475	0.17795	0.00229	0.07246	0.00181	1037.2	32.72	1055.8	25.0	998.9	100.0	-1.8	-5.7	1055.8	25.0
CZ01-083	498	207	0.42	10.9655	0.19811	0.48185	0.00574	0.1651	0.00286	2520.2	33.62	2535.3	50.0	2508.5	57.8	-0.6	-1.1	2508.5	57.8
CZ01-084	405	413	1.02	1.75917	0.03575	0.17077	0.00207	0.07473	0.00148	1030.5	26.32	1016.4	22.8	1061.3	78.7	1.4	4.2	1016.4	22.8
CZ01-085	710	274	0.39	1.45866	0.02856	0.1528	0.00184	0.06926	0.00131	913.5	23.6	916.6	20.5	906.4	77.3	-0.3	-1.1	916.6	20.5
CZ01-086	177	68	0.38	18.9133	0.34874	0.59909	0.00725	0.22903	0.00406	3037.4	35.56	3026.2	58.4	3045.3	56.3	0.4	0.6	3045.3	56.3
CZ01-087	82	85	1.04	11.4187	0.22947	0.50089	0.0063	0.16538	0.00324	2558	37.52	2617.6	54.1	2511.5	65.1	-2.3	-4.2	2511.5	65.1
CZ01-088	160	89	0.56	0.54445	0.01898	0.07095	0.00098	0.05567	0.00195	441.4	24.96	441.9	11.8	439	152.6	-0.1	-0.7	441.9	11.8
CZ01-089	290	161	0.55	0.55359	0.016	0.07273	0.00095	0.05522	0.00159	447.3	20.92	452.6	11.4	421	125.4	-1.2	-7.5	452.6	11.4
CZ01-090	459	595	1.30	4.29013	0.08172	0.28466	0.00343	0.10934	0.00201	1691.5	31.38	1614.8	34.4	1788.4	66.3	4.7	9.7	1788.4	66.3
CZ01-091	450	132	0.29	0.73676	0.01726	0.0887	0.0011	0.06026	0.00139	560.5	20.18	547.8	13.0	612.9	98.2	2.3	10.6	547.8	13.0
CZ01-092	548	145	0.26	5.19712	0.09775	0.3355	0.00402	0.11238	0.00204	1852.1	32.04	1865	38.8	1838.3	64.9	-0.7	-1.5	1838.3	64.9
CZ01-093	226	289	1.28	1.65423	0.03845	0.16627	0.00209	0.07218	0.00165	991.2	29.42	991.5	23.1	991	91.8	0.0	-0.1	991.5	23.1
CZ01-094	222	119	0.54	0.55638	0.01723	0.07124	0.00095	0.05666	0.00176	449.2	22.48	443.6	11.4	477.5	135.8	1.3	7.1	443.6	11.4
CZ01-095	258	240	0.93	3.46448	0.07088	0.26493	0.00325	0.09487	0.00189	1519.2	32.24	1515	33.1	1525.5	74.1	0.3	0.7	1525.5	74.1



1  
2  
3  
4  
5  
6  
7  
8  
9  
10  
11  
12  
13  
14  
15  
16  
17  
18  
19  
20  
21  
22  
23  
24  
25  
26  
27  
28  
29  
30  
31  
32  
33  
34  
35  
36  
37  
38  
39  
40  
41  
42  
43  
44  
45  
46  
47  
48  
49  
50  
51  
52  
53  
54  
55  
56  
57  
58  
59  
60

sample	concentrations				ratios					ages					discordance		preferred ages		
	ppm U	ppm Pb	atomic Th/U	Pb207/Pb206	1 sigma	Pb207/U235	1 sigma	Pb206/U238	1 sigma	age 206/238	1 sigma	age 207/235	1 sigma	age 207/206	1 sigma	%disc ord.68-75	%disc ord.68-76	preferr ed age	1 sigma
CZ03-001	409	126	0.31	0.46401	0.01121	0.05959	0.00073	0.0565	0.00137	387	15.56	373.2	8.9	471.5	106.1	3.7	20.8	373.2	8.9
CZ03-002	327	535	1.63	1.26435	0.02426	0.13653	0.00161	0.0672	0.00127	829.9	21.76	825	18.3	844.1	77.8	0.6	2.3	825	18.3
CZ03-003	132	177	1.34	1.39432	0.03498	0.14635	0.00185	0.06914	0.00174	886.5	29.66	880.5	20.8	902.9	102.1	0.7	2.5	880.5	20.8
CZ03-004	652	443	0.68	1.63601	0.02826	0.15697	0.00183	0.07564	0.00128	984.2	21.76	939.9	20.4	1085.5	66.9	4.7	13.4	939.9	20.4
CZ03-005	366	240	0.66	9.44019	0.14083	0.42901	0.00497	0.15968	0.00229	2381.7	27.4	2301.3	44.8	2452.3	48.1	3.5	6.2	2452.3	48.1
CZ03-006	446	288	0.65	4.83439	0.07729	0.30411	0.00355	0.11536	0.00179	1790.9	26.9	1711.6	35.1	1885.5	55.3	4.6	9.2	1885.5	55.3
CZ03-007	248	216	0.87	0.25827	0.01009	0.03626	0.0005	0.05169	0.00205	233.3	16.28	229.6	6.3	271.5	176.4	1.6	15.4	229.6	6.3
CZ03-008	271	121	0.45	5.2651	0.08286	0.33147	0.00385	0.11527	0.00176	1863.2	26.86	1845.5	37.3	1884.1	54.3	1.0	2.0	1884.1	54.3
CZ03-009	880	101	0.11	2.04966	0.03117	0.18839	0.00215	0.07895	0.00115	1132.2	20.76	1112.6	23.3	1171	57.3	1.8	5.0	1171	57.3
CZ03-010	150	89	0.59	2.14246	0.04553	0.19487	0.00239	0.07979	0.00169	1162.6	29.42	1147.7	25.8	1191.7	82.4	1.3	3.7	1191.7	82.4
CZ03-011	197	71	0.36	0.59297	0.02056	0.07492	0.00102	0.05744	0.00202	472.8	26.22	465.7	12.2	508	151.7	1.5	8.3	465.7	12.2
CZ03-012	298	54	0.18	6.80177	0.10286	0.38056	0.00439	0.1297	0.00189	2086	26.78	2078.9	41.0	2093.9	50.7	0.3	0.7	2093.9	50.7
CZ03-013	126	113	0.90	1.51996	0.04222	0.1501	0.00198	0.07349	0.00206	938.5	34.02	901.5	22.2	1027.4	111.4	4.1	12.3	901.5	22.2
CZ03-014	212	108	0.51	11.0207	0.16413	0.47398	0.00549	0.16873	0.00241	2524.9	27.72	2501	48.0	2545.1	47.5	1.0	1.7	2545.1	47.5
CZ03-015	198	101	0.51	0.38049	0.0137	0.05089	0.00069	0.05425	0.00198	327.4	20.14	320	8.5	381.5	158.7	2.3	16.1	320	8.5
CZ03-016	284	127	0.45	5.21716	0.08997	0.33361	0.00397	0.11349	0.00192	1855.4	29.38	1855.8	38.4	1856	60.4	0.0	0.0	1856	60.4
CZ03-017	410	65	0.16	5.80878	0.0864	0.33288	0.00382	0.12663	0.00181	1947.7	25.78	1852.3	37.0	2051.7	50.0	5.2	9.7	2051.7	50.0
CZ03-018	469	10	0.02	0.56105	0.01943	0.06734	0.00093	0.06046	0.00212	452.2	25.28	420.1	11.2	620.2	148.1	7.6	32.3	420.1	11.2
CZ03-019	461	226	0.49	5.31808	0.07911	0.33502	0.00384	0.11519	0.00164	1871.8	25.42	1862.7	37.1	1882.9	51.0	0.5	1.1	1882.9	51.0
CZ03-020	472	225	0.48	1.64451	0.02944	0.16369	0.00192	0.07291	0.00128	987.4	22.6	977.2	21.2	1011.3	70.4	1.0	3.4	977.2	21.2
CZ03-021	454	346	0.76	9.88317	0.1418	0.44438	0.00507	0.16139	0.00221	2423.9	26.46	2370.2	45.3	2470.3	45.8	2.3	4.1	2470.3	45.8
CZ03-022	265	375	1.42	1.10281	0.02408	0.12369	0.0015	0.0647	0.00141	754.7	23.26	751.8	17.2	764.6	90.3	0.4	1.7	751.8	17.2
CZ03-023	249	72	0.29	6.01474	0.09383	0.34616	0.00402	0.12609	0.0019	1978	27.16	1916.2	38.5	2044.2	52.9	3.2	6.3	2044.2	52.9
CZ03-024	208	80	0.38	4.85861	0.07976	0.32078	0.00376	0.10991	0.00176	1795.1	27.64	1793.5	36.7	1797.9	57.6	0.1	0.2	1797.9	57.6
CZ03-025	481	177	0.37	8.85192	0.12718	0.42477	0.00485	0.15123	0.00207	2322.9	26.22	2282.1	43.8	2359.8	46.4	1.8	3.3	2359.8	46.4
CZ03-026	675	97	0.14	5.62869	0.08144	0.34121	0.00388	0.11971	0.00165	1920.5	24.94	1892.5	37.3	1951.9	49.0	1.5	3.0	1951.9	49.0
CZ03-027	296	125	0.42	7.94086	0.11881	0.39168	0.00452	0.14712	0.00212	2224.3	26.98	2130.6	41.9	2312.7	49.0	4.4	7.9	2312.7	49.0
CZ03-028	328	196	0.60	5.1136	0.07895	0.32175	0.00372	0.11533	0.00172	1838.4	26.22	1798.3	36.3	1885	53.2	2.2	4.6	1885	53.2
CZ03-029	392	72	0.18	0.5061	0.01254	0.06657	0.00082	0.05517	0.00137	415.8	16.92	415.4	9.9	419	107.8	0.1	0.9	415.4	9.9
CZ03-030	1041	581	0.56	1.64055	0.02519	0.16423	0.00187	0.07249	0.00107	985.9	19.38	980.2	20.7	999.7	59.5	0.6	2.0	980.2	20.7
CZ03-031	362	139	0.39	1.57073	0.02876	0.15228	0.00179	0.07485	0.00135	958.7	22.72	913.7	20.0	1064.4	71.6	4.9	14.2	913.7	20.0
CZ03-032	534	4	0.01	0.51366	0.01128	0.06759	0.00081	0.05515	0.0012	420.9	15.14	421.6	9.8	418.1	94.9	-0.2	-0.8	421.6	9.8
CZ03-033	99	91	0.92	9.54502	0.16045	0.44293	0.00534	0.15638	0.00257	2391.9	30.9	2363.8	47.7	2416.8	55.4	1.2	2.2	2416.8	55.4
CZ03-034	732	172	0.24	5.58633	0.08087	0.35192	0.004	0.11519	0.00159	1914	24.94	1943.8	38.2	1882.8	49.4	-1.5	-3.2	1882.8	49.4
CZ03-035	419	308	0.74	9.12467	0.13262	0.419	0.00479	0.15803	0.0022	2350.6	26.6	2255.9	43.6	2434.7	46.8	4.2	7.3	2434.7	46.8
CZ03-036	253	65	0.26	5.56867	0.08669	0.34432	0.00399	0.11736	0.00177	1911.3	26.8	1907.4	38.2	1916.4	53.5	0.2	0.5	1916.4	53.5
CZ03-037	355	162	0.46	0.60897	0.01415	0.07722	0.00094	0.05723	0.00133	482.9	17.86	479.5	11.2	499.8	101.6	0.7	4.1	479.5	11.2
CZ03-038	35	38	1.08	7.07447	0.19273	0.36835	0.00549	0.13937	0.00387	2120.8	48.48	2021.6	51.8	2219.4	94.7	4.9	8.9	2219.4	94.7
CZ03-039	54	59	1.09	4.68347	0.1084	0.31364	0.00411	0.10836	0.00252	1764.3	38.74	1758.6	40.3	1771.9	83.9	0.3	0.8	1771.9	83.9
CZ03-040	464	303	0.65	6.67945	0.09817	0.3706	0.00424	0.13079	0.00184	2069.9	25.96	2032.2	39.8	2108.6	49.0	1.9	3.6	2108.6	49.0
CZ03-041	129	96	0.75	0.36415	0.01727	0.0461	0.00071	0.05732	0.00277	315.3	25.7	290.5	8.8	503.4	206.7	8.5	42.3	290.5	8.8
CZ03-042	236	50	0.21	5.44179	0.08727	0.33939	0.00396	0.11635	0.00181	1891.5	27.52	1883.7	38.1	1900.9	55.5	0.4	0.9	1900.9	55.5
CZ03-043	747	565	0.76	10.5752	0.15	0.47073	0.00534	0.16302	0.0022	2486.5	26.32	2486.8	46.8	2487.2	45.2	0.0	0.0	2487.2	45.2
CZ03-044	659	330	0.50	1.48537	0.02476	0.14825	0.00171	0.07271	0.00118	924.4	20.22	891.1	19.2	1005.8	65.2	3.7	11.4	891.1	19.2
CZ03-045	276	199	0.72	10.6215	0.15838	0.46567	0.00537	0.16551	0.00237	2490.6	27.68	2464.6	47.3	2512.8	47.8	1.1	1.9	2512.8	47.8



1  
2  
3  
4  
5  
6  
7  
8  
9  
10  
11  
12  
13  
14  
15  
16  
17  
18  
19  
20  
21  
22  
23  
24  
25  
26  
27  
28  
29  
30  
31  
32  
33  
34  
35  
36  
37  
38  
39  
40  
41  
42  
43  
44  
45  
46  
47  
48  
49  
50  
51  
52  
53  
54  
55  
56  
57  
58  
59  
60

CZ03-095	122	135	1.11	6.57406	0.11898	0.37989	0.00458	0.12556	0.00225	2055.9	31.9	2075.8	42.8	2036.7	62.6	-1.0	-1.9	2036.7	62.6
CZ03-096	242	120	0.49	1.21368	0.02998	0.13398	0.00167	0.06572	0.00163	806.9	27.5	810.6	19.0	797.6	102.4	-0.5	-1.6	810.6	19.0
CZ03-097	327	499	1.53	10.7712	0.16698	0.47669	0.00549	0.16394	0.00247	2503.6	28.8	2512.9	47.9	2496.8	50.2	-0.4	-0.6	2496.8	50.2
CZ03-098	432	170	0.39	5.35222	0.0852	0.33997	0.00391	0.11423	0.00177	1877.2	27.24	1886.5	37.7	1867.7	55.4	-0.5	-1.0	1867.7	55.4
CZ03-099	503	58	0.12	0.93879	0.0189	0.10203	0.00121	0.06676	0.00134	672.2	19.8	626.3	14.2	830.2	82.4	7.3	24.6	626.3	14.2
CZ03-100	124	97	0.79	1.59781	0.0412	0.16208	0.00207	0.07152	0.00186	969.4	32.2	968.3	22.9	972.5	104.2	0.1	0.4	968.3	22.9
CZ03-101	441	119	0.27	10.9871	0.16857	0.48592	0.00557	0.16405	0.00244	2522	28.56	2553	48.3	2497.9	49.6	-1.2	-2.2	2497.9	49.6
CZ03-102	1349	225	0.17	10.6633	0.15928	0.47188	0.00535	0.16396	0.00236	2494.2	27.74	2491.8	46.9	2496.9	48.1	0.1	0.2	2496.9	48.1
CZ03-103	60	54	0.89	4.37614	0.12699	0.29857	0.00431	0.10634	0.00314	1707.8	47.96	1684.2	42.8	1737.6	106.3	1.4	3.1	1737.6	106.3
CZ03-104	64	43	0.67	1.21622	0.04761	0.12928	0.00193	0.06826	0.00272	808	43.62	783.8	22.1	876.4	161.0	3.1	10.6	783.8	22.1
CZ03-105	290	193	0.67	0.3884	0.01246	0.05122	0.00067	0.05501	0.00179	333.2	18.22	322	8.2	412.7	140.7	3.5	22.0	322	8.2